# TEXTILE RESEARCH JOURNAL

*Publication of*

TEXTILE RESEARCH INSTITUTE

VOLUME XXVIII AUGUST 1958 NUMBER 8

# Fiber Facts from Du Pont

***number 5, August, 1958***

The fifth in a series of advertisements containing technical data on properties and characteristics of Du Pont fibers . . . information which may be useful in your research activities. Here, for example, are some properties of "Super Cordura"* high tenacity rayon yarn.

## *"SUPER CORDURA"* HIGH TENACITY RAYON YARN*

| | |
|---|---|
| **Fiber Cross-Section** | **Irregular shape; smooth contour** |
| **Color** | **White** |
| **Density** | **1.52** |
| **Breaking Tenacity, Dry** | **4.6 to 5.0 g.p.d. at 76°F., 56% R.H.<br>5.6 to 6.0 g.p.d. at minus 70°F.<br>3.5 to 3.8 g.p.d. at 300°F.** |
| **Breaking Tenacity, Wet** | **2.9 to 3.3 g.p.d. in water at 70°F.<br>2.2 to 2.5 g.p.d. in water at 210°F.** |
| **Tensile Strength** | **89,500 to 97,300 lbs./sq. in. at 76°F., 56% R.H.** |
| **Elongation at Break, Dry** | **8 to 10% at 76°F., 56% R.H.** |
| **Elongation at Break, Wet** | **22 to 26% in water at 70°F.** |
| **Initial Modulus, Dry** | **100 to 120 g.p.d. at 76°F., 56% R.H.** |
| **Initial Modulus, Wet** | **5 g.p.d. in water at 70°F.** |
| **Work-to-Break, Dry** | **About 0.30 g.cm./d.cm. at 76°F., 56% R.H.** |
| **Heat Resistance** | **Fiber retains about 25% of its original strength after 40 days in air or water (under pressure) at 250°F.** |
| **Useful Environmental Temperature** | **−100°F. to +250°F.** |
| **Zero Strength Temperature** | **626°F. (Fiber breaks under load of 0.1 g.p.d.)** |
| **Melting Point** | **Does not melt** |
| **Specific Heat** | **0.3 BTU/lb./°F.** |
| **Flammability** | **Similar to cotton** |
| **Chemical Resistance** | **Good resistance to organic solvents. Also good resistance to dilute acids and alkalis at room temperature. Hot dilute or cold concentrated acids may degrade or dissolve the fiber.** |
| **Moisture Absorption** | **About 27% at 70°F., 95% R.H.** |

- Our "Technical Information Bulletins" cover subjects such as properties, characteristics, dyeing and processing of Du Pont's six textile fibers. More than 200 Bulletins are now in print; we'll be glad to forward you an Index.
- You may also be interested in our recently-published handbook, "Du Pont Fibers in Industry," which details technical and performance data for most industrial fiber applications.
- If you have specific questions about "Super Cordura" . . . or about any Du Pont fibers . . . write to Technical Service Section, Textile Fibers Department, Du Pont Company, Wilmington, Del.

DU PONT
REG. U.S. PAT. OFF.

BETTER THINGS FOR BETTER LIVING
. . . THROUGH CHEMISTRY

**NYLON** **"ORLON"*** REG. U. S. PAT. OFF. Acrylic fiber **"DACRON"*** REG. U. S. PAT. OFF. Polyester fiber **RAYON** **ACETATE** **"TEFLON"*** REG. U. S. PAT. OFF. TFE-fluorocarbon fib

* Registered Du Pont trademark

# TEXTILE RESEARCH JOURNAL

VOL. XXVIII *August 1958* NUMBER 8



***Editor:*** **Julian S. Jacobs**

***Production Editor:*** **Candida Frenking**

***Advisory Board***

**H. J. Ball**
**Earl E. Berkley**
**Henry Eyring**
**W. J. Hamburger**
**Milton Harris**
**K. L. Hertel**
**Harold P. Lundgren**
**H. Mark**
**E. R. Schwarz**



TEXTILE RESEARCH JOURNAL, published monthly at Prince and Lemon Streets, Lancaster, Pa., is devoted to the interest of research in textile and allied industries. It is published by Textile Research Institute.

Entered as second-class matter, April 27, 1945, at the post office at Lancaster, Pa., under the Act of August 24, 1912. Accepted for mailing at special rate of postage provided for in paragraph (d-2), Section 34.40, P. L. & R. of 1948, authorized May 9, 1950.

Manuscripts and communications should be sent to the Publications Department, P.O. Box 625, Princeton, N. J.

Subscription rates: $20.00 per year; additional for postage, 50 cents to Canada, $1.00 to all other countries. Single copies, $2.00 each.



Contents copyrighted © 1958 by Textile Research Institute. Advertising rates supplied on request.


## IN THIS ISSUE


High Speed Tensile Testing of Fibers. *J. W. Ballou and J. A. Roetling* ..... 631

The Polarographic Estimation of Sulfhydryl and Disulfide Groups in Wool. *J. P. E. Human* ..... 647

The Nature of Permanent Set in Keratin Fibers. *M. Feughleman, A. R. Haly, and T. W. Mitchell* ..... 655

The Preparation and Properties of Partially Benzylated Cotton. *Elias Klein, David J. Stanonis, Pieter Harbrink, and Ralph J. Berni* ..... 659

Empirical Relations of Crease Recovery and Time. *P. R. Wilkinson and H. E. Stanley* ..... 669

The Creasometer—An Apparatus for Measuring Crease and Pleat Sharpness and Retention. *P. R. Wilkinson and D. W. Ireland* ..... 674

The Mothproofing of Wool with Dieldrin. *M. Lipson and J. R. McPhee* ..... 679

Evaluation of Formaldehyde Pretreatment for Wool Bleaching. *J. E. Moore and R. A. O'Connell* ..... 687

Findings and Recommendations on the Use of the Vibroscope. *D. H. Patt* ..... 691

Response to Environmental Changes and an Equation of State for Nylon Yarn. *Bernard H. Eckstein, Earl H. Olson, and William F. Ames* ..... 701

Nonsilicate Stabilization of Hydrogen Peroxide Bleach Solutions. *David M. Cates and Winifred H. Cranor* ..... 708


### LETTERS TO THE EDITOR


Maximum Alkali-Combining Capacity of Wool. *J. R. McPhee* ..... 714

A Tex–Cotton Count Conversion Scale. *Gain L. Louis* .... 716

Cause of Wool Felting. *O. K. Dobozy* ..... 717

Dynamometric Measurements on Wool Fibers in Tops: Mean Value of Specific Strength, Work of Stretching, and Rate of Loading. *J. Grignet and F. Monfort* ..... 719


REPRINT REQUESTS SHOULD BE DIRECTED TO THE AUTHORS
SEE ARTICLES FOR ADDRESSES

AUGUST 1958
VOL. XXVIII NO. 8

TEXTILE RESEARCH JOURNAL

# High Speed Tensile Testing of Fibers[1]

**J. W. Ballou and J. A. Roetling**

*Pioneering Research Division, Textile Fibers Department, E. I. du Pont de Nemours & Co., Wilmington, Delaware*

**Abstract**

The requirements placed on the stress recording device of a tensile tester (usually a stress-transducer and recorder) become more stringent as the time to complete the test decreases. Unless these requirements are met, the difference between the true stress–strain curve and the indicated stress–strain curve becomes so large as to make the latter meaningless.

In this paper, the response of a stress–strain tester to the forces arising in testing a sample having a linear stress–strain curve is examined theoretically. An equation is derived which gives the indicated stress in terms of the true stress, the strain, the rate of strain, the resonance frequency and damping of the stress-transducer, and the upper and lower cut-off frequencies or bandwidth of the amplifier-recorder system. Wave effects, however, are not considered. This equation has been solved for a variety of conditions using a small scale digital computer. Indicated stress–strain curves are presented showing their increased deviation from the true stress–strain curve as the rate of testing is increased, as the resonance frequency is lowered, or as the bandwidth is decreased. These results show that certain minimum requirements involving the ratio of the rate of strain to the resonance frequency, damping, and upper and lower cut-off frequencies must be met for accurate indication of stress. As each requirement fails to be met, certain characteristic faults in the recorded stress–strain curve appear.

The principles developed above were put to use in designing and constructing a simple stress–strain tester capable of true stress recording at a strain rate of $10^3$ %/min., using a 5-in. gauge length. This tester is described and data taken on textile fibers at 1, $10^2$, and $10^3$ %/min. strain rates presented by way of example.

The structural basis of fiber behavior at different experimental time-scales is discussed briefly.

## Introduction

The main object of this paper is to provide information on the requirements imposed on a tensile tester if it is to record the true stress–strain curve of the specimen tested. Additionally, the characteristic faults which appear as distortions of the true stress–strain curve as various requirements fail to be met will be examined. In particular, the effect of high rates of testing on the accuracy of recording will be studied in detail.

The theoretical performance of a tensile tester consisting of a stress-transducer, amplifier, and

[1] Given at the Fall Meeting of The Fiber Society, Boston, Mass., September 4, 1957.

cathode ray oscilloscope as recorder will be analyzed with the help of an equation for the indicated stress in terms of the true stress, the strain, and the various constants describing the tester. This equation will then be solved for various conditions, including high rates of testing, and the resulting performances shown in the form of both indicated and true stress–strain curves. The equation also will allow generalizations to be made on requirements for testing with desired accuracy. Finally, a simple high-speed tensile tester will be described along with examples of results obtained with it; the structural basis of fiber behavior at high rates of testing will be touched upon.

*Strain Rates and Velocities*

A fiber or yarn in use or being tested for such properties as tensile strength, breaking elongation, etc. may experience stresses and strains which vary with time. Thus the characteristics of its environment include not only the magnitude of the stresses or strains which it encounters, but also how fast they are applied. Either stress or strain may be the primary variable, but because many tensile testers operate as controlled straining devices, let us consider strain and its time rate of application as fundamental in the discussion to follow. Strain rate $R$ will be defined as the change of strain occurring in a specimen per unit of time, where the strain is always based on the initial unstrained specimen length, in such units as cm./cm./sec. or %/min. If the specimen is in a tensile tester operating at a constant rate of strain as defined above and the gauge length between the upper and lower jaws (at zero strain) is $L$, the velocity of the crosshead or lower jaw is $V$, where

$$V = RL \tag{1}$$

In Figure 1 is shown a chart of testing velocities in m./sec. and corresponding strain rates in %/min. based on a 5-in. (12.7-cm.) gauge length. It is seen that conventional fiber testing velocities, such as one encounters with an Instron[2] Tensile Tester, are two or three decades below those velocities which it is estimated a fiber experiences in high speed sewing, tire cord impact, and in safety and parachute lines. Thus it is of interest to know what the physical properties of fibers are at these higher velocities. These velocities have been at-

[2] T. M. Instron Engineering Corp., Quincy, Mass.

**Symbols Used**

$C$ = velocity of sound
$D$ = denier
$E_0$ = input voltage to amplifier
$E_1$ = voltage output from high-pass filter
$E_2$ = voltage output from low-pass filter
$F_1$ = high-pass filter factor
$F_2$ = low-pass filter factor
$F_3$ = transient factor
$G$ = spring constant
$K$ = proportionality constant
$L$ = gauge length
$M$ = (elastic) modulus
$R$ = strain rate
$V$ = straining (impact) velocity
$e$ = strain
$e_b$ = break strain
$e_0$ = magnitude of strain pulse
$\bar{e}$ = average strain
$f_i$ = indicated force
$f_i'$ = force indicated by stress-transducer
$f_t$ = true force
$f_0$ = resonance frequency of stress-transducer
$f_1$ = lower cut-off frequency of amplifier
$f_2$ = higher cut-off frequency of amplifier
$g$ = gravitational constant
$l$ = damping constant
$m$ = mass of moving element of transducer
$s_i$ = indicated stress
$s_i'$ = stress indicated by stress-transducer
$s_t$ = true stress
$t$ = time
$t_b$ = time to break
$x$ = displacement of stress-transducer
$x_1 = \omega_1/R$
$x_2 = \omega_2/R$
$x_3 = \omega_0/R$
$x_4 = l/R$
$x_5 = \omega_r/R$
$\beta$ = phase angle
$\epsilon = 2.71828$
$\eta$ = dashpot viscosity
$\omega_0 = 2\pi f_0$
$\omega_1 = 2\pi f_1$
$\omega_2 = 2\pi f_2$
$\omega_r = G/\eta$

tained in testers built by Meredith [4] in England and by Schiefer, Smith, and others [2] at the Bureau of Standards, to name a few. In general, fiber properties change with velocity of testing, in some cases very markedly, so that it is risky to predict high speed behavior from data taken at low speed.

*Problems in High Speed Tensile Testing*

As speed of testing is increased, the stress–strain curve indicated by a particular tensile tester will, in general, deviate from the true stress–strain curve more and more. The first difficulty to be encountered as speed is increased is associated with inadequate response of the stress measuring device and the associated recorder used. One effect, for example, is that as the time-scale of the test decreases, the inertia possessed by any mechanical system such as a conventional stress-transducer makes itself felt. Eventually, at very high speeds (short time-scales), no response will occur at all, and the indicated stress–strain curve coincides with the strain axis at zero stress.

The second difficulty, generally at still higher speeds, results from the finite velocity of strain transmission along the specimen (sound velocity). If the end of the specimen is moved at high velocity to develop strain, it is possible for an appreciable local strain to build up in the vicinity of the end before being propagated very far along the specimen. The result is a strain pulse which moves along the specimen to the stationary end, where it would show up as a corresponding stress pulse if it were measured at that point. Upon reflection, the strain pulse returns to the moving end, is reflected again, and returns to the stationary end, where the stress is doubled by the addition of the second reflection. Thus a stepwise rather than a continuous stress–strain curve is developed. Further, as the velocity with which the end is moved increases, a speed is reached where the local strain developed is equal to the break strain and the fiber breaks at the moving end. At this "critical velocity," no strain pulse propagates to the fixed end before failure and no stress is developed at this point.

*Wave Effects*

Whether or not wave effects and stepwise stress–strain curves occur depends on two factors: the velocity with which the end of the specimen being strained moves and the velocity of sound in the

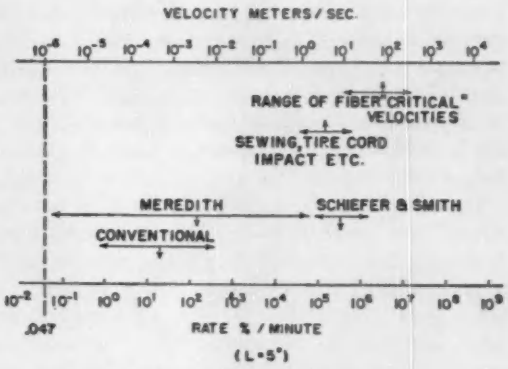


**Fig. 1.** Testing velocities and the corresponding strain rates based on a 5-in. gauge length.

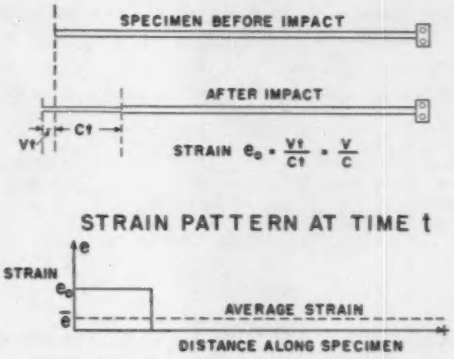


**Fig. 2.** Strain wave magnitude and propagation.

specimen. This can easily be seen by reference to Figure 2, which shows a specimen of length $L$ clamped at one end being strained by moving the other end with a velocity $V$. In a time $t$, the free end will move a distance $Vt$, but the average strain $\bar{e}$ in the sample will not always be $Vt/L$, since the whole specimen may not be strained if $t$ is relatively short. Instead, it is seen that the actual strain developed will have moved only a distance $Ct$, where $C$ is the velocity of sound in the specimen. Thus the actual strain is

$$e_0 = Vt/Ct = V/C \qquad (2)$$

and the average strain in the specimen at time $t$ is less than $e_0$. This is the strain pulse resulting in stepwise loading and a stepped stress–strain curve. Ordinarily $V$ is small so that the strain pulse $e_0$ is relatively small and the time $t$ to strain a sample appreciably is relatively large. Thus a very small strain pulse suffers a very large number of reflec-

tions during the time of the experiment, and the average strain $\bar{\epsilon}$ will be essentially equal to $Vt/L$ in all parts of the specimen, since dynamic equilibrium will have been established. That is, the steps in the stress–strain curve will have been reduced in size and increased in number so that they are no longer noticeable.

In real fibers, the sound velocity $C$ is between about 1000 and 6000 m./sec., depending upon molecular orientation. Thus if the velocity of the moving end of the specimen $V$ is 1 m./sec., the strain pulse amplitude $e_0 = V/C$ will vary between 0.1% and 0.017%, depending upon the specimen tested. If, on the other hand, $V$ = 50 m./sec., the corresponding $e_0$ values are 5–0.84%, which would be very noticeable as step distortions in the stress–strain curve, at least in specimens with sound velocities in the lower range, since it must be remembered that each step would be $2e_0$ as a result of reflection doubling the strain (see Figure 3).

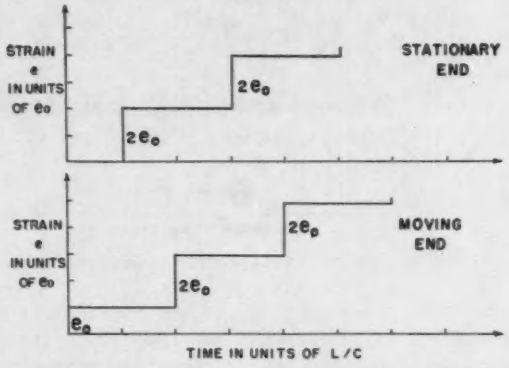


**Fig. 3.** Stepwise increase in strain resulting from strain wave reflection.

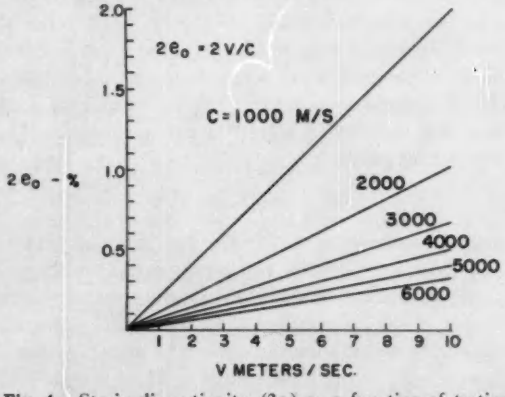


**Fig. 4.** Strain discontinuity ($2e_0$) as a function of testing velocity ($V$) for various sound propagation velocities ($C$).

Since a tensile tester operating at a strain rate $R$ of $10^5$ %/min. and having a 5-in. (12.7-cm.) gauge length $L$ will be described below, it is of interest to calculate the range of strain pulse amplitudes which might be encountered and see if they will be noticeable. Since $V = RL$, these conditions correspond to $V$ = 2.12 m./sec. Therefore, if an oriented specimen having a sound velocity of $C$ = 2120 m./sec. were tested, $e_0$ would be $10^{-3}$ or 0.1% and $2e_0$, the strain discontinuity, 0.2%. If the situation is idealized a bit and the stress–strain curve assumed to be linear with a slope of 50 g./den., this strain pulse would result in stress steps on the stress–strain curve of 0.1 g./den. at every 0.2% of strain, which might be expected to be noticeable. However, this small step in the stress–strain curve would be damped out, unless the stress-transducer fulfilled certain conditions which are generally not realized; i.e., it corresponds to a rather high-frequency ($10^4$ cycles/sec.), small, sharp, repetitive pulse modulation on the stress–strain curve to which the system ordinarily would not respond. On the other hand, if the testing velocity $V$ were increased, a point would be reached where the discontinuities would be great enough to be noticeable. Smith [3] makes the statement that the effects of tension-wave propagation along the fiber must be considered when the testing velocity exceeds about 10 m./sec.

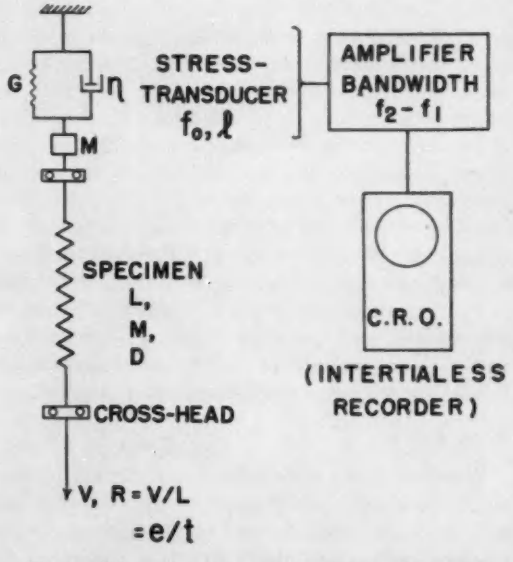


**Fig. 5.** Schematic representation of the testing system.

In Figure 4 is shown a plot of the strain discontinuity $2e_0$ vs. testing velocity for various sound velocities in the specimen. As mentioned, at 1 or 2 m./sec. no discontinuities should be noticeable in the tester to be described below.

Since the strain pulse generated at the moving end of the specimen before any reflections occur is $e_0$, it can be seen that if $e_0$ is equal to the impact breaking strain $e_b$ in a specimen with a sound velocity $C$ in the unstrained state, then the "critical velocity" is given by

$$V_c = e_0 C = e_b C \tag{3}$$

This is the velocity which will break the specimen at the moving clamp end before reflection at the fixed end. That is, $e_b$ is developed at once by the strain pulse without the necessity for multiple reflections to occur.

## Theory of High Speed Tensile Testing in the Absence of Wave Effects

### *Specimen and Tester Characteristics*

In Figure 5 is shown a schematic of the system to be considered. The first element is a stress-transducer which provides a d.c. electrical signal proportional to stress. It may, for example, consist of a cantilever beam having a bonded strain gauge attached to it, suitably powered. It will be represented, insofar as its mechanical behavior is concerned, by a model consisting of a mass $m$ attached to a spring and dashpot in parallel. The spring has a spring constant $G$ and the dashpot a viscosity $\eta$. The system will also have a resonance frequency $f_0$ and damping constant $l$. Attached to the mass is an upper (essentially fixed) clamp holding the specimen of length $L$ which terminates at the movable crosshead clamp. The specimen will be represented by a spring but will be thought of as a fiber or yarn sample having a certain denier $D$ and elastic modulus $M$. The crosshead will move with a certain velocity $V$ and strain the specimen at a corresponding strain rate $R$. The electrical signal from the stress-transducer goes through an amplifier assumed for simplicity to have a gain of unity over most of its pass band, which is described by a low cut-off frequency $f_1$ and a high cut-off frequency $f_2$. Finally the signal is fed to a cathode ray oscilloscope. Since it is assumed that the sample is strained at a constant rate, the horizontal time axis is proportional to strain; the vertical axis will be proportional to stress. Actually the amplifier gain will not be unity in practice but it is sufficient to specify that its gain, plus the electrical sensitivity of the stress-transducer, be sufficient to give a usable deflection on the oscilloscope. The responses of the stress-transducer and amplifier will be considered separately and then combined to obtain the theoretical performance of the system.

### *Stress-Transducer Differential Equation*

In order to find the response characteristics of the stress-transducer, i.e., the electrical signals generated for a given force or stress vs. time input, it is necessary to set up the differential equation describing the motion of the mechanical system and solve it for a specific case; i.e., obtain the displacement of the mass to which the upper clamp is attached (Figure 5) as a function of time. It is assumed that the electrical output is proportional to this displacement, which in turn is proportional to the indicated stress $s_t'$ sensed by the transducer.

A specimen with a linear stress–strain curve will be considered, since this is easy to handle theoretically and will suffice to show the principles involved. The true stress $s_t$ developed in such a specimen on its being strained an amount $e$ is, if wave effects are neglected,

$$s_t = Me \text{ g./den.} \tag{4}$$

where $M$ = specimen modulus, g./den., and $e$ = specimen strain, cm./cm. If the specimen has a denier $D$, the true force $f_t$ or tension developed is

$$f_t = MDe \text{ g.} \tag{5}$$

However, since the time to strain a specimen to a strain $e$ at a strain rate $R$ (cm./cm./sec.) is

$$t = e/R \text{ sec.} \tag{6}$$

Equation 5 may be written as $f_t = MDRt$ g. or $f_t = gMDRt$ dynes. This will be the input to the stress-transducer, a force increasing linearly in time. The reaction of the stress-transducer to this force function is governed by the usual complete linear differential equation discussed in such books as that of Page [5]. If $x$ is the downward displacement of the mass in the transducer, to which the upper clamp is attached, then the equation is as follows, using the notation in Figure 5:

$$m\frac{d^2x}{dt^2} + \eta\frac{dx}{dt} + Gx = gMDRt \text{ dynes} \tag{7}$$

where $m$ = grams, $x$ = cm., $\eta$ = dyne-sec./cm., $G$ = dyne/cm., $M$ = g./den., $D$ = denier units, $R$ = cm./cm./sec., and $t$ = sec. If this equation is solved for $x$ as a function of time, this will be proportional to the indicated force as a function of time.

*Complete Solution of Differential Equation*

The general integral of Equation 7 is the sum of the complementary function and any particular integral. The complementary function is the solution with $gMDRt = 0$, while the particular integral is *any* solution of the complete equation. In this case, the complementary function is given by Page [5] and the particular integral was obtained by well-known methods [1]. The general integral is as follows, for the periodic case:

$$x = \frac{gMDRt}{G} + \frac{gMD}{G}\left[\frac{R}{\omega_0}\epsilon^{-lt}\cos(\omega_0 t - \beta) - \frac{R}{\omega_r}\right] \quad (8)$$

where

$$l = \eta/2m \qquad \omega_0^2 = k^2 - l^2$$

$$k^2 = G/m \qquad \beta = \tan^{-1}\frac{1}{2}\left[\frac{l}{\omega_0} - \frac{\omega_0}{l}\right]$$

$$k^2 > l^2 \qquad \omega_r = \frac{\omega_0^2 + l^2}{2l}$$

$l$ is the damping constant (sec.$^{-1}$) and $\omega_0$ is the resonant angular frequency (sec.$^{-1}$) characteristic of the stress-transducer.

However, since $G$ is the stress-transducer spring constant, $\frac{Gx}{g}$ is the force in grams sensed by the stress-transducer. Thus the indicated force $f_i'$ is, in grams,

$$f_i' = \frac{Gx}{g} = MDRt + MD\left[\frac{R}{\omega_0}\epsilon^{-lt}\cos(\omega_0 t - \beta) - \frac{R}{\omega_r}\right] \quad (9)$$

but $e = Rt$ (Equation 6) so

$$f_i' = MDe + MD\left[\frac{R}{\omega_0}\epsilon^{-le/R}\cos\left(\frac{\omega_0 e}{R} - \beta\right) - \frac{R}{\omega_r}\right] \quad (10)$$

or

$$f_i' = MDe\left\{1 + \left[\frac{R}{\omega_0 e}\epsilon^{-le/R}\cos\left(\frac{\omega_0 e}{R} - \beta\right) - \frac{R}{\omega_r e}\right]\right\} \quad (11)$$

By dividing by the denier $D$, Equation 11 becomes

$$s_i' = Me\left\{1 + \left[\frac{R}{\omega_0 e}\epsilon^{-le/R}\cos\left(\frac{\omega_0 e}{R} - \beta\right) - \frac{R}{\omega_r e}\right]\right\} \quad (12)$$

This is the indicated stress as a function of strain. Since $Me = s_t$ (Equation 4),

$$s_i' = s_t(1 + F_3) \quad (13)$$

where $F_3$ is a superimposed damped oscillation, a transient modulation or perturbation of the true stress–strain curve, which is a function of strain at a given rate of strain.

*Effect of Band-Width on Response*

Equation 12 (or 13) governs the response of the stress-transducer only. It would describe the complete response of the system only if the amplifier in the system (Figure 5) had a frequency pass-band flat from 0 cycles/sec. to a very high frequency. In general, an amplifier has a limited pass-band; this will modify the overall response.

To get a simple approximation to the effect of the amplifier, let the equivalent circuit be that given in Figure 6. The voltage signal from the stress-transducer, $E_0$, which is proportional to $s_i'$ in Equation 13; i.e.,

$$E_0 = \text{constant} \times s_i' \quad (14)$$

is shown going through a high-pass $RC$ network which results in a voltage $E_1$. This, in turn, goes through the low-pass network, resulting in a voltage $E_2$. The dashed line represents an ideal isolation coupling of unity gain having no frequency characteristics of its own. In practice the gain is greater than unity by an amount depending on the sensitivity of the stress-transducer, but it is not necessary to take this into account in working out the response to voltages varying with time.

It is easy to show that such an idealized amplifier will have a frequency response approximately like that shown also in Figure 6, where the upper and lower cut-off angular frequencies, defined in terms

of the voltage gain dropping 3 db to 0.707, are given by

$$\omega_1 = 2\pi f_1 = \frac{1}{R_1 C_1} \tag{15}$$

$$\omega_2 = 2\pi f_2 = \frac{1}{R_2 C_2} \tag{16}$$

One must determine what effect such an amplifier will have on a voltage varying linearly in time, such as is produced by the stress-transducer. Actually, as shown by Equation 13, if the true stress varies linearly in time, the indicated stress or voltage proportional to it may have a transient perturbation $F_3$ superimposed. In this approximation it will be assumed that $F_3$ is small and that the input to the amplifier will be approximately

$$E_0 = Kt \tag{17}$$

Qualitatively, the frequency response diagram in Figure 6 shows that if this limitation in frequency range has any effect at all on the stress–strain curve, the low-pass filter tail at $f_2$, in cutting off the high frequencies, will affect the initial part of the stress–strain curve at low strains, but not the final part. This is because high frequencies correspond to short times and therefore low strains. Conversely, the high-pass filter tail at $f_1$, in cutting off the low frequencies, will affect the final part of the stress–strain curve, but not the initial part. Thus if the voltage input to the amplifier is linear in time, passage through the high-pass filter will not affect the early portion of the linear voltage-time curve which will subsequently be affected by the low-pass filter. That is, the important early part of the voltage-time curve input to the low-pass filter will be approximately linear. Similarly, the later part of voltage-time curve affected by the high-pass filter will not be affected by the low-pass filter. While this analysis is approximate, it permits easy solution of the differential equations describing the two filters, since it can be assumed that the input to each is approximately linear over the time range where an effect takes place.

The solutions based on these assumptions show that

$$E_1 = E_0 \frac{1}{\omega_1 t}\left(1 - \epsilon^{-\omega_1 t}\right) \tag{18}$$

$$E_2 = E_1\left[1 - \frac{1}{\omega_2 t}\left(1 - \epsilon^{-\omega_2 t}\right)\right] \tag{19}$$

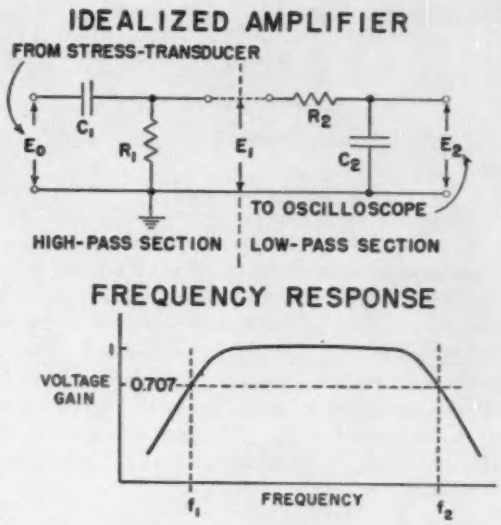


Fig. 6. Idealized amplifier response.

These equations can be combined (remember that $t = e/R$) to give

$$E_2 = E_0\left[\frac{R}{\omega_1 e}\left(1 - \epsilon^{-\omega_1 e/R}\right)\right] \times \left[1 - \frac{R}{\omega_2 e}\left(1 - \epsilon^{-\omega_2 e/R}\right)\right] \tag{20}$$

or

$$E_2 = E_0 \times F_1 F_2 \tag{21}$$

This equation gives the approximate effect of the amplifier, as a function of strain, on the sensibly linear voltage output of the stress-transducer, $E_0$, which is proportional to $s_i'$ (Equation 14). $E_2$ is the signal fed to the oscilloscope; it is this signal, after the amplifier has had an effect, which will be taken as proportional to the final stress $s_i$ indicated on the oscilloscope; i.e.,

$$E_2 = \text{constant} \times s_i \tag{22}$$

*Final Approximation to Overall Response*

Equations 12 or 13 would be the complete response of the system in the absence of any amplifier characteristics. However, when an amplifier is present, added modification of the signal from the stress-transducer ($E_0$) occurs in the form given by Equation 20 or 21. Thus it is necessary to combine Equations 13, 14, 21, and 22 as follows, to eliminate $E_0$, $E_2$, $s_i'$, and constant:

$$\text{constant} \times s_i = E_2 \tag{22}$$

$$= E_0 \times F_1F_2 \tag{21}$$

$$= \text{constant} \times s_i' \times F_1F_2 \tag{14}$$

$$= \text{constant} \times s_t(1 + F_3)F_1F_2 \tag{13}$$

or

$$s_i = s_t(1 + F_3)F_1F_2 \tag{23}$$

This is the complete overall approximate response equation and shows that the stress indicated on the oscilloscope $s_i$ is equal to the true stress $s_t$, with an added transient perturbation represented by $F_3$, multiplied by the effect of the amplifier bandwidth in the form of two functions, $F_1$ and $F_2$. Thus the ratio of the indicated stress to the true stress at any strain is $(1 + F_3)F_1F_2$. Alternatively, since $s_t = Me$ (Equation 4), Equation 23 may be rewritten as

$$s_i = Me(1 + F_3)F_1F_2 \tag{24}$$

which is the equation of the indicated stress–strain curve. Note that the strain $e$, as well as being explicit in Equation 24, is implicit in $F_1$, $F_2$, and $F_3$. Equation 24 can be compared to the equation of the true stress–strain curve given by Equation 4; i.e., $s_t = Me$. In Figure 7 the functions are expanded so that the complete equation is given, along with the two auxiliary equations defining $\beta$ and $\omega_r$.

Note that

$$\lim_{x \to 0} \frac{1}{x}(1 - \epsilon^{-x}) = 1$$

and

$$\lim_{x \to \infty} \frac{1}{x}(1 - \epsilon^{-x}) = 0$$

so that, if the low cut-off angular frequency $\omega_1 = 0$, $F_1 = 1$; if the high cut-off angular frequency $\omega_2 \to \infty$, $F_2 = 1$. In other words, an amplifier with a very wide pass band starting at 0 cycles/sec. has no effect on the response of the system. The influences of other variables are also evident. For example, the higher the resonance frequency of the stress-transducer $\omega_0$, the smaller the amplitude of the transient and the greater the number of oscillations to a given strain. The greater the damping constant $l$, the faster the oscillations are damped out; i.e., they disappear at a smaller strain. Also, the higher the rate of strain $R$, the greater the amplitude of the transient oscillations, the smaller their number to a given strain, and the slower their damping out. These effects will be investigated quantitatively below.

$$s_i = Me\left[1 + \left[\frac{R}{\omega_0 e}\epsilon^{-\frac{lt}{R}}\cos\left(\frac{\omega_0 e}{R} - \beta\right) - \frac{R}{\omega_r e}\right]\left[\frac{R}{\omega_1 e}\left(1 - \epsilon^{-\frac{\omega_1 e}{R}}\right)\right]\left[1 - \frac{R}{\omega_2 e}\left(1 - \epsilon^{-\frac{\omega_2 e}{R}}\right)\right]\right] \tag{25}$$

$$s_i = Me\left[1 + [F_3]\right][F_1][F_2]$$

$$\beta = \tan^{-1}\frac{1}{2}\left[\frac{l}{\omega_0} - \frac{\omega_0}{l}\right] \tag{26}$$

$$\omega_r = \frac{\omega_0^2 + l^2}{2l} \tag{27}$$

$$\omega_1 = 2\pi f_1 \qquad \omega_2 = 2\pi f_2$$

$$\omega_0 = 2\pi f_0$$

**Fig. 7.** Indicated stress–strain curve equation.

A feature of Equation 25 (Figure 7) is that the rate of strain over an angular frequency times the strain, or its inverse, consistently appears. Thus we have

$$\frac{R}{\omega_0 e} \quad \frac{R}{\omega_1 e} \quad \frac{R}{\omega_2 e} \quad \text{and} \quad \frac{R}{\omega_r e}$$

plus $\frac{R}{le}$, which has the same dimensions since $l$ is in units of sec.$^{-1}$, as is angular frequency. The frequencies $\omega_0$, $\omega_1$, and $\omega_2$ have been defined; $\omega_r$ can be shown to be the relaxation frequency of the stress-transducer $(G/\eta)$. Since $e/R = t$, these combinations represent the ratio of two times; i.e., they are of the form $\frac{1/\omega}{t}$ or $\frac{1/l}{t}$. The numerator in each case is a period characteristic of the stress-transducer or amplifier and the denominator is the time-scale of the test. Thus if a specimen breaks at a strain $e_b$ when being tested at a rate $R$, the time-scale of the breaking test is $e_b/R = t_b$. On the other hand, if the secant modulus of a nonlinear specimen is measured out to 3% strain, the time-scale of the secant modulus measurement is $0.03/R$. Thus a stress–strain curve at a constant rate of strain has a spectrum of time-scales covering the range 0 to $e_b/R$.

Now, as mentioned, combinations of variables such as $\frac{R}{\omega e}$ and $\frac{R}{le}$ are important since they determine the values of the functions $F_1$, $F_2$, and $F_3$ and therefore the response of the tester. Since $e$, the strain, is common to all these combinations and is the independent variable, let us consider the following ratios as characteristics of the system under study: $x_1 = \omega_1/R$, $x_2 = \omega_2/R$, $x_3 = \omega_0/R$, $x_4 = l/R$, and $x_5 = \omega_r/R$.

It is clear that these ratios control the response of the system, since their values determine the values of $F_1$, $F_2$, and $F_3$ at any given strain. Equations 25, 26, and 27 are rewritten in terms of these ratios in Figure 8, where this is more evident. It is seen that the response is invariant so long as $x_1$, $x_2$, $x_3$, and $x_4$ do not change. Thus an increase in rate can always be compensated for by a proportional increase in three frequencies and a damping constant.

*Examples of Response Characteristics*

Equation 25 or 28, if solved for a range of strains from 0 out to the break strain $e_b$ with appropriate values of $M$, $R$, $f_1$, $f_2$, $f_0$, and $l$ (Equation 25) or $M$, $x_1$, $x_2$, $x_3$, and $x_4$ (Equation 28), yields a theoretical or indicated stress–strain curve characteristic of a given tester and specimen. In order to show the effects of varying $x_1$, $x_2$, $x_3$, and $x_4$ on the indicated stress–strain curve, the solutions of Equations 28, 29, and 30 were programmed on a small scale digital computer[3] and various indicated stress–strain curves developed for comparison with a true curve. In all cases $s_i$ values for 50 strain points from 0.2% to 10% in steps of 0.2% were calculated and plotted. The machine computation and plotting took about 15 min. per set of 50 points. If $x_2 = \omega_2/R$ is less than $x_3 = \omega_0/R$, the transient $(1 + F_3)$ is automatically suppressed in computation, since to a first approximation it would not be passed by the amplifier. In order to show the separate effects of $F_1$, $F_2$, and $(1 + F_3)$ for low, medium, and high strain rates, two of the three factors are suppressed in any one case by substituting values of the appropriate variables which make the two factors essentially equal to unity. That is, to see the effect of $x_1$ or $F_1$ (the high-pass filter) at different rates, $F_2$ and $(1 + F_3)$ were made to equal unity. Three cases are considered in connection with each factor; i.e., values of the appropriate variable corresponding to low, medium, and high strain rates are substituted.

Consider first the effect of the low cut-off frequency on the final part of the stress–strain curve. To show up the effect of change of strain rate for a fixed low cut-off frequency $\omega_1$, three values of $x_1 = \omega_1/R$ were selected such that the deviations from the true stress–strain curve at 10% strain were about 4%, 21%, and 33%. Of course, these three values could also be interpreted as arising from a change in $\omega_1$ at a fixed strain rate. The

[3] Bendix G-15-D.

$$s_i = Me\left[1+\left[\frac{1}{x_2^2}e^{-x_4\theta}\cos(x_3\theta-\beta)-\frac{1}{x_2^2}\right]\right]\left[\frac{1}{x_1^2}(1-e^{-x_1\theta})\right]\left[1-\frac{1}{x_1^2}(1-e^{-x_1\theta})\right] \quad (28)$$

$$\beta = \tan^{-1}\frac{1}{2}\left[\frac{x_4}{x_3}-\frac{x_3}{x_4}\right] \quad (29)$$

$$x_5 = \frac{1}{2}\left[\frac{x_3^2+x_4^2}{x_4}\right] \quad (30)$$

$$x_1 = \omega_1/R \qquad x_2 = \omega_2/R$$
$$x_3 = \omega_0/R \qquad x_4 = \beta/R$$
$$x_5 = \omega_t/R$$

**Fig. 8.** Alternate form of the indicated stress–strain curve equation.

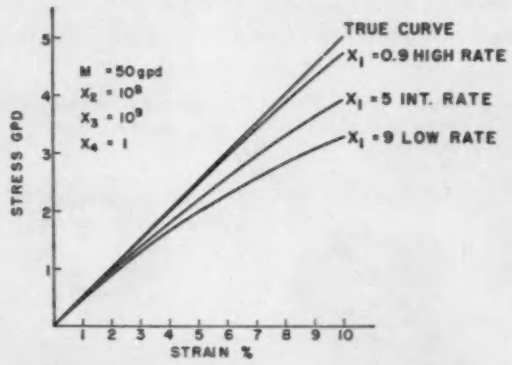


**Fig. 9.** Comparison of true and indicated stress–strain curves showing the effect of the high-pass filter (low frequency cut-off) on the indicated curve at three test rates.

computed stress–strain curves are shown for comparison with the true curve for a linear specimen having a modulus of 50 g./den. in Figure 9. The upper cut-off frequency and resonance frequency were assumed large compared to $R$ and their effects suppressed. The ratio $\omega_1/R = x_1$ was taken as 0.9, 5, and 9, which corresponds to going from a high to a low rate of strain. As shown in Figure 9, the longer it takes to complete the test, the more error is introduced if $\omega_1/R$ covers a range such that any error is introduced at all. The effect, when it occurs, is in the final part of the curve.

In Figure 10, on the other hand, is shown the effect of change of strain rate when $\omega_2/R = x_2$ covers a range where appreciable error is introduced by the low-pass filter. Again, the effect of the high-pass filter and transducer transient are suppressed by appropriate choice of $x_1$ and $x_3$. It is seen that, first of all, the effect is in the initial part of the curve (but persists to the final part) and secondly, that it becomes more serious as the strain rate is increased, i.e., as the time to do the test

becomes shorter. This increase in the effect also can be interpreted as occurring as a result of lowering $\omega_1$ at a fixed strain rate.

The effect of change of strain rate on the transient term is shown in Figures 11, 12, and 13. In this case, the effect of the amplifier is suppressed and both $x_3 = \omega_0/R$ and $x_4 = l/R$ are changed by the same factor; i.e., the transducer is assumed to have the same $\omega_0$ and $l$ at different rates. As the rate is increased from a relatively low value (Figure 11) to an intermediate value (Figure 12) to a relatively high value (Figure 13), the damped oscillation shows a decrease in the number of cycles, an increase in amplitude, and a decrease in damping. This behavior can be interpreted as a decrease in resonance frequency $\omega_0$ and damping constant $l$ of the transducer at a fixed strain rate.

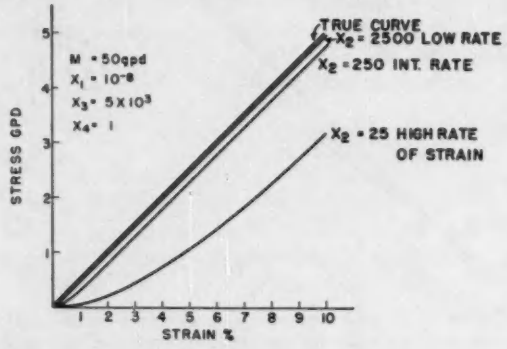


**Fig. 10.** Comparison of true and indicated stress–strain curves showing the effect of the low-pass filter (high frequency cut-off) on the indicated curve at three test rates.

Figure 14 shows all of these effects occurring at once in a very unfavorable case. All three effects are evident and the figure shows how badly an indicated stress–strain curve can deviate from the true stress–strain curve in the case where the resonance frequency is too low, the low cut-off frequency too high, and the high cut-off frequency too low relative to the strain rate of the test.

A summary of the effect of change of strain rate on the response of a given tensile tester of the kind considered is given below. The indicated stress–strain curve will show the following as the strain rate is increased:

a. The initial part of the curve will deviate more from the true.

b. The final part will deviate less, except for the persistence of effect a.

c. Any transient will increase in amplitude.

d. The transient will persist to greater strains.

e. The number of cycles of the transient apparent will be cut down.

In Figure 15 is plotted the value of $F_1$ vs. $\omega_1 e/R$ and the value of $F_2$ vs. $\omega_2 e/R$ on a log scale. It is seen that when $\omega_1 e/R = 0.02$, $F_1 = 0.99$, or a 1% error is introduced, and when $\omega_2 e/R = 100$, $F_2 = 0.99$; again a 1% error is introduced. Thus if we

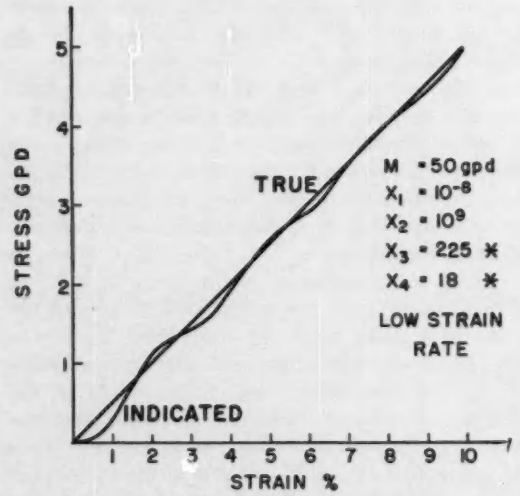


**Fig. 11.** Comparison of true and indicated stress–strain curves showing the effect of stress transducer characteristics on the indicated curve at a low test rate.

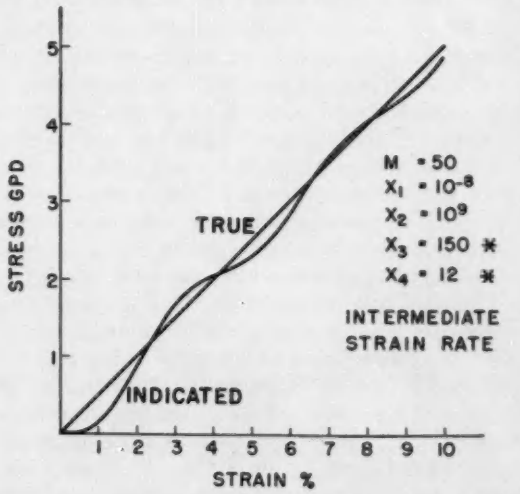


**Fig. 12.** Comparison of true and indicated stress–strain curves showing the effect of transducer characteristics on the indicated curve at an intermediate test rate.

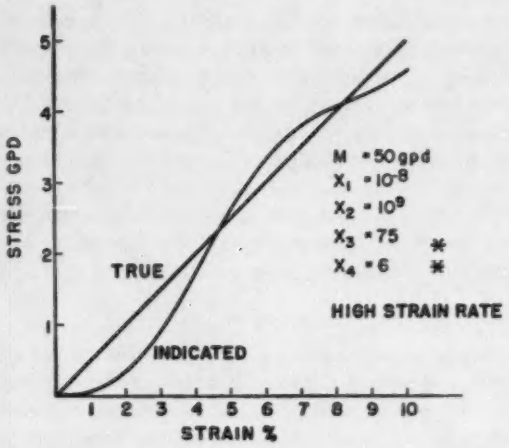


**Fig. 13.** Comparison of true and indicated stress–strain curves showing the effect of transducer characteristics on the indicated curve at a high test rate.

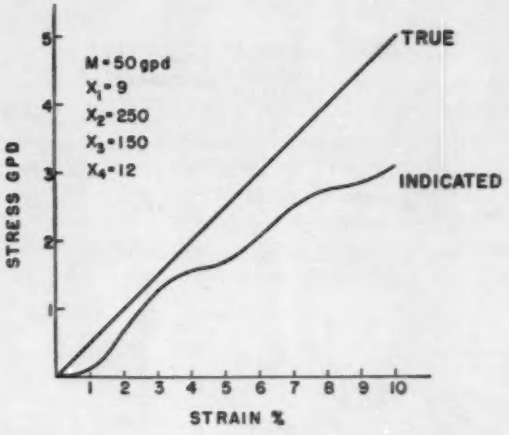


**Fig. 14.** Comparison of true and indicated stress–strain curves showing the combined effects of inadequate frequency response and transducer characteristics on the indicated curve.

wanted to keep the maximum error at 10% strain, due to the high-pass filter, equal to 1%, it would be necessary for the amplifier to have a lower cut-off angular frequency $\omega_1$ equal to $\frac{0.02\,R}{0.1} = 0.2\,R$. Because of the nature of the function $F_1$, the error would be smaller at smaller strains. However, if we wanted the maximum error at 1% strain, due to the low-pass filter, to be 1% also, it would be necessary for $\omega_2 e/R$ to be equal to 100 and therefore $\omega_2 = \frac{100\,R}{0.01} = 10^4\,R$. These considerations provide some rules of thumb for amplifier design.

The effect of the stress-transducer characteristics on the error introduced is more complex. It is noted, however, referring to Figure 7, that the amplitude of the transient term in $F_2$ is $\frac{R}{\omega_0 e}$. If this factor is 0.01, the maximum error which can ever be introduced in the indicated stress due to the transient is $\pm 1\%$ and may be less if damping is appreciable. However, $F_2$ has limits of $\pm 1$, as can easily be seen by expanding the cosine term for the zero damping case, so transient error is at most 100%. In addition, we note that $0 \leqslant F_1 \leqslant 1$, $0 \leqslant F_2 \leqslant 1$, and $0 \leqslant (1 + F_2) \leqslant 2$ as above, so that $0 \leqslant [(1 + F_2)F_1F_2] \leqslant 2$. This means that no matter how poorly a stress–strain tester is designed, the indicated stress can never be more than $\pm 100\%$ in error.

In regard to optimum tensile tester design, it is important to keep in mind that in studying the

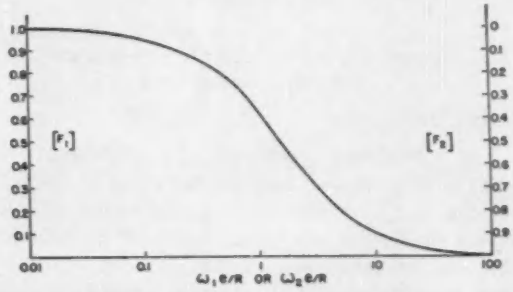


**Fig. 15.** Filter factors for determination of necessary amplifier frequency response.

behavior of a specimen, the time-scale of the test is the fundamental variable, as will be discussed in more detail below. The greater the range of time-scales available in testing, the greater will be the effect on behavior, at least up to a certain point. Thus, if a tensile tester is to have as short a time-scale of test as possible, it is of advantage to obtain it by making the strain rate $R$ high rather than the velocity $V$ with which the specimen end moves to minimize wave effects. This means keeping the gauge length $L$ as short as practicable, since $V = RL$. Practically, short gauge lengths have advantages as well as disadvantages. In general, higher specimen tenacities result because of reduction in the probability of flaws in the specimen. On the other hand, if there is appreciable slippage of the specimen in the clamp or appreciable motion of the clamp attached to the stress-transducer, the measured breaking strain will be greater than the true.

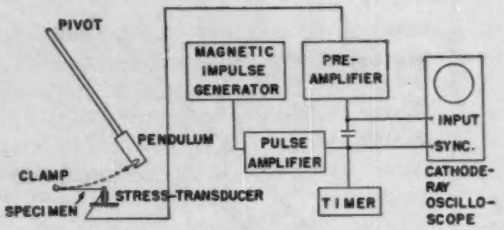


**Fig. 16.** Schematic representation of the high speed tensile tester.

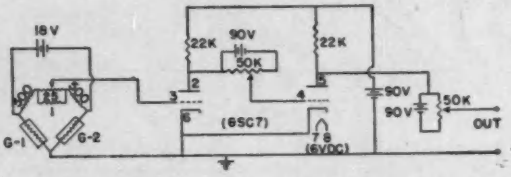


**Fig. 17.** Circuit diagram of the strain gauge bridge and preamplifier.

## Design of Tensile Tester to Operate at $10^5$%/Min. Strain Rate

*General Description*

Figure 16 shows a schematic of a pendulum type tester which has been built to operate at an impact velocity of 2.12 m./sec. and a gauge length of 5 in. This is equivalent to a strain rate of $10^5$ %/min. or 16.7 cm./cm./sec. The specimen to be tested is mounted with one end attached to a transducer and the opposite end attached to a clamp (referred to as the head clamp) which rests upon a support (support not illustrated) but is otherwise free to move. This clamp is picked up by a falling pendulum and moves with the velocity of the pendulum to strain the yarn. The stress–strain curve is obtained by connecting the amplified output signal of the transducer to the vertical deflection plates of an oscilloscope while at the same time applying a signal proportional to strain to the horizontal plates. Thus the stress–strain curve is displayed on the face of the oscilloscope and is recorded by means of a 35-mm. camera.

Pick-up of the head clamp by the pendulum without "bounce" is accomplished by making the clamp wedge-shaped to fit into a wedge-shaped recess in the pendulum so that the clamp and pendulum become firmly joined on impact. This is patterned after a method described by Parker [6] at a recent Fiber Society meeting. To make certain the clamp is firmly wedged to the pendulum before any measurable stress is applied to the specimen, the clamp is retarded to some extent by its support. Pick-up of the clamp by the pendulum results in some loss of velocity by the pendulum (about 2% in the present apparatus), but this loss occurs before the specimen is strained. The actual loss in mean velocity during the test as a result of energy required to break the yarn specimen is less than 1% and could be reduced further by increasing the pendulum mass.

*Characteristics and Operation*

The pendulum used has a length of approximately 24 in. and is counterbalanced to adjust the velocity. Pick-up of the clamp occurs at the point where velocity is a maximum, and since the velocity of a pendulum is constant to within 1% through an arc of 11 degrees to either side of this point, the pendulum used provides essentially a constant rate of elongation up to about 100% elongation (for a 5-in. specimen). Coupled with the loss in velocity as a result of energy used to break the specimen, this would be a total decrease in velocity of about 2%. However, most specimens break at less than 20% elongation, so that the total velocity change is nearer 1%.

Since the pendulum velocity is essentially constant, the internal sweep of the oscilloscope (which is linear) can be triggered to provide a deflection or trace proportional to strain. Synchronized triggering is accomplished by mounting a knife-edged fin on the pendulum so that it passes by a magnetic impulse generator[4] just prior to the instant the pendulum picks up the clamp. This provides a pulse which is amplified and used to trigger the oscilloscope. By using two such knife-edges separated by a known distance, two pulses are obtained which are fed to the vertical deflection plates of the oscilloscope and provide strain calibration marks. In the present apparatus the knife-edges are separated by 0.950 in., so that the distance between the two pulses corresponds to a strain of 19%. As these calibration marks occur as the test is run, strain calibration is accomplished automatically. If, however, the specimen breaks just before the second marker occurs, the marker is "lost" in the oscillations (transducer vibrating) which occur following specimen failure. In this case it is necessary to run a separate calibration trace (this could be avoided

[4] Electro Products Laboratories, Inc., Chicago, Illinois; Model 3010-A.

by using 3 markers instead of 2). At present when a separate calibration trace is run the pendulum is not slowed down by the presence of the clamp or specimen and, since the oscilloscope trace is linear with time, the spacing of the markers on the separate calibration trace corresponds to an elongation (on the test trace) of something less than 19%, the exact elongation being determined by dividing 19 by the ratio of the time between calibration pulses during the test to the time between these pulses during the calibration. These times are measured by means of an electronic counter (Berkeley Model 5510). Use of this counter also provides a check on the rate of elongation and provides an indication if the spacing of the calibration knife-edges is accidentally altered.

The transducer used for stress measurement consists of an aluminum alloy cantilever beam approximately 2.6 cm. long, 1.2 cm. wide, and 0.5 cm. thick with two SR-4 strain gauges (type C-5) bonded on opposite faces. These gauges form two arms of a Wheatstone bridge circuit (Figure 17), the output of which is proportional to the force applied to the beam. Resonant frequency of the transducer is 3280 cycles/sec. The output signal of the transducer is amplified by a DC preamplifier (Figure 17) and the vertical deflection amplifier (DC) of the oscilloscope (Du Mont Model 304-A). The preamplifier has a gain of approximately 200, is flat to 7 Kc. (down 3 db at 7 Kc.), and has a noise of only 2 $\mu$v. (referred to input). Long term drift of the DC amplifiers is fairly low; since the test duration is a matter of a few milliseconds, drift is not a problem. There is also a slight drift in gain with time, so that it is necessary to run a stress calibration at the conclusion of each test for maximum precision. This is accomplished by hanging a known weight on the transducer and photographing the oscilloscope trace with and without the weight applied. Overall sensitivity and signal-to-noise ratio is such that for essentially noiseless recording of the indicated stress–strain curve, the breaking force of the specimen should be a minimum of 1000 g.

A typical test result is shown in Figure 18 with the stress and strain calibrations indicated. Fig-

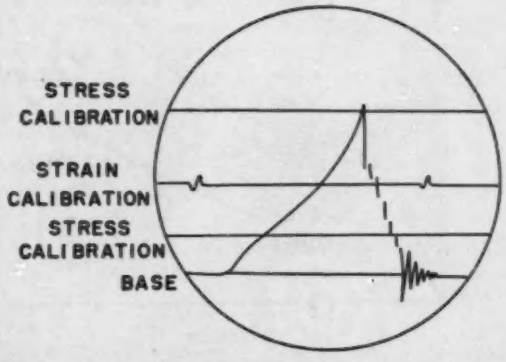


**Fig. 18.** Typical test result obtained with the high-speed tensile tester at a strain rate of 100,000%/min.

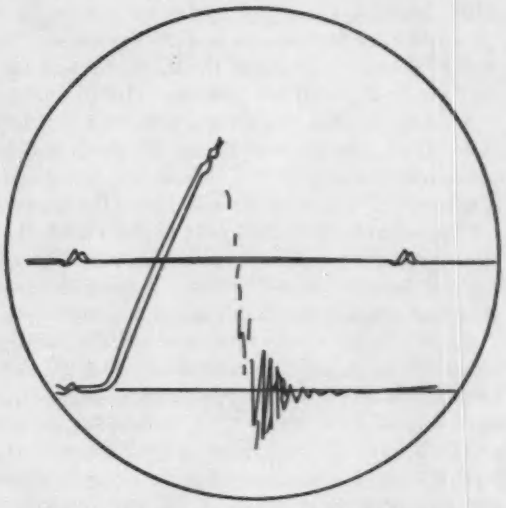

**Fig. 19.** Test results showing reproducibility on two successive tests. Rate = 100,000%/min.

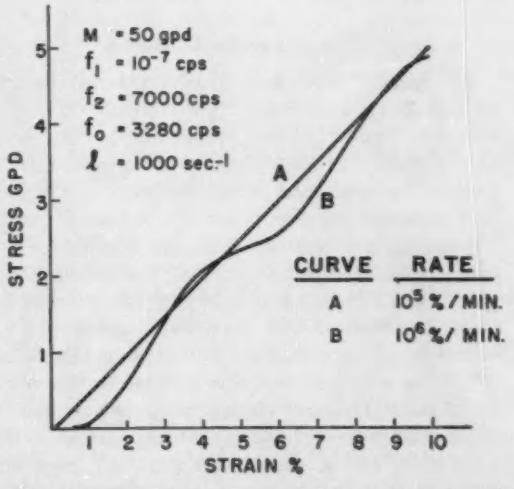


**Fig. 20.** Theoretical response of the high-speed tensile tester to a sample having a linear stress–strain curve. Response of the system is very good at a test rate of $10^5$%/min. but is inadequate for testing at a rate of $10^6$%/min.

ure 19 shows two separate tests recorded on the same negative to illustrate reproducibility.

*Theoretical Performance*

The characteristics of the tensile tester described above were substituted into the equation for indicated stress, which was solved for two high strain rates. In Figure 20 are shown the results when, in Case A, $M$ = 50 g./den., $R$ = 16.7 cm./cm./sec. ($10^5$ %/min.), $f_1 = 10^{-7}$ cycles/sec. (actually 0), $f_2$ = 7000 cycles/sec., $f_0$ = 3280 cycles/sec., and $l$ = 1000 sec.$^{-1}$. In Case B, $M$, $f_1$, $f_2$, $f_0$, $l$ are as in Case A; $R$ = 167 cm./cm./sec. ($10^6$ %/min.).

It is noted that the error introduced at $10^5$ %/min. strain rate is about 3% at 1% strain and progressively less out to 10%, where it is a fraction of a percent. This latter error is due to the factor $F_2$, which controls the initial part of the curve; if the upper cut-off frequency $f_2$ in the amplifier were higher, this error would be less. A small sinusoidal transient error is detectable below 1% strain.

At $10^6$ %/min. strain rate, however, the indicated stress curve is wholly unreliable. The $F_2$ factor error is greater; in addition, a large sinusoidal transient due to $F_3$ is present. This is a flag to work at $10^5$ %/min. at most with this particular tester. Notice that if a specimen known to be nonlinear and having a break strain of 3% were tested, the indicated curve might look very reasonable, when as a matter of fact it is grossly in error.

## Typical Results Obtained

In Figure 21 are shown three stress–strain curves at different strain rates characteristic of the behavior of Type 81 Orlon[5] acrylic fiber. The curves at 1%/min. and 100%/min. were obtained on an Instron Tensile Tester, while the one at $10^5$ %/min. was obtained on the pendulum tester described. These data were selected from the large number we have obtained on commercial and experimental yarns, since they show behavior characteristic of many textile materials—an increase in tenacity and modulus and a reduction in breaking elongation. While tenacity and modulus increase in the majority of cases, breaking elongation is just as likely to increase as decrease as strain rate is increased. The tests made at the three rates shown in Figure 21 were made with a common type of simple (non-snubbing) specimen clamp, at 5-in. gauge length and at 65% RH and 70° F. The curves given are averages of 8 specimen breaks.

To give some idea of the time scales involved, the times required to reach 5% strain are shown. One way to interpret the differences in stress at 5% strain is to associate them with differences in stress-relaxation. Thus in $3 \times 10^{-3}$ sec., the stress is high because there is little time for the stress to decay. On the other hand, in 300 sec. there is ample time for the stress to decay almost 2 g./den.

In Figure 22 are given some of the data calculated from the curves of Figure 21. Notice that the work-to-break or toughness (area under stress–strain curve) is almost 50% greater at the highest rate of testing compared to the lowest. Since break elongation may increase or decrease as strain-rate is increased, it is clear that work-to-break may also increase or decrease.

## Structural Basis of Fiber Response

Most synthetic and natural fibers are composed of aggregates of long chain molecules, more or less oriented and ordered, glass fibers being the notable exception. This type of structure results in a fiber's having a broad spectrum of relaxation times or characteristic times of response of its structure. The relaxation time can most simply be defined as the time it takes for a strained simple viscoelastic element showing recovery properties to recover, not to zero strain, but to $1/e$ of the original strain on release of the stress causing the strain. An alternative definition involves the time it takes the

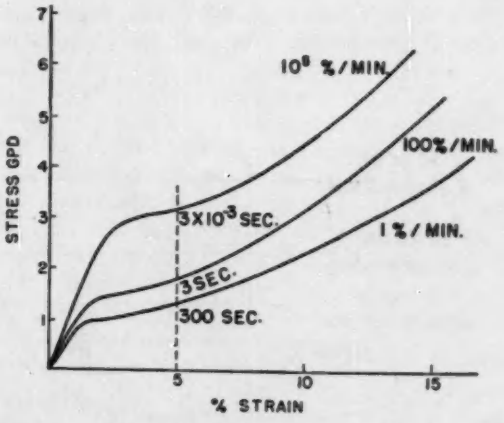


**Fig. 21.** Stress–strain behavior of Type 81 Orlon acrylic fiber at three test rates.

[5] Du Pont trademark.

stress to relax to $1/e$ of the original stress at fixed strain in a system exhibiting stress-decay.

In general there are two characteristics which determine relaxation time; the stiffness and the viscosity associated with response. These are pictured as an elastic spring and a viscous dashpot respectively. The spring alone has a zero relaxation time and the dashpot alone has an infinite one. There are, in principle, an infinite number of combinations of stiffness and viscosity values giving rise to correspondingly different relaxation times. Thus, in a structure such as we are considering, there is not just one but many relaxation times forming a spectrum. A perfectly elastic specimen has a zero relaxation time and thus no spectrum in the sense of a range. A simple viscoelastic system may have just one relaxation time and again no real spectrum. In discussing relaxation spectra, one way to represent them is to plot the distribution function $N(\tau)$ vs. $\tau$ or log $\tau$; i.e., plot the number of elements having a given relaxation time vs. that relaxation time and so on over the $\tau$ range of interest.

*Ideal Case*

Consider the relaxation spectrum shown in Figure 23, which is characterized by a sharply defined "box" distribution. Let us further assume that this distribution remains invariant when the specimen of which it is characteristic is strained. Note that there are, to a first approximation, two regions; an essentially elastic region with zero relaxation time and a viscoelastic region. What this means in terms of specimen response when a stress–strain curve is run is simply this: so long as the time it takes to run the test is much shorter than $\tau_1$, the stress–strain curve will be essentially linear and elastic; as it approaches $\tau_1$, there will probably be some concave downward character to the curve, since stress-decay will take place, and the behavior will be nonlinear and viscoelastic. Thus, in general a decrease in strain rate means a longer time-scale, more elements relax in the time of the test, and therefore a lower stress and average modulus result. Notice that it is the time-scale of the test that is important here, not the rate *per se* but only in combination with the strain, since

$$t = e/R$$

Thus, with reference to Figure 23, if the specimen breaks at a strain $e_b$ and it is strained at a rate $R$

| RATE | TENACITY | BREAKING ELONGATION | MODULUS | WORK TO BREAK |
|---|---|---|---|---|
| 1%/MIN. | 4.2 GPD | 16.5% | 90 GPD | 0.35 GPD |
| 100%/MIN. | 5.5 GPD | 15.5% | 110 GPD | 0.42 GPD |
| $10^5$%/MIN. | 6.3 GPD | 14.3% | 141 GPD | 0.52 GPD |

ALL DATA ± 5%
CONDITIONS 70°F - 65% R.H.
5" GAGE LENGTH
MULTIFILAMENT YARN
NON-SNUBBING JAWS

**Fig. 22.** Tensile properties of Type 81 Orlon acrylic fiber at three test rates.

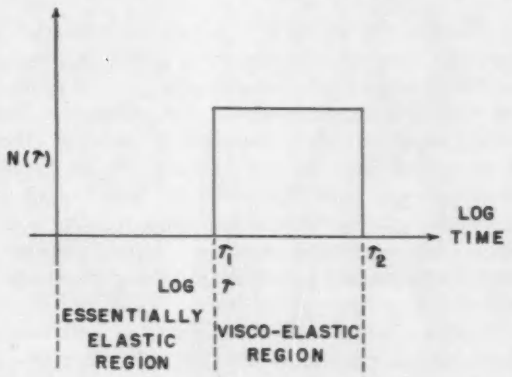


**Fig. 23.** Ideal relaxation time spectrum.

such that the time to break $t$ is greater than $\tau_1$, the specimen will generally show a nonlinear curve. If, by increasing the strain rate, the strain $e_b$ is reached in a time considerably less than $\tau_1$, the same specimen will show a linear curve and a higher modulus. When the range of time-scales is such that it encompasses a relaxation time or band, rate sensitivity of stress at a given strain or average modulus will be evident.

*Real Fibers*

Needless to say, the relaxation spectra of real fibers are not simple box-type distributions. In addition, the distribution will change with strain as a result of molecular orientation. Nevertheless, the simple principles elucidated above can be applied qualitatively to real fibers. It is difficult to see how any real fiber response can be truly elastic, since the distribution should have a very broad range; for example, as sketched in Figure 24. It is perfectly possible for a linear viscoelastic response to occur, however; all this means is that the distri-

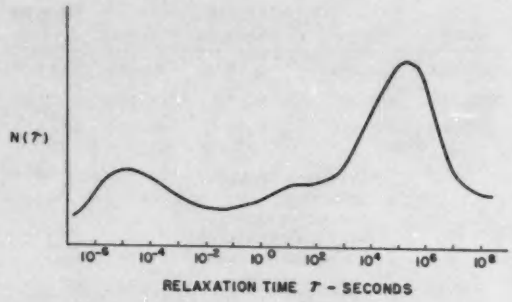


**Fig. 24.** A hypothetical "real" relaxation time spectrum.

bution function is such that the percent stress-decay remains constant over the whole curve as a result of the time-scale selected and perhaps of the effect of molecular orientation on the distribution. The virtue of the simple picture given is that it gives a structural "feel" to the interpretation of stress–strain curves. All that must be remembered is that, for a given relaxation spectrum, the time-scale determines the character of the specimen response, and the time-scale, in a constant rate-of-strain case, is $t = e/R$.

It should also be remembered that it is the time-scale which determines the response of a given testing apparatus in the absence of wave-effects. That is, terms such as $\frac{R}{\omega e}$ or $\frac{R}{le}$ govern the response; since $\omega$ and $l$ are characteristic of a given tester, it is $e/R$ or $t$ which is the important variable in a specific situation.

**Acknowledgment**

The authors wish to acknowledge the assistance of Mr. J. E. Owens in the designing of the electronic circuits used in the high-speed tensile tester.

**Literature Cited**

1. Ayers, Frank, Jr., "Theory and Problems of Differential Equations," New York, Schaum Pub. Co., Chap. 16 (1952).
2. *J. Research Nat. Bur. Standards* (a) **54**, 269–276 (May 1955); (b) **54**, 276–280 (May 1955); (c) **55**, 19–28 (July 1955); (d) **57**, 83–89 (August 1956).
3. *J. Research Nat. Bur. Standards* **55**, 24 (July 1955).
4. Meredith, R., "The Effect of Rate of Extension on the Tensile Behavior of Viscose and Acetate Rayons, Silk and Nylon," *Shirley Inst. Mem.* **26**, 247–260 (November 1953).
5. Page, Leigh, "Introduction to Theoretical Physics," 2nd Ed., New York, Van Nostrand, 74 ff. (1935).
6. Parker, J. P. and Kemic, C. S., "Energy Absorption in Tire Cord During Impact Breaks," Fiber Society Meeting, New York City, September 6–7, 1956.

*Manuscript received October 29, 1957.*

# The Polarographic Estimation of Sulfydryl and Disulfide Groups in Wool

**J. P. E. Human**

*Biochemistry Unit, Wool Textile Research Laboratories, C. S. I. R. O., Parkville, N.2. (Melbourne) Victoria, Australia*

**Abstract**

Methods for determining sulfydryl sulfur only and sulfydryl plus disulfide sulfur in intact wool are described. In the first case, the wool is allowed to react with an excess of an organic mercurial in a buffer containing urea at pH 7–8.5, while in the second case sulfite as well as urea is present in a buffer at pH 8.5. In both, the excess mercurial is determined polarographically.

Two existing methods for the polarographic determination of sulfydryl plus disulfide sulfur in protein hydrolysates, namely amperometric titration with mercuric chloride and the use of the catalytic wave produced by cysteine and cystine in the presence of cobalt ions, have been adapted for the special case of wool, to cope with 10–100 mg. samples and 0.05–0.10 mg. samples, respectively.

An indication of the reliability of the nonhydrolytic methods is also given.

## Introduction

The chemical and physical properties of wool and changes in these properties very often may be correlated with the sulfur content, and it is important to have accurate and reliable methods for the analysis of the sulfur in its two most important forms of combination—sulfhydryl and disulfide sulfur.

Until the recent work of Burley [5] and Burley and Horden [6] on intact wool, demonstrating the presence of about 22–30 μmoles of sulfhydryl sulfur/g. of dry fiber, little significance was attached to the small amounts of sulfhydryl sulfur shown to be present by the usual colorimetric methods (e.g., modified Folin method [16]) because of the rather vigorous conditions required for the preliminary hydrolysis.

In the present paper, another method for estimating the sulfhydryl groups of intact wool is described, which confirms Burley's findings that free sulfhydryl groups are indeed present, but which favors the higher value—i.e., about 30 μmoles/g. of dry wool. The method consists in treating the wool with organic mercurials of the type RHgCl and estimating the excess mercurial by polarography.

Most of the sulfur in normal untreated wool occurs as combined cystine, and the sulfur content is usually expressed as "% cystine" on the dry weight of wool. Since, however, cystine is usually estimated after conversion to cysteine, the result obtained is a measure of cystine + cysteine, but for most purposes this is sufficient.

All methods of determination of cystine in wool hydrolysates are open to some uncertainty, as in the case of cysteine determinations, due to possible destruction of the amino acid in question during hydrolysis. For this reason, it was of interest to devise a method for the determination of cystine, as well as cysteine, in intact wool and to compare the results with those obtained by hydrolysis and amperometric titration. Such a method is outlined and the results are discussed.

For the routine estimation of cystine in wool, where samples of 100 mg. are available, Leach [15] adapted the method of Stricks, Kolthoff, and Tanaka [17], which was developed for other peptides and proteins. In Leach's procedure, the cystine content of a wool hydrolysate is estimated by amperometric titration with mercuric chloride in the presence of sulfite. The apparatus has been described previously [12]; the method is given in detail below. A further modification of the same method enables one to use 10 mg. of material.

For quantities of wool 100–200 times smaller than this—that is, weighing about 0.1–0.05 mg. and corresponding to a single fiber of Merino wool or to short lengths of coarser wool fibers, a method of

much greater sensitivity is required. It has been found that, by suitable modification, the method of Brdička [3, 13], using the catalytic wave produced by cystine (and cysteine) in ammoniacal solutions of cobaltous chloride, can be used in these cases. The method, however, yields results which are consistently low and is therefore of more use for comparative studies.

## Materials

All reagents were of "Polaritan" quality (Hopkins and Williams) where possible; otherwise they were of analytical reagent quality.

*p*-Chloromercuribenzoic acid (*p*-CMB) was kindly prepared and purified by Mr. I. W. Stapleton in this laboratory. Neohydrin ($Cl \cdot Hg \cdot CH_2 \cdot CH(OMe) \cdot CH_2 \cdot NH \cdot CO \cdot NH_2$) was a gift from Lakeside Laboratories Inc., Wisconsin. (The above two mercurials were analyzed for mercury and found to be 99.9% pure or better.) All water was twice distilled, finally from glass. The nitrogen was oxygen-free and was saturated with water before being passed through the test solutions. The chloroform was successively treated with sulfuric acid, water, caustic soda solution, and water, and finally dried and distilled, the foreruns being rejected. It was stored in dark glass bottles for not more than 2 or 3 weeks before use.

Kolthoff's phosphate-borate buffers were made according to Britton [4a]. Britton-Robinson buffers [4b] were made up from a solution which was 0.1 *M* in acetic, boric, and phosphoric acids (Benesch and Benesch [2]). Sufficient 0.4 *M* NaOH was added so that the pH had the value required when the solution was diluted to twice the original volume. This solution is subsequently referred to as the "concentrated buffer." In addition, all solutions for polarography were made up in 0.1 *M* KCl.

The wool used, unless otherwise stated, was a standard Merino 64's of known moisture content and containing 3.36% total sulfur; it was solvent degreased before use.

## Apparatus

A Tinsley Model 15 5 recording polarograph was used, modified to take the type of cell described by Human and Leach [12]. In addition to two cells of this type having capacities of 10 and 20 ml., another cell was designed for following the uptake of mercurial reagents by samples of intact wool (Figure 1). It consisted of two sections—a "reaction chamber," A, and a modified form of the polarographic cell described previously [12], B. These two sections were connected at the base via a coarse sintered disk, C, and a tap, D, and at the top via a tap, E. The wool was placed in A together with the reagent in a suitable buffer, with tap D closed. From time to time the concentration of the reagent could be determined polarographically by opening D, closing E, and introducing nitrogen under slight pressure through F. When sufficient liquid had been transferred to B, tap D was closed and tap E opened, thus allowing the nitrogen to pass over the surface of the liquid in B and escape via G. After the polarogram had been run, the solution in B could be returned without loss to A by closing E, opening D, and introducing nitrogen through G. The mercury which collects from the dropping mercury electrode falls to the bottom of the trap H. It is convenient to have G and F connected to a reversing tap system which can be arranged to supply nitrogen to F and vent G to the atmosphere, or vice versa.

## Methods

### *The Determination of Sulfhydryl Sulfur in Intact Wool*

It is well known that mercuric chloride reacts with the —SH in intact wool (see, for example, Burley [5], p. 335); however, when an approximately twofold excess of this reagent in buffers of pH 8 or 9 was added to a sample of wool, the reaction, followed over a period of days in the apparatus shown in Figure 1, was not limited to —SH only, for mercuric ions continued to be removed slowly from the solution after the 30 μmoles/g. stage. This shows that reaction with other sites, presumably —S—S—, also occurred.

When a lower pH (2–3) was employed to avoid this reaction, following the recommendation of Cecil [7], who was thereby able to reduce the reaction of —S—S— with silver ions, mercuric ions apparently were removed from the solution by the free mercury from the dropping mercury electrode to give a scum, probably HgCl, on the mercury surface. The use of chloride-free solutions with acetate buffers was abandoned, as the mercuric acetate solutions appeared to be unstable, yielding minute red crystals on the walls of the storage vessel. It seemed therefore that while mercuric ions undoubtedly react with the —SH groups in wool, they cannot be used conveniently to determine these groups quantitatively.

It has been shown recently by Hata [10] that, under certain conditions, *p*-CMB can be determined in the polarograph, enabling its reaction with —SH groups in solution to be followed. Benesch and Benesch [2] have also characterized a number of organic mercurials in the polarograph and have examined the reaction of some of these with thiols [1]. However, the reaction of *p*-CMB with intact wool in buffers from pH 7 to 9 (Hata [10]) was too slow to be followed until urea was introduced to swell the fibers. After it had been shown that the height of the first reduction wave of *p*-CMB increased linearly with concentration in Kolthoff's pH 7 buffer which had been made approximately 8 *M* in urea, a sample of wool was placed in A (Figure 1) with a solution of *p*-CMB and urea in this buffer. The concentration of the *p*-CMB was determined initially and at intervals up to 220 hr. after thorough outgassing of the solution with nitrogen by measuring the height of the wave between 0.0 V. and −1.0 V.[1] It can be seen (Figure 2) that the concentration of *p*-CMB fell rapidly over a period of 48 hr., then more slowly until after 180 hr. it had reached a value which remained constant for a further 40 hr. A check on a solution of the same composition, but without the wool, showed that the concentration of the *p*-CMB, as measured by the polarograph, remained substantially constant over a period of 300 hr.; thus, the decrease observed in the previous experiment represented the reaction of the *p*-CMB with the wool. This value corresponded to a reaction with —SH groups to the extent of about 30 μmoles/g. of wool.

This result was confirmed by the use of neohydrin which, in the polarograph, behaved very like mercurials examined by Benesch and Benesch [2]. In solutions of pH 4, it showed one wave only ($E_{\frac{1}{4}} = -0.36$ V), while with increasing pH, the wave progressively split until at pH 9 it showed two distinct waves, $(E_{\frac{1}{4}})_1 = -0.40$ V and $(E_{\frac{1}{4}})_2 = -1.02$ V. The single wave formed at pH 4 had a very large maximum spread over the range of about −0.4 V to −1.0 V, but this could be completely suppressed with gelatin (0.01%). In the alkaline region of two waves, no maximum was observed; the first wave was clearly defined and increased linearly with concentration over the range used, $0.8\text{–}4.0 \times 10^{-4}$ *M*.

The ability of the neohydrin to react with —SH groups was checked using solutions of cysteine and of human and bovine serum albumin. In each case the concentration was first determined by amperometric titration with $10^{-3}$ *M* mercuric chloride at the rotated platinum electrode (Kolthoff, Stricks, and Morren [14]) and then by titration with neohydrin ($4 \times 10^{-3}$ *M* by weight; i.e., assuming 100% purity).

The procedure for cysteine was to take concentrated pH 8.5 buffer (10 ml.), neohydrin (0.6 ml.), 0.1 *M* NaOH (0.3 ml.), and make up to 20 ml. with water. After the solution had been outgassed, cys-

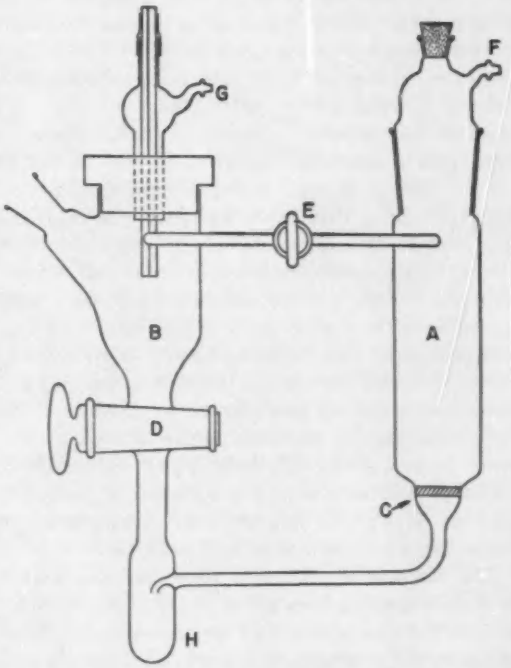


**Fig. 1.** Polarographic cell for following the uptake of organic mercurials by intact wool.

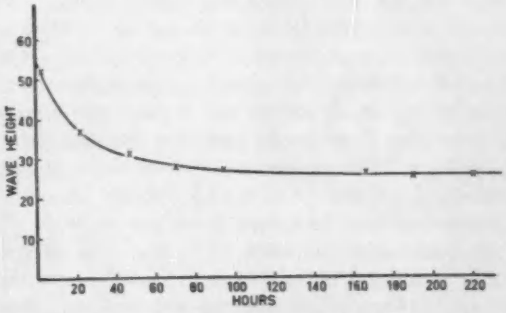


**Fig. 2.** Reaction of *p*-CMB with wool, as measured by the height of the polarographic wave.

[1] All voltages are expressed versus the Standard Calomel Electrode.

teine hydrochloride in 0.1 $N$ HCl (0.3 ml.) was added and the solution mixed. A polarogram was run on the solution and after each of four or five additions of neohydrin (0.1 ml. each). The wave heights were plotted against the total volume of neohydrin added and the straight line extrapolated to zero wave height. There was some scatter in the final values, but ten determinations gave the concentration of neohydrin as $4.05 \pm 0.25 \times 10^{-3}$ $M$. The bovine serum albumin was Armour's batch P67403 with an —SH content of 0.78 $M$/molecular wt. of 69,000. The human serum albumin was a partially purified sample from the Commonwealth Serum Laboratories, having an —SH content of approximately 0.2–0.3 $M$/molecular wt. of 69,000.

In the case of serum albumin, a solution was made such that 2 ml. was equivalent to 0.8–1.0 ml. of $10^{-3}$ $M$ $HgCl_2$. It was found that in the usual pH 8.5 buffer the neohydrin wave was poorly defined; use was therefore made of the single wave at pH 4, which, under these conditions, is quite well defined. Portions of the protein solutions (10 ml.) were mixed with the concentrated pH 4 buffer (10 ml.) and neohydrin (1.0 ml.) was added. Two drops of *sec*-octyl alcohol were added to suppress foaming and the whole outgassed and allowed to stand for 1 hr. A polarogram was then run on the solution at slow speed (6 min. 40 sec./V) between 0.0 and −0.08 V, and after each of four or five additions of neohydrin (0.1 ml. each). In this way, the concentration of neohydrin was shown to be $4.02 \times 10^{-3}$ $M$.

The reaction of neohydrin with wool was studied in buffers ranging from pH 4 to pH 10.5. In pH 4 buffers, the concentration of the mercurial, as determined in the polarograph, falls off, until after 9 days it has a value of about 90% of the original. With buffers of pH 5 and 6, the shape of the wave is not very suitable for quantitative determinations, although values from 26 to 30 μmoles of —SH/g. of wool were obtained for pH 6 buffers. Above pH 6, solutions of neohydrin appear to be stable for at least 15 days. At pH 10 and higher, the reaction fails to come to a definite endpoint, due again, presumably, to further reaction with —S—S— groups. Buffers of pH from 7 to 8.5 were finally chosen as suitable and have been used as set out below.

*Recommended procedure.* To the concentrated buffer is added ½ of its volume of water, urea (8 g. for every 15 ml. of the resulting solution), and gelatin to make a 0.005% solution. Wool samples (equivalent to 100 mg. dry) are placed in 50-ml. conical flasks equipped with spring-loaded ground glass stoppers. Aliquots (about 22.5 ml.) of the urea-buffer mixture are introduced into the flasks from a dispenser such as that described by Human [11], and neohydrin (or *p*-CMB) ($4 \times 10^{-3}$ $M$, 1.5 ml.) added. The stoppers are greased, the springs fitted, and the flasks and contents placed on a shaker of the type used in microbiological work. After the flasks have been gently shaken for 10–12 days, the contents are transferred to a cell and two or three polarograms of each solution are run in the usual way. A flask containing all the reagents except the wool is treated in the same manner and is used to obtain the wave height given by the reagent in the absence of the wool. This "blank" solution should give a polarogram identical with that of a similar solution made up freshly. From the difference between the average heights of the polarograms of the blank and the polarograms of the solutions containing the wool, the amount of reagent consumed by the various weights of wool can be calculated.

### *The Determination of Sulfhydryl plus Disulfide Sulfur (% Cystine) in Intact Wool*

The observation that organic mercurials will react with sulfhydryl groups in intact wool and that under certain conditions this reaction tends to proceed past the expected endpoint for sulfhydryl only, coupled with the finding of Gross and Egan [8] that the —S—S— bonds of chymotrypsin are completely reduced in the presence of potassium sulfite, 6 $M$ urea, and excess *p*-CMB, suggested that these reagents might induce the —S—S— bonds as well as the —SH bonds of wool to react.

The polarographic behavior of *p*-CMB in pH 8.5–9.0 buffers and in the presence of 8 $M$ urea and 0.25 $M$ $Na_2SO_3$ was first examined. The first reduction wave was still well defined under these conditions, and its height increased linearly with concentration over the range 0.8 to $4.8 \times 10^{-4}$ $M$. Trial runs with a two-fold excess of reagent to the expected cystine content of the wool showed that about 7 days was required to approach a steady state, the wool becoming gelatinous in the process. However, the consumption of *p*-CMB corresponded to a cystine content which was impossibly high. A check on the keeping quality of the reagent alone over this period showed an apparent decrease in concentration of the *p*-CMB of about 15%, which is not satisfactory for this type of experiment.

Neohydrin, in the presence of urea and sulfite and at the same pH, with 0.005% gelatin added, gave a well-defined first reduction wave ($E_{\frac{1}{4}} = -0.57$ V), the height of which, however, did not increase linearly with concentration above $2.5 \times 10^{-4}$ *M*, although below this concentration good linearity was found. Further, the solution of neohydrin, urea, sulfite, and gelatin at about pH 9 remained substantially unaltered in its behavior in the polarograph over a period of 15 days, especially if undue exposure to air and light were avoided.

Preliminary runs in the cell in Figure 1 showed that the time to reach a steady concentration of neohydrin was about 7 days and that the amount of neohydrin consumed corresponded to a cystine value slightly higher than that obtained using the 100-mg. sample method described for wool hydrolysates.

*Recommended procedure.* To the concentrated buffer (pH 8.5) is added ½ of its volume of water; urea and powdered $Na_2SO_3 \cdot 7H_2O$ (8 g. and 1.6 g., respectively, for every 15 ml. of diluted buffer) and gelatin, dissolved in a minimum of water to make a final 0.005% solution, are added. Wool samples (equivalent to 6.5–8.5 mg. dry) are weighed on a torsion balance in a conditioned atmosphere and placed in 50-ml. conical flasks fitted with spring-loaded ground glass stoppers. Aliquots (about 22.5 ml.) of the urea-sulfite-buffer mixture are dispensed as before into the flasks and neohydrin ($4 \times 10^{-3}$ *M*, 1.5 ml.) added. The stoppers are greased, the springs fitted, and the contents of the flasks gently agitated for 8–9 days. After this time, the contents are transferred to the cell and two or three polarograms of each solution run between −0.2 V and −0.9 V, using the slow rate of decrease of potential across the cell. As before, a flask containing all the reagents except the wool is used as a blank; the height of the neohydrin wave of this blank should not differ by more than 2% from that of a similar solution made up freshly. From the difference between the average heights of the polarograms of the blank and of the solutions containing the wool, the amount of reagent consumed by the various weights of wool can be calculated.

### *The Determination of Sulfhydryl plus Disulfide Sulfur (% Cystine) in Wool Hydrolysates*

*Recommended procedure (using 100-mg. samples*[2]). The sample is placed in a 25-ml. test tube provided with a ground glass stopper which can be held down with springs. Concentrated HCl (11.5 *N*, 1.0 ml.) and 98–100% formic acid (1.0 ml.) are introduced into the tube, the stopper well greased with silicone grease, and the springs fitted. The tube is immersed to about one-half its depth in an oil bath at 110 ± 0.5° C. For the first few minutes, excess pressure in the tube may lift the stopper, but after this a steady pressure inside is maintained.

After 5 hr., the contents are allowed to cool, the pH brought to about 5.5 (B.D.H. Universal Indicator) with 2.5 *N* NaOH and made up to 25 ml. A freshly made solution (15 ml.) containing sodium borate (25.4 g./l.), $Na_2SO_3 \cdot 7H_2O$ (67.4 g./l.) and KCl (49.7 g./l.) is placed in the cell, together with $CHCl_3$ (1.5 ml.). The dropping mercury electrode and KCl bridge are introduced, a small stopper is placed at E in the side arm (Figure 1, [12]) and nitrogen passed through the cell. The waste nitrogen is further passed through the neutralized hydrolysate. After 15 min., the stopper is removed and 5 ml. of the hydrolysate is introduced into the cell and mixed thoroughly. With the least possible delay, a slight excess of $10^{-2}$ *M* $HgCl_2$ solution is run in from a burette, and the diffusion current at −0.35 V is noted. Three successive additions of 0.15 ml. of reagent are made, and the diffusion current after each addition is recorded. The residual current of the borate buffer is determined separately.

A plot of the diffusion current, corrected for volume increase, against the volume of $HgCl_2$ added enables the amount of cystine in the aliquot, and hence in the original sample, to be calculated [17].

*Recommended procedure (using 10-mg. samples).* The above method may be modified as follows. The wool sample is weighed on a 10-mg. torsion balance in a constant temperature and humidity room and placed in the ground glass test tube as before. Concentrated HCl and 98–100% formic acid (0.4 ml. each) are introduced; the stopper is greased and held down with springs. After 4 hr. at 110 ± 0.5° C. in an oil bath, the tube is removed and the hydrolysate freeze-dried to a brown oil. This is taken up in 10 ml. of a solution containing sodium borate (29.4 g./l.) and KCl (57.6 g./l.). A sample (7.8 ml.) of this solution is transferred to a 10-ml. cell [12] containing $CHCl_3$ (1 ml.) and outgassed for 15 min. Sodium sulfite (2 *M*, 1.2 ml.) is added and the solutions mixed. A slight excess of $HgCl_2$ ($5 \times 10^{-3}$ *M*) is run in quickly from the burette and the titration and calculation carried out as before.

[2] Adaptation of the method of Stricks, Kolthoff, and Tanaka [17] by Dr. S. J. Leach [15].

*Recommended procedure (using 0.05–0.10-mg. samples).* The sample, if a Merino fiber, may be suspended directly from the hook of a 1-mg. torsion balance and weighed in a constant temperature and humidity room. If the fiber is a short length of a coarser fiber, it may be necessary to tie it into an open knot to enable it to be hung from the balance hook.

The fiber is transferred to the bottom of a 20-ml. test tube having a male standard taper joint: concentrated HCl and 98–100% formic acid (0.2 ml. each) are added, the joint greased at the bottom, and the tube closed with a cap carrying a small cold finger condenser (Figure 3) which can be held down with springs.

**Fig. 3.** Tube for hydrolysis of single fibers.

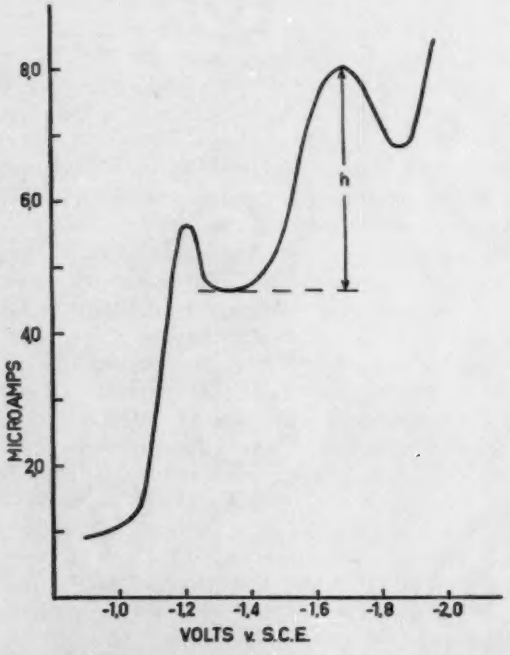


**Fig. 4.** Polarographic wave given by a wool hydrolysate in the presence of $CoCl_2$.

The hydrolysis is carried out in an oil bath at $110 \pm 0.5°$ C., with occasional gentle shaking of the tube and inspection to see that no part of the fiber is left adhering to the walls. The cold finger condenser prevents condensation of the hydrolysis acids in the upper parts of the tube.

After 4.5 hr. the tube is removed; the contents are freeze-dried and transferred to a 20-ml. cell with 4 portions, each of 5 ml., of a solution which is 0.1 *N* with respect to $NH_4OH$ and $NH_4Cl$ and which contains 0.005% gelatin. A dispenser [11] is convenient for this operation.

The solution in the cell is then outgassed with nitrogen (Kolthoff and Lingane, *loc. cit.*) which has been previously washed with a fresh solution of 0.1 *N* $NH_4OH$. A solution of $CoCl_2$ ($2 \times 10^{-2}$ *M*, 1.0 ml.) is next added through the side arm of the cell and thoroughly mixed with the solution. A polarogram is then run on the solution between $-0.8$ and $-2.0$ V. The height of the maximum *h* (Figure 4) is a measure of the cystine content.

To obtain an absolute value for the cystine content, it is necessary to construct a calibration curve, preferably from a hydrolysate of a larger sample of the same fiber. This should automatically allow for any reduction in the height of the maximum due to interfering substances in the hydrolysate (Kolthoff and Lingane, *loc. cit.*, 855). The comparison is conveniently made by hydrolyzing 100 mg. of the fiber according to the method above. The hydrolysate is then made up to 10 ml. (Solution A). From this, 4 ml. is taken, neutralized, and made up to 10 ml. (Solution B). This has the same composition as if the whole hydrolysate has been neutralized and made up to 25 ml. in the usual way. Solution B (5 ml.) is titrated amperometrically, and the cystine content of solution A is calculated.

Solution A (1 ml.) is now diluted to 250 ml. (Solution C) and successive quantities of 0.2, 0.4, 0.6, 0.8, 1.0, and 1.2 ml. (or more if necessary) are measured out into tubes, freeze-dried, and treated as for single fiber hydrolysates. A plot of the heights of the maxima against the amounts of cystine known to be present will be found to yield a straight line (Figure 5). The amount of cystine in an unknown

sample can be read from this graph. The calibration and the determinations should be carried out using the same fresh solutions of reagents.

## Discussion of Results from the Recommended Procedures

### *The Determination of Sulfhydryl Sulfur in Intact Wool*

*Merino wool (pH 7 buffer).* The mean cysteine content of the intact wool was found to be 0.37% (31 μmoles/g.), with a standard error of 0.007. The variance of determinations made between runs was not significantly greater than within runs; *viz.*, $S_B^2 = 0.000745$, $S_W^2 = 0.000666$, $S_W = 0.026$, and the the coefficient of variation was 7%.

*Merino wool (pH 8.5 buffer).* The mean cysteine content was found to be 0.39% (32 μmoles/g.), with a standard error of 0.024. The variance within runs was $S_W^2 = 0.000171$, although the between run variance component was $S_B^2 = 0.001699$. The coefficient of variation within runs was 3.3%.

*Woolen fabrics after various treatments (pH 8.5 buffer).* Three determinations were made in three runs on each of five fabrics, representing (a) a control, (b) and (c) two levels of treatment with $H_2O_2$, (d) and (e) two levels of treatment with alcoholic KOH. Analysis of the data showed that the variance between determinations within a run was $S_W^2 = 0.000142$, $S_W = 0.012$, while the component of variance between runs was $S_B^2 = 0.000290$, $S_B = 0.017$. The first of these variance estimates provided an upper limit for the variance of the method, as it included a component due to the sampling variance within the fabrics. As the variance $S_B^2$ is significantly greater than zero (as also in the intact wool at pH 8.5), the method is more precise for comparisons made within runs than for those made between runs. The coefficient of variation within runs was 3.6% and the —SH content of the untreated fabric was 0.32% (26.5 μmoles/g.).

The value of the —SH content of the intact Merino wool used may be less than the figures given, namely 31–32 μmoles/g., as there is evidence that up to 5 μmoles of the mercurial may be held by absorption to each gram of wool. This is indicated by the fact that wool samples, after treatment by this method followed by thorough washing, may, on retreatment, show an uptake of from 4 to 6 μmoles of neohydrin after the usual time. Burley and Horden [6] found similar absorption with their reagent. As, however, we have used the method solely for comparative purposes, this has been ignored.

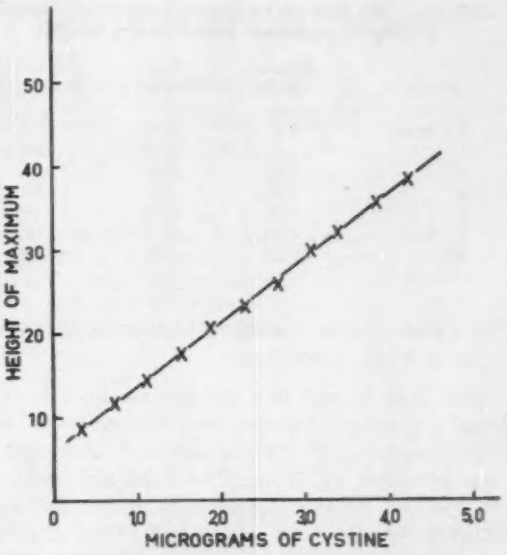


**Fig. 5.** Relationship between the height of the maximum *h* (Figure 4) and the cystine content of a wool hydrolysate.

### *The Determination of Sulfhydryl plus Disulfide Sulfur in Intact Wool*

Analysis of the data from the determination of cystine in intact wool by reaction with neohydrin in the presence of sulfite showed that the component of variance between runs was not significantly greater than zero. The estimate within runs was $S_W^2 = 0.1188$. The mean cystine content of all samples was 12.28%, or 512 μmoles/g., with a standard error of 0.07; the coefficient of variation within runs was 2.8%. The results are significantly higher than those obtained by the methods involving hydrolysis, and this implies that some cystine or cysteine is lost during the hydrolysis.

All the "% cystine" figures are based on the assumption that each —S—S— upon reaction with sulfite yields one —SH (Stricks, Kolthoff, and Tanaka [17]), and no account is taken of the —SH originally present. If allowance is made for this, then a value of 12.3 "% cystine" for a wool containing about 30 μmoles/g. of —SH represents 11.6% actual cystine, or 482 μmoles/g., and about 0.36% cysteine.

**TABLE I. The Variation of Cystine Content from Root to Tip along Single Lincoln Fibers (% Dry Weight)**

| Position | Primary lateral | Early secondary | Late secondary |
|---|---|---|---|
| 1 (root) | 8.65 | 7.94 | 7.60 |
| 2 | 7.52 | 6.82 | 6.80 |
| 3 | 7.62 | 6.36 | 6.74 |
| 4 | 7.35 | 7.02 | 6.82 |
| 5 | 7.25 | 6.76 | 5.88 |
| 6 (tip) | 6.55 | 5.92 | 5.66 |
| SE | 0.27 | 0.22 | 0.29 |

*The Determination of Sulfhydryl plus Disulfide Sulfur in Wool Hydrolysates*

The value of the first method for hydrolysates given above has been discussed adequately by the original authors [17]. When applied to wool, agreement to within 3% is found for duplicates, and the "% cystine" for the Merino wool in question was found to be 11.8 (491 μmoles/g.). The modified (second) technique yielded the values 11.8, 11.9, 12.2, and 11.6 for four determinations, or an average of 11.9. The method has found application in the determination of cystine in porcupine quill tip (9.5%), light and heavy cortical cell preparations (14 and 17%, respectively) and in samples of U.V. irradiated Corriedale fibers (Haly, Feughelman, and Griffiths [9]). In each case, only about 10 mg. of the material was available for analysis.

The third method was used in cases where the supercontraction or mechanical behavior of one or two fibers was to be correlated with a change in cystine content. The values obtained were found to be reproducible to within 3%, but appeared to be appreciably low when compared with a bulk sample of the same fibers. However, for comparative purposes, this was not considered to be serious, especially as large changes were involved. The method was also used to follow the change in cystine content from root to tip in a long-staple fiber. Thus a sample of 36's wool from a previously unshorn Lincoln lamb was sorted into primary laterals, early secondary, and late secondary fibers (no primary centrals could be found, and the bulk of the fibers fell into the early secondary category). The cystine content of the fibers was followed section by section for each fiber type, and an analysis of variance was made to separate position and fiber variation. In each case, the differences between positions are significant ($P < 0.01$; Table I). Since the bulk sample had a cystine content of 9.3% (first method), it was clear that the results were low, but even so, this represented a clear demonstration of the variation from root to tip in the one fiber. The lower values obtained for tip sections could well be due to weathering, but the variations lower down the fiber must have been due to variations in diet or changes in metabolism. It is hoped to investigate this point using hand-fed sheep whose fleece has been protected from weathering.

## Acknowledgment

The author is greatly indebted to Miss E. M. J. Parkhill for technical assistance and to Mr. W. B. Hall for the statistical analyses.

## Literature Cited

1. Benesch, R. and Benesch, R. E., *Arch. Biochem. and Biophys.* **38**, 425 (1952).
2. Benesch, R. and Benesch, R. E., *J. Am. Chem. Soc.* **73**, 3391 (1951).
3. Brdička, R., *Coll. Czech. Chem. Communs* **5**, 238 (1933).
4. Britton, H. T. S., "Hydrogen Ions," Vol. 1, London, Chapman and Hall, (a) 307, (b) 313 (1942).
5. Burley, R. W., TEXTILE RESEARCH JOURNAL **26**, 232 (1956).
6. Burley, R. W. and Horden, F. W. A., TEXTILE RESEARCH JOURNAL **27**, 615 (1957).
7. Cecil, R., *Biochem. J.* **47**, 572 (1950).
8. Gross, E. M. and Egan, R., *Fed. Proc.* 265 (1956).
9. Haly, A. R., Feughelman, M., and Griffith, J. C., *Nature* **180**, 1064 (1957).
10. Hata, T., *Mem. Res. Inst. Food Science,* Kyoto Univ., No. 1, 19 (1951).
11. Human, J. P. E., *Chem. and Ind.* 108 (1955).
12. Human, J. P. E. and Leach S. J., *Chem. and Ind.* 149 (1956).
13. Kolthoff, I. M. and Lingane, J. J., "Polarography," Vol. 2, New York, Interscience, 852 (1952).
14. Kolthoff, I. M., Stricks, W., and Morren, L., *Anal. Chem.* **26**, 366 (1954).
15. Leach, S. J., *Proc. Int. Wool Text. Res. Conf. Austr.* **C**, 469 (1955).
16. Simmonds, D. H., *Proc. Int. Wool Text. Res. Conf. Austr.* **C**, 65, refs. 6–8, 20, and 21 (1955).
17. Stricks, W., Kolthoff, I. M., and Tanaka, N., *Anal. Chem.* **26**, 299 (1954).

*Manuscript received March 17, 1958.*

# The Nature of Permanent Set in Keratin Fibers

**M. Feughelman, A. R. Haly, and T. W. Mitchell**

*Physics and Engineering Unit, Wool Textile Research Laboratories, Commonwealth Scientific and Industrial Research Organization, The Hermitage, Ryde, N.S.W., Australia*

**Abstract**

It has been shown by Farnworth that permanent set of keratin fibers in water is mainly due to strong polar linkages formed during the setting process. In this paper these linkages are identified with the bonds broken in the second stage of supercontraction of a fiber in a concentrated lithium bromide solution. These bonds are probably formed by groups of cooperative hydrogen bonds which are closely associated in the keratin structure with a tyrosine residue.

## Introduction

When a keratin fiber is held strained in boiling water for a period it acquires a set which is not completely released by boiling the fiber in water in a slack state. Speakman and others [1, 10, 15] have examined this permanent set in keratin fibers and have concluded that

1. Permanent set [15] is obtained in fibers heated strained in water at temperatures above 90° C.

2. Permanent set [10] is due to disulfide bond breakdown, followed by rebuilding of new covalent links.

3. The fiber [1] prior to the formation of bonds which cause permanent set (at the early stages of the setting process), if released from strain, will supercontract.

Recently Farnworth [2] has examined permanent set in crossbred wool fibers and found that permanent set could be detected in fibers set in water at temperatures above 70° C. Further, he has shown that permanent set could be released by water heated to a temperature above the temperature at which the fiber was set. He concluded that permanent set was due mainly to strong polar linkages (possibly hydrogen bonds) and not to covalent links of the type previously indicated.

The aim of the present work was to investigate and attempt to identify the bonds broken and re-formed which contribute to permanent set. From previous work [7] it had been pointed out that the ability of a fiber to set is correlated with ability to supercontract. Supercontraction [6] of wool fibers in concentrated LiBr solutions has been shown to proceed in two stages. The birefringence [9] of the fiber has almost entirely disappeared at the end of the first stage of supercontraction. However, washing out the LiBr with water causes the birefringence to be completely regained. On the other hand, if the supercontraction of the fiber has proceeded into the second stage, recovery of birefringence is only partially obtained, the amount recovered depending on how far the supercontraction has proceeded. Permanent disappearance of some birefringence was observed in fibers that had been permanently set. This could mean that the bonds broken during set correspond to the bonds broken in going into the second stage of supercontraction of a fiber in concentrated LiBr solution. Further, the amount and time rate of reduction in length of fibers which had been held strained in water at 100° C., on being treated in cold water, in water at 100° C., and in lithium bromide

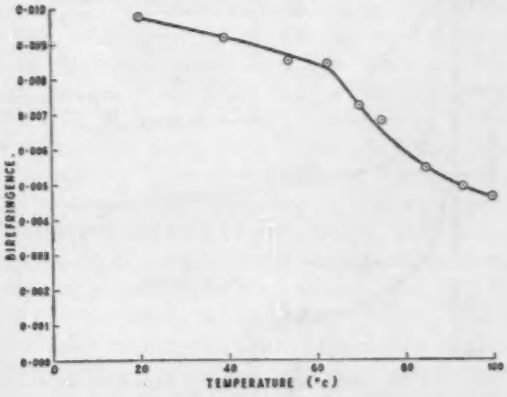


**Fig. 1.** The birefringence of a wool fiber plotted against the temperature at which the fiber had been held stretched 40% in water for 1 hr., then released for 1 hr.

solutions at a number of temperatures between room temperature and 100° C., indicated the formation during set of polar bonds of a wide energy range.

## Experimental

By use of the straining frame described elsewhere [7], single wool fibers were strained 40%, heated in water at various fixed temperatures for 1 hr., and released for 1 hr. in a slack condition at the same temperature as that at which the fiber was held strained. The birefringence at room humidity and temperature

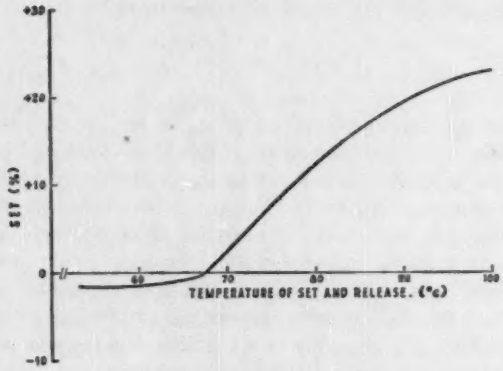


**Fig. 2.** The percentage permanent set obtained for different temperatures of setting of single wool fibers. In each case the fiber was held stretched at 40% in water for 1 hr. and released for 1 hr. at the temperature indicated (after Farnworth).

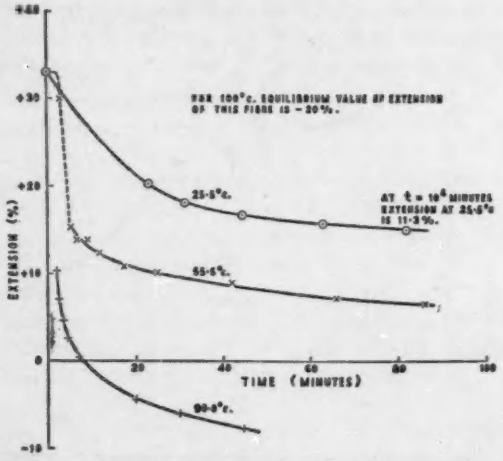


**Fig. 3.** The rate of contraction of wool fiber snippets in LiBr solution at various temperatures. These snippets are from a fiber that has been held at 40% extension in water at 100° C. for 1 hr. and then released at room temperature (20° C.) for 1 hr.

(20° C. ± 0.5° C. and 55 ± 5% relative humidity) of these treated fibers was then measured using the technique described by Goranson and Adams [5] adapted to a standard microscope. The essential components were a substage polarizer, a rotating analyzer above the microscope eyepiece, and between these a quarter-wave plate.

The wool fibers used for this birefringence experiment were from Corriedale sheep penned and handfed for uniformity of growth rate by the Sheep Biology Laboratory of the C.S.I.R.O. All wool fibers were scoured in petroleum ether at room temperature, washed in cold ethanol and then water. For each temperature, measurements were made on four fibers. About twenty readings of diameter and difference of optical path at varying positions along each fiber were taken. The optical path difference measurements were made in the plane of the fiber axis. An average value was calculated for each fiber and divided by the average fiber diameter to obtain the birefringence. The mean value of the birefringence for at least four fibers at each temperature was estimated. The readings for each fiber lay within a range $\pm 0.02 \times 10^{-2}$ about the mean at each temperature.

For the contraction experiments two more wool samples available to this laboratory were used, one a 50s crossbred and the other a finer Corriedale wool. Wool fibers from these samples were held strained at 40% extension in boiling water for 1 hr. The fibers were then released in water at room temperature until they came to equilibrium. Snippets from these fibers were contracted at a number of temperatures in LiBr solution. Observations of the contraction in the solution were made with microscope, using fiber snippets of about 1-mm. length; this technique has been described in a previous paper [9]. Bromine-free 8.13 *M* LiBr solution was used in all cases.

## Results

The birefringence of fibers which had been treated as indicated in the previous section was plotted against the temperature at which the fibers had been strained and released (Figure 1). From 20° C. to 63° C. the value of the birefringence changes slowly from $0.975 \times 10^{-2}$ to $0.84 \times 10^{-2}$. From 63° C. to 100° C. the birefringence drops rapidly to $0.46 \times 10^{-2}$, the rapid change starting between 63° C. and 70° C. The temperature region around 70° C. is

that at which Farnworth [2] (see Figure 2) observed the commencement of permanent set. As a control experiment, unstrained fibers were boiled in water for 2 hr.; no change of birefringence was detectable.

A typical set of contraction versus time curves for snippets from the same fiber is given in Figure 3. For each temperature in the lithium bromide solution, the snippets contract asymptotically to a final figure. The final extensions of these snippets relative to the original natural length of the fiber were averaged and are summarized in Table I. Also in Table I is given the permanent set of each of the wool varieties if extended to 40% in boiling water for 1 hr. and released in boiling water for 1 hr.

Further, the equilibrium supercontraction in lithium bromide at 100° C. of the natural unstretched wool fiber is given in Table I.

**TABLE I. Set Retained by Wool Fibers Which Were Held at 40% Strain While in Boiling Water for 1 Hr., Then Released Under the Conditions Indicated**

| Condition of release | Equilibrium extension for SW1 Corriedale, % | Equilibrium extension for Cross-bred 50s, % |
|---|---|---|
| Cold water 20° C. | 33 | 33 |
| Boiling water (100° C.) for 1 hr. | 12 | 19 |
| Cold 8.13 *M* LiBr (25.5° C.) | 12 | 2 |
| 8.13 *M* LiBr at 100° C. | −23 | −28 |
| Supercontraction in 8.13 *M* LiBr at 100° C. for the same wool starting from the natural unstretched fiber | −35 | −41 |

## Discussion

The supercontraction in lithium bromide solution of set fibers supports the findings of Farnworth [2] that much of the so-called permanent set in wool fibers is due to the creation of polar bonds during the setting of the fiber. It is suggested that the energy of these bonds is distributed over a wide range so that some are released in cold water and others progressively released in LiBr solution as the temperature of the solution is increased (see Table I and Figure 3). There is a discrepancy of some 12–13% between the final supercontraction in lithium bromide at 100° C. of a set fiber and of an unset fiber of the same wool, the set fiber contracting less. It is possible that this discrepancy can be accounted for by the creation of covalent links of the type proposed by Speakman [10].

The next problem to arise concerns the nature of the strong polar bonds formed during the setting process. It has been reported elsewhere [8] that supercontraction of single wool fibers in lithium bromide beyond the first stage is inhibited if the tyrosine groups in the wool have been iodinated by the method of Richard and Speakman [14]. The same wool [7] is extremely difficult to set. Also, Whewell and De Silva [16] found that application of nitric acid to wool, which probably nitrates the tyrosine in the wool, inhibits permanent set. However, if a wool fiber [8] is exposed to ultraviolet irradiation, the rate of second-stage supercontraction in lithium bromide is accelerated. This irradiated wool also has been shown [7] to set more rapidly. It appears likely, therefore, that the bonds which are broken in the second stage of supercontraction in concentrated lithium bromide must be the ones broken during the setting process to obtain permanent set.

The present work on birefringence is further evidence in favor of this proposal. During the supercontraction of a wool fiber, birefringence becomes irretrievably destroyed once the fiber contracts beyond the first stage [9]. Similarly, the birefringence of a wool fiber is reduced in rapidly increasing amounts as the temperature at which the fiber is strained is increased beyond the temperature range over which onset of permanent set is noted (Figures 1 and 2).

The second stage of supercontraction of wool fibers in concentrated lithium bromide solution has an activation energy deduced from the temperature coefficient of the process of about 30 kcal./mol. [6]. The strong polar bonds involved in this stage could be cooperative secondary links such as exist in crystalline regions. It is worth noting that Fraser and MacRae [3] have observed a reduction of crystallinity of fibers (from x-ray diffraction studies) due to exposure to ultraviolet irradiation. Kaplan and Fraser [11] and also Maybury [13] have examined the effect of radiation on egg albumin. Kaplan and Fraser, in the case of ultraviolet irradiation of egg albumin, proposed that the radiation energy is initially absorbed by a chromophore in the protein (possibly tyrosine) and then transferred to adjacent labile bonds. Maybury found in egg albumin that exposure to γ-radiation caused a latent damage which showed itself up in rate of change of optical rotation during denaturation by urea. He suggested that the

latent damage could be the rupture of a bond in a hydrogen bonded group.

A similar situation appears to exist in wool. When a stretched wool fiber is heated in water at a temperature above 70° C., cooperative secondary links, probably a network of hydrogen bonds, are broken. If, soon after commencement of heating in water (about 2 min. at 100° C.) the wool fiber is released, it supercontracts. Astbury and Woods [1] have shown that under optimum conditions full supercontraction can be obtained. This is compatible with the fact that cooperative secondary links control the supercontraction in the second stage. If the fiber is heated further in the strained state, it sets. The bonds involved in this set are mainly polar (being broken by heating in lithium bromide solution). These bonds are probably the cooperative secondary bonds re-formed (possibly only partially) while the fiber is held in an extended form. The re-formation of these bonds, especially if they are groups of cooperative bonds, would tend not to be as complete as the original bonds. This would result in a lowering and a widening of the range of energies associated with these polar bonds.

Chemical modification of the tyrosine residue appears certain to inhibit the rupture of the cooperative bonds. However, radiation, probably absorbed by the tyrosine, speeds up their breakdown [8]. This points to the association of a tyrosine residue with these cooperative bonds. This tyrosine residue seems capable of transferring energy absorbed to these bonds, causing their rupture.

Le Roux and Speakman [12] have suggested that tyrosine in wool (as in silk), due to its bulkiness, may cause the termination of crystalline regions. They found a relationship between tyrosine content and crystallinity. Fraser and MacRae [4] have shown that at least a portion of the tyrosine in wool occurs in a very ordered manner. This evidence suggests that the cooperative bonds in question, associated with the tyrosine residue, may be in the crystalline regions. This idea is further reinforced by the fact mentioned previously that ultraviolet irradiation causes a reduction in crystallinity of wool fibers.

## Summary

When a fiber is being permanently set in water it goes through the following stages:

1. It is strained and heated in the water at a temperature above 70° C. This causes not only weak polar bonds of the Van der Waal force type to be broken, but also disrupts strong polar bonds (probably cooperative hydrogen bonds). These strong bonds are those broken in the second stage of supercontraction of a wool fiber heated in concentrated lithium bromide solution. At this early stage, if the fiber is released it will supercontract.

2. The broken bonds are re-formed with the fiber in the strained state. The energy associated with these re-formed bonds is widely distributed because of the partial manner in which these bonds are reformed.

3. When the fiber is released slack in the heated water, it contracts to its permanently set length. The process of release disrupts the weak polar bonds, and the set length depends on the relative number of re-formed strong polar bonds.

The rupture of the strong polar bonds is controlled by the condition of the tyrosine residues in the wool fiber. Chemical modification of the tyrosine, such as iodination or introduction of nitrogroups, inhibits the rupture of these bonds. Ultraviolet radiation absorbed by the tyrosine residues is transferred to the polar bonds, causing a partial disruption of them.

It should be pointed out that some covalent linkages may be formed during the setting process, since the maximum supercontraction of the set fibers in lithium bromide never attains the full value of supercontraction for the natural fiber. However, the major portion of the permanent set is due to strong polar bonds, as Farnworth [2] already has pointed out.

## Literature Cited

1. Astbury, W. T. and Woods, H. J., *Phil. Trans. Roy. Soc.* **A232**, 333–394 (1933).
2. Farnworth, A. J., TEXTILE RESEARCH JOURNAL **27**, 632 (1957).
3. Fraser, R. D. B. and MacRae, T. P., private communication.
4. Fraser, R. D. B. and MacRae, T. P., *Nature* **179**, 732–733 (1957).
5. Goronson, R. W. and Adams, L. H., *J. Franklin Inst.* **216**, 475 (1933).
6. Haly, A. R. and Feughelman, M., TEXTILE RESEARCH JOURNAL **27**, 919 (1957).
7. Mitchell, T. W. and Feughelman, M., TEXTILE RESEARCH JOURNAL **28**, 453 (1958).
8. Haly, A. R., Feughelman, M. and Griffith, June, *Nature* **180**, 1064 (1957).
9. Haly, A. R. and Griffith, June, TEXTILE RESEARCH JOURNAL **28**, 32 (1958).

10. Hind, J. R. and Speakman, J. B., *J. Textile Inst.* **36**, T19 (1945).
11. Kaplan, J. G. and Fraser, M. J., *Biochem. et Biophys. Acta* **9**, 585–596 (1952).
12. Le Roux, P. L. and Speakman, J. B., TEXTILE RESEARCH JOURNAL **27**, 1–7 (1957).
13. Maybury, R. H., *J. Phys. Chem.* **61**, 140–141 (1957).
14. Richards, H. R. and Speakman, J. B., *Int. Wool Text. Res. Conf. Austr.* **C**, 308 (1955).
15. Speakman, J. B., *Trans. Faraday Soc.* **25**, 169 (1929).
16. Whewell, C. S. and De Silva, M. A., *J. Textile Inst.* **48**, T98 (1957).

*Manuscript received January 20, 1958.*

# The Preparation and Properties of Partially Benzylated Cotton

**Elias Klein, David J. Stanonis, Pieter Harbrink, and Ralph J. Berni**

*Southern Regional Research Laboratory,[1] New Orleans, Louisiana*

**Abstract**

Ternary systems, such as alcohol, water, and sodium hydroxide, have been used in the pretreatment bath or have been added in fixed quantities to cotton prior to etherification with benzyl chloride. Evidence has been obtained which supports an hypothesis that increased reagent solubility, coupled with control of the cellulose: sodacellulose equilibrium, can lead to essentially homogeneous cotton cellulose modifications. In addition, the experiments have resulted in the preparation of interesting fibrous cellulose ethers. These ethers retained many of the desirable mechanical properties of the original cotton and showed increases in elastic recovery, decreased permanent set, substantivity to disperse dyes, microbiological resistance, and a high degree of thermoplasticity.

As a continuation of a program to study the fundamentals of cellulose etherification, the benzylation of cotton has been investigated. Under proper conditions benzyl chloride can be made to react with alkali cellulose to give benzyl ethers of cellulose. For a single cellulosic hydroxyl group the overall reaction can be pictured as

$$\text{Cell(OH)}_2 + \text{NaOH} + \text{C}_6\text{H}_5\text{CH}_2\text{Cl} \rightarrow \text{Cell(OH)}_2\text{OCH}_2\text{C}_6\text{H}_5 + \text{NaCl} + \text{H}_2\text{O}$$

By consecutive reactions of the other hydroxyl groups the process theoretically can be continued until a degree of substitution (DS) of 3.0 is reached.

A review of early work dealing with the preparation of these ethers is given by Worden [12]; a summary of more recent research has been published under the editorship of Ott and Spurlin [11]. Much of the previous work described the preparation of soluble cellulosic ethers having a high DS. Okada [8] prepared benzene-soluble benzylcellulose in a two-stage reaction; in the first stage, alkali cellulose prepared by soaking sulfite pulp (96% alpha cellulose) in 17.5% NaOH was heated at 100° C. in benzyl chloride. This partially benzylated intermediate was not soluble in benzene and retained the fibrous structure of the pulp. Repetition of the process led to a soluble product and complete loss of fiber structure.

Lorand and Georgi [6] studied the benzylation of alkali cellulose from cotton linters under conditions favorable to the preservation of the fibrous structure. Using 25% NaOH they prepared alkali cellulose and treated it at 60° C. with benzyl chloride. They pointed out the importance of water in the reaction, and stated that "its immiscibility with benzyl chloride further accentuates the heterogeneity of the system."

[1] One of the laboratories of the Southern Utilization Research and Development Division, Agricultural Research Service, U. S. Department of Agriculture.

Using cotton yarns instead of pulp we repeated the experiments of Okada [8] using 17.5% NaOH and obtained the expected yield as measured by the DS; as anticipated, the samples lost a major portion of their mechanical strength. It was felt that much of this degradation was attributable to the prolonged heating of the yarn in the presence of the base. To avoid this degradation, experiments utilizing lower base concentration were conducted. This technique led to improvements in the final mechanical strength but also caused significant decreases in the yield of the reaction. This dilemma—increased yields leading to loss of strength—represented the essentials of the problem.

In our first attempts to circumvent this dilemma we employed hydrotropes; these had proven interesting and useful in previous studies on the cyanoethylation of cotton [4]. The net effect of hydrotropic compounds in cellulose reactions is to increase the solubility of the organic reagent in the aqueous phase about the fiber and to shift the cellulose:soda-cellulose equilibrium in favor of the soda-cellulose form. Sodium xylenesulfonate and dioxane were employed in the preliminary experiments. The latter, while not a true hydrotropic compound, could be expected to yield similar results by changing the character of the solvent system.

### The Water–Dioxane–NaOH System

The preferential absorption of sodium hydroxide by cellulose from this ternary system was determined by analyzing samples padded with constant pressure after immersion in varying compositions of the ternary solution. The experimental details have been described previously [4]. Previous experiments along such lines have been reported for ethanol–water–NaOH by Kolthoff [5]. In the case of the dioxane system the range of compositions available is limited by the ternary phase diagram of the system; this has been reported by Duhamel and Laurent [3].

As was pointed out previously, this system was chosen with the expectation of obtaining increased preferential absorption of sodium hydroxide by the cellulose. As indicated in Table I, these expectations were realized to some extent. At any given level of base content, increased dioxane percentages led to increased preferential absorption.

The maximum amount of dioxane compatible with the system is determined by the sodium hydroxide content of the system, as indicated by the phase diagram. When these saturated systems are employed as padding solutions prior to benzylation, increased yields result. In Table II are presented the results of a series of experiments at 95° C. using these saturated ternary solutions and suitable controls. Note that in addition to increasing the preferential absorption, the ternary system dissolves more of the benzyl chloride. The data also indicate that the preferential absorption is more influential on the yield than the solubility; it should be emphasized, however, that the solubility determinations relate to the padding solution, and do not necessarily represent the situation on the fiber after absorption has taken place.

These experiments represented the maximum effect available with this system, since they were carried out at the compatibility limits. Comparison with the binary padding solution of water and sodium hydroxide substantiated the early hypothesis regarding reaction yields, but were not very promising when viewed with respect to retention of mechanical strength. Even under these relatively mild conditions, excessive degradation occurred. In view of these limitations, a search for other ternary systems was initiated.

### The Water–Ethanol–Sodium Hydroxide System

The preferential absorption of sodium hydroxide from this ternary system has been studied [5]. These data indicate that a high degree of preferential absorption occurs, especially at a 30% ethanol level. Preliminary experiments established that in 15% NaOH and 35% ethanol the solubility of benzyl chloride is 5.15 g./100 g. of solution at 25° C. This solubility is 34.3 times as great as the benzyl chloride solubility in a 30% dioxane solution containing only 6% NaOH. The combination of these data warranted an investigation into the use of this ternary system in the benzylation reaction.

The procedure adopted in these experiments was relatively simple. Small skeins (1.250 g.) were prepared from a commercially mercerized linker yarn (7/2); to these were added predetermined quantities of aqueous sodium hydroxide and ethanol; after the ternary system had been well distributed, 20.0 cc. of benzyl chloride was added and the container shaken in an oil bath controlled at 95° C. After 2 hr. of reaction the samples were washed in methanol, dilute acid, and water; after the last wash they were steam distilled to remove residual benzyl chloride. Table III represents a typical series of such experiments.

In this instance 2.2 ml. of 22.9% NaOH was added to the yarn and the quantities of ethanol indicated in the first column of the table.

There are several points of interest in these data. Foremost, of course, is the apparent solution to the original dilemma; increased yields result in increased mechanical strength. In addition, it appears that there should be a simple relationship between the amount of ethanol employed, the yield, and the strength retained. The only discrepancy is the 27.2% yield figure obtained at the highest alcohol level. Later experiments showed that this was a temperature effect resulting from the delayed rise of the reaction temperature. In these first experiments no attempt was made to contain any highly volatile vapors; later experiments showed that in the first few minutes of reaction the vapor phase above the system contained 18% water, 75% ethanol, and 7% benzyl chloride. Distillation of these components out of the reaction system led to a decrease in the alcohol content of the system and a concomitant temperature rise in the reaction mixture.

These promising results led to a time study of the reaction. The alcohol content was fixed at 1.5 cc.; while not yielding an optimum product, this quantity was experimentally convenient. The only variation from the procedure described previously was the addition of a spiral air condenser to each flask so that the temperature and composition would remain constant. The consumption of benzyl chloride was followed indirectly by assuming that each mole of the chloride produced one mole of acid, which in turn neutralized one equivalent of base. At the end of the reaction each sample was transferred to aqueous methanol and titrated with 0.1 *N* HCl. After the titration each sample was worked up as described previously and the degree of substitution calculated from the weight gain. By comparing the DS with the decrease in NaOH content, an approximate efficiency calculation for the reaction can be carried out. These data are presented in Table IV, together with the sodium hydroxide:anhydroglucose mole ratio at the end of the indicated reaction time.

The data indicate that the reaction essentially stops when the mole ratio of NaOH to anhydroglu-

**TABLE I. Preferential Absorption of NaOH from Dioxane–Water Solvents**

| Composition of padding solution | | |
|---|---|---|
| Wt. % NaOH | Wt. % Dioxane | Mole ratio NaOH : $C_6H_{10}O_5$ |
| 3.0 | 20.0 | 0.21 |
| 3.0 | 30.0 | 0.27 |
| 3.0 | 35.0 | 0.32 |
| 4.0 | 20.0 | 0.28 |
| 4.0 | 30.0 | 0.37 |
| 4.0 | 35.0 | 0.46 |
| 5.0 | 20.0 | 0.35 |
| 5.0 | 30.0 | 0.51 |
| 5.0 | 35.0 | 0.67 |

**TABLE II. Benzylation of Cotton with Benzyl Chloride for 2 Hr. at 95° C. Using Dioxane Saturated Padding Solutions**

| Composition of original solution | | Mole ratio NaOH : $C_6H_{10}O_5$ | Solubility of benzyl chloride in padding soln. g./100 g. soln. | Wt. % gain through benzylation |
|---|---|---|---|---|
| Wt. % NaOH | Wt. % Dioxane | | | |
| 4.0 | 39.6 | 0.68 | 0.42 | 7.6 |
| 5.0 | 34.7 | 0.69 | 0.26 | 7.6 |
| 6.0 | 29.5 | 0.73 | 0.15 | 8.0 |
| 7.0 | 27.1 | 0.74 | 0.09 | 9.6 |
| 8.0 | 23.4 | 0.77 | 0.04 | 10.4 |
| 4.0 | 0 | 0.22 | <0.02 | 0 |
| 5.0 | 0 | 0.27 | <0.02 | 0.8 |
| 6.0 | 0 | 0.33 | <0.02 | 1.6 |
| 7.0 | 0 | 0.39 | <0.02 | 3.2 |
| 8.0 | 0 | 0.45 | <0.02 | 3.2 |

**TABLE III. Benzylation of Cotton with Benzyl Chloride for 2 Hr. at 95° C.**

| Ml. ethanol added | Wt. % gain through benzylation | Breaking strength, g. | Ultimate elongation | Tenacity, g./tex |
|---|---|---|---|---|
| 0 | 12.4 | 1463 | 14.1 | 6.09 |
| 0.5 | 14.0 | 2282 | 12.8 | 9.85 |
| 1.0 | 19.2 | 2915 | 14.4 | 12.24 |
| 2.0 | 30.0 | 3055 | 14.3 | 12.73 |
| 3.0 | 27.2 | 3630 | 12.0 | 14.45 |

**TABLE IV. Benzylation of Cotton with Benzyl Chloride at 95° C. in the Presence of Ethanol (1.5 ml.)**

| No. | Reaction time, hr. | Wt. % gain | DS, calc. | Mole ratio NaOH : $C_6H_{10}O_5$ | Efficiency, % |
|---|---|---|---|---|---|
| 1 | 0 | | 0 | 2.01 | — |
| 2 | 1 | 6.8 | 0.12 | 1.39 | 19.4 |
| 3 | 2 | 20.8 | 0.37 | 0.66 | 27.4 |
| 4 | 3 | 27.6 | 0.49 | 0.43 | 31.0 |
| 5 | 4 | 31.2 | 0.55 | 0.30 | 32.2 |
| 6 | 5 | 35.6 | 0.63 | 0.22 | 35.2 |
| 7 | 6 | 35.6 | 0.63 | 0.15 | 33.9 |

cose approaches 0.2; this is supported by the data presented previously in Table II. The latter, determined in the absence of alcohol, showed that no benzylation occurred at a mole ratio lower than 0.27.

### Microscopical Observations

The partially benzylated fibers were similar in gross appearance to mercerized cotton, indicating that swelling had occurred during their preparation. Their refractive indices were lower than for mercerized fibers. An electron micrograph of a thin section of fiber benzylated to weight gain of 26% is shown in Figure 1. It is apparent that the benzylated fiber undergoes a limited amount of swelling as the result of the embedding process with methacrylic esters. The uniformity of texture of the whole cross-sectional area indicates that benzylation occurs throughout the fiber. There is no evidence that the highly topochemical process observed by Lorand and Georgi [6] obtains in benzylation of cotton under these reaction conditions. It is also possible to discern discrete microfibrils in the section illustrated. These observations were confirmed by examination of fragments of the same benzylated cotton obtained by beating fibers in water in a Waring blendor. The typical appearance of the fragments is shown in Figure 2. The microfibrillate character of the modified cellulose is still strongly evident. Some specimens gave the impression of having undergone plastic deformation as the result of the beating process, but other than having a slightly swollen appearance they were undistinguishable from unbenzylated cotton treated with NaOH and ethanol in the same manner. Benzylated cotton was fibrillated only with great difficulty, a characteristic of modified celluloses whose swelling in water has been seriously reduced.

### X-Ray Analysis

Since a more complete analysis of the x-ray diffraction patterns obtained from benzylated cotton is planned for a separate report [2], only a brief outline of the results will be mentioned here. Figure 3 shows the fiber bundle pattern of a sample benzylated to a DS of 0.55. The diffraction from the 101 plane of Cellulose II is still in evidence, as well as a new arc closer to the central beam, indicating a larger lattice spacing as the result of the benzylation. The appearance of a new crystal form at such low substitution indicates that the reaction is taking place essentially homogeneously throughout the entire fiber

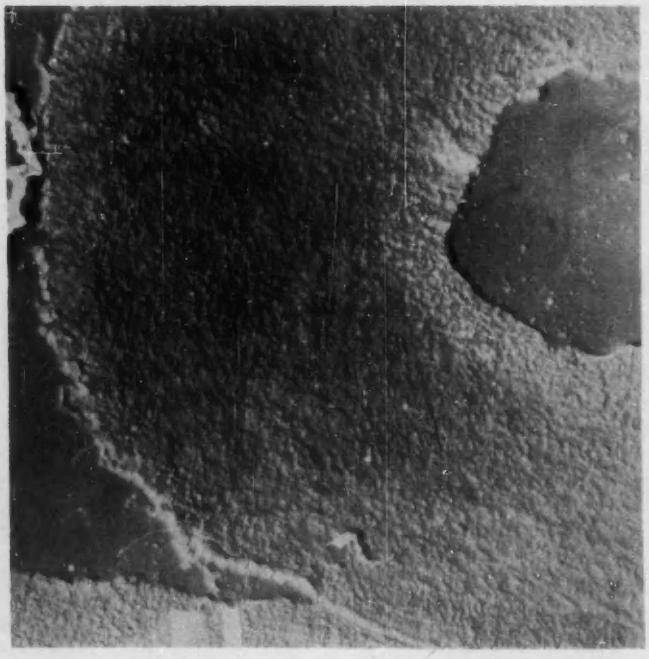

**Fig. 1.** Electron micrograph of cross section of benzylated cotton fiber (26% weight gain); sectioned after embedding in polymethyl methacrylate; platinum shadowing (6000×).

structure; this is supported by the electron microscopy data.

At higher substitutions, the appearance of the new arc is more pronounced. A sample rebenzylated especially for x-ray analysis to a DS of 0.81 gives a pattern as shown in Figure 4. When this sample is heat stretched, the pattern in Figure 5 results. The inner arcs are shorter and sharper, indicating increased crystallization and perhaps better orientation.

### Thermal Response of Partially Benzylated Cotton

Since commercially prepared benzylcellulose is known to have a softening temperature in the neighborhood of 100° C., depending on its degree of substitution and chain length, it was of interest to determine the temperature responses of the fibrous benzylcellulose. The first technique chosen was essentially that described by Brown [1]. Benzylated yarns were extended to fixed elongations using a TRI Shaevitz Tensile Tester, modified by the addition of an oven. The entire 10-in. sample length was inside the oven. The stress necessary to reach this elongation was recorded; the temperature was increased for subsequent measurement. The data are shown in Figure 6 on a semilogarithmic plot. The ordinate is in arbitrary units for convenience in showing the several samples. In addition to a control sample, the plot shows three yarns having a benzyl DS of 0.25, 0.34, and 0.81; the inflection points, and by inference the second order transition temperatures occur at 167° C., 160° C., and 125° C., respectively. The control yarn shows no evidence of a transition in the temperature range studied.

To check the validity of the apparent second order transition temperatures, fiber samples were placed between crossed Nicol prisms on a microscope hot stage. Birefringence remained even after the temperature exceeded 220° C., indicating that true melting had not taken place. The inflection points of Figure 6 therefore may be taken to represent second order transition temperatures.

This was investigated in greater detail using a more convenient technique. In the second method, fiber samples were mounted with a torsion pendulum cemented to their bottom inside a 1-in. diameter oven. The fiber was made to oscillate by an external magnet; the period of oscillation was determined. The temperature inside the oven was determined by means of a thermocouple arrangement. For fibers undergoing small deformations the logarithm of the oscillation period is proportional to the torsional modulus of the fiber. By plotting the logarithm of the period of oscillation versus the temperature, both in the dry and saturated water vapor state, one finds rapid decreases in stiffness over a short temperature range. This again is indicative of a transition temperature. Figure 7 represents such data obtained from samples described in Table IV; these data were collected with a drying agent in the oven. Figure 8 shows similar data measured in a saturated water

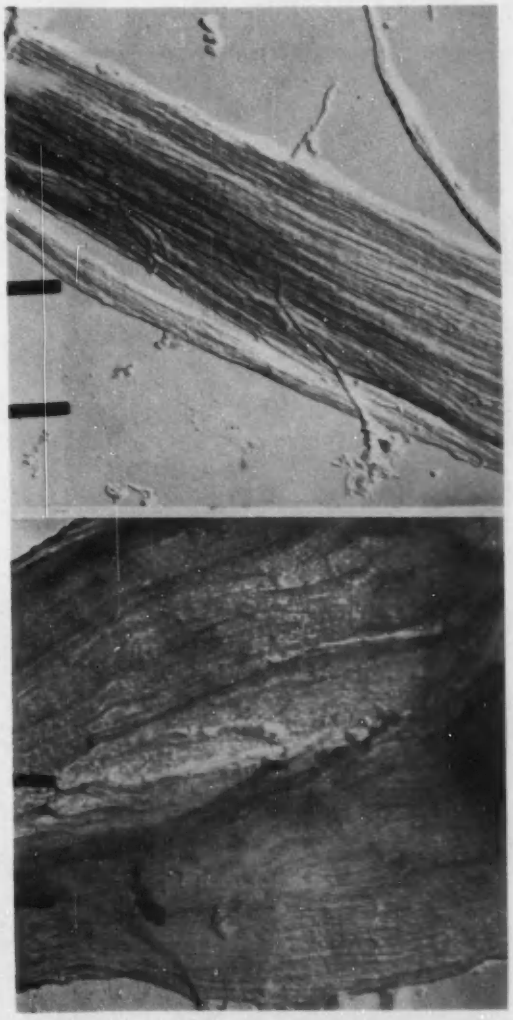

**Fig. 2.** Electron micrograph of fiber fragments obtained by wet beating; chromium shadowing; 10,000 ×. Top: partially benzylated (Sample 5, Table IV). Bottom: control (Sample 1, Table IV).

vapor atmosphere. Both figures contain control cotton samples and an acrylic fiber for comparison.

The data obtained with the drying agent present indicate that at higher temperatures the stiffness tends toward a plateau. In the presence of water vapor the tendency is absent; this suggests a plasticization effect by the water.

### Mechanical Properties of Partially Benzylated Cotton

Since the use of alcohol in the benzylation reaction resulted in higher strength retention, and additionally offered a means of introducing thermoplastic properties into cotton, a detailed mechanical analysis was desirable. The samples employed were those previously described in Table IV in connection with a time study. They were well suited for this purpose,

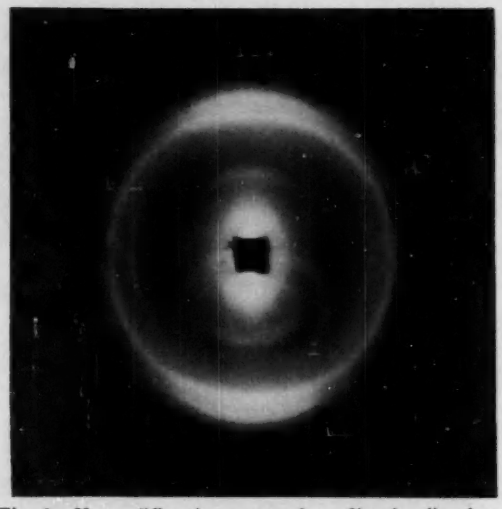

Fig. 3. X-ray diffraction pattern from fiber bundle of partially benzylated cotton (DS = 0.55).

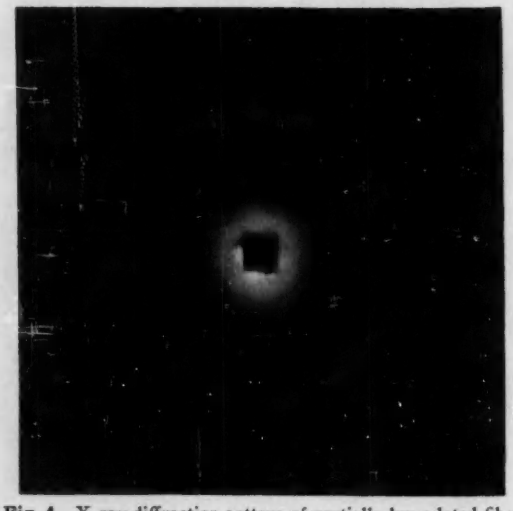

Fig. 4. X-ray diffraction pattern of partially benzylated fiber bundle (DS = 0.81).

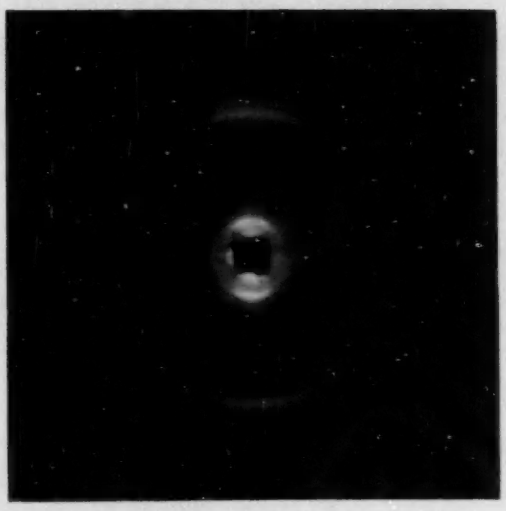

Fig. 5. X-ray diffraction pattern of partially benzylated cotton fiber bundle after heating under stress (DS = 0.81).

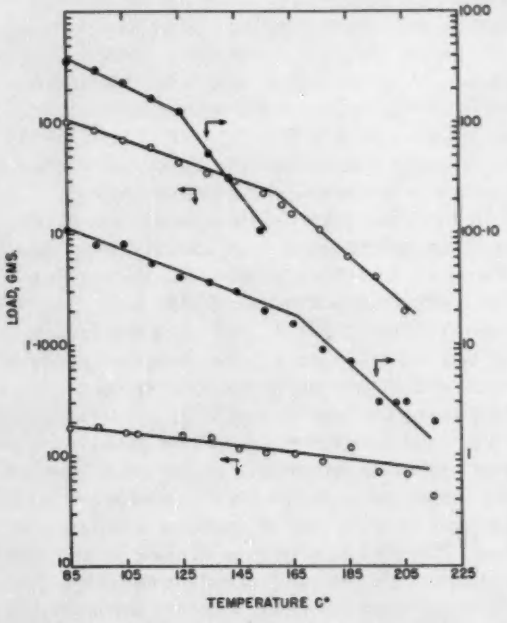


Fig. 6. Variation of load required for fixed elongations of partially benzylated yarns and control as a function of temperature. Degree of substitution, top to bottom: 0.81, 0.34, 0.25, and control.

since considerable effort had been made to keep both their chemical and mechanical histories identical. Since the pretreating solutions and conditions were identical for all the samples, any changes in mechanical properties are attributable to the varying degrees of substitution and the time-dependent degradation reactions remaining in the system.

Two series of tests were performed, both using an Instron tester. In the first, the stress–strain curves were determined and the energy to rupture measured by means of an attached integrator. In the second series, the yarns were evaluated for immediate recovery, delayed recovery, and permanent set essentially according to the method of Orr et al. [9]. Two variations of this latter technique were employed: the first loading of the samples was carried out with 10.0 g. pretension as indicated by the recorder, and, instead of cycling to predetermined loads, the samples were cycled to predetermined elongations. These were minor differences, however, and employed only for convenience. In addition to the linear extension data, resilience values were calculated for each extension cycle with the aid of an integrator. The extensions employed were 1, 2, 4, 6, 8, and 10% based on a 10-in. specimen.

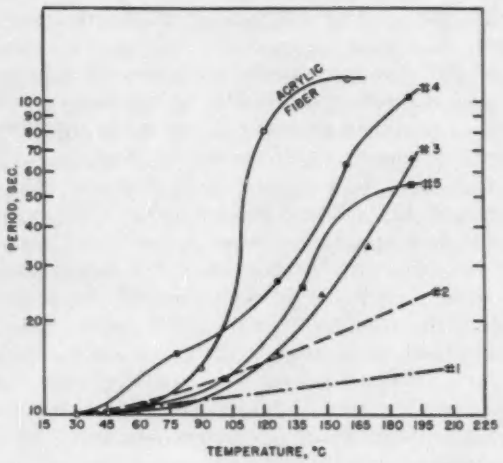


**Fig. 7.** Torsional period of partially benzylated, control, and acrylic fibers as a function of temperature; dry air.

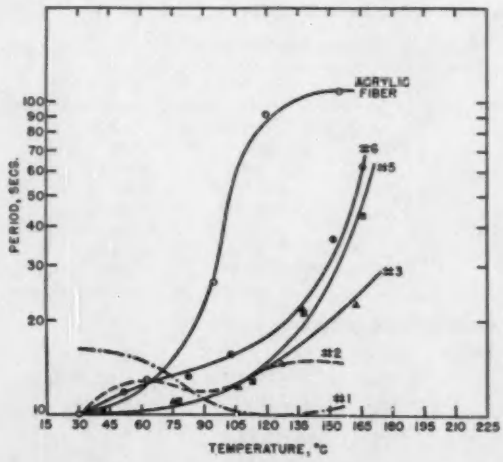


**Fig. 8.** Torsional period of partially benzylated, control, and acrylic fibers as a function of temperature; water vapor saturated atmosphere.

In Figure 9 the resilience of several samples is plotted as a function of elongation. In the range of 2–6% elongation there are significant increases in resilience with increasing DS. At both the low and high extremes of elongation these differences vanish. It should be kept in mind that the control sample (No. 1) in these tests is not a mercerized yarn as usually encountered, but a sample pretreated with base, alcohol, and water in the same manner as the etherified samples. In fact, the control was taken through a 2-hr. heating period in toluene and worked up exactly as the other samples in order to impose the same stresses and temperature conditions.

In Table V is a summary of the pertinent mechanical data obtained from the stress–strain curves. In addition, linear density and volume density were determined; the latter was done by means of the gradient column technique [10].

Figures 10 through 13 represent the immediate recovery and permanent set data from Samples 1

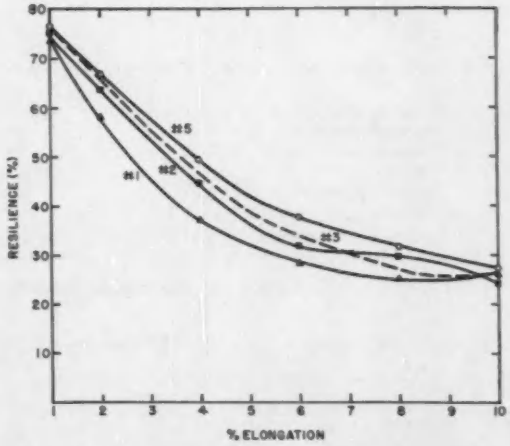


**Fig. 9.** Resilience as a function of elongation of partially benzylated and control yarns.

through 4 of Table IV; the values are plotted against both the absolute elongation and the percentage of ultimate elongation. Two changes are immediately apparent; one is the increased elastic recovery due to benzylation and the other is decreased permanent set up to 60% of the ultimate elongation. The shapes of the curves indicate that no yield point is encountered even at the higher elongations. A characteristic difficult to explain is the appearance of a definite negative permanent set.

### Miscellaneous

Because all of the experiments characterizing this modified cellulose were carried out on a laboratory scale, a larger run was initiated to determine what, if any, difficulties would arise. Accordingly a 1-lb. sample of 15/1 yarn was scoured, soaked in 17.5% NaOH, and centrifuged to 225% wet pickup. These conditions had been established to give the same chemical composition on the fiber as the laboratory method. It did cause variations in the mechanical properties, however, since the excess padding solution allowed unrestricted swelling and gave the fibers an opportunity to reach an equilibrium state with the padding solution. After they were centrifuged the skeins were wound wet on a package dyer spindle and reacted in the package dyer for 2 hr. at 95° C. with benzyl chloride containing 20% ethanol. At the end of the reaction period the reagent was drained; the package was washed with methanol, dilute acid, water, and then steamed. The weight gain of the sample was 20%. Yarn samples were taken from each 500-yd. portion of the package and dyed with Celliton Fast Red GGA. Microscopic examination indicated that the treatment was homogeneous throughout the fiber; comparison of the samples from fifteen layers in the package showed no color or shade differences.

The mechanical properties of this sample and a control are shown in Table VI. The control in the table consisted of yarns taken off the spindle just prior to the benzylation. Its value is limited by the fact that the sample was allowed to relax prior to neutralization, whereas the benzylated sample was under the winding and package tension the entire time. Our experience with this reaction system has indicated that the ultimate elongation of a given sample is determined primarily by the swelling and tension conditions encountered, and not to any great extent by the degree of reaction obtained.

Data from the x-ray and mechanical cycling experiments had indicated that tensioning of the product leads to significant changes in mechanical properties. Accordingly, specimens of this sample were strained to 50% of their ultimate elongation and held at this point for 2 min. After a 5-min. relaxation period their stress–strain curves were determined. The last column in Table VI shows this latter breaking stress. A noticeable improvement in the benzylated sample is apparent compared to the scoured yarn and the control.

Qualitative evaluations on this and other samples

**TABLE V. Mechanical Properties of Partially Benzylated Cotton Yarns Described in Table IV**

| | Sample numbers | | | |
|---|---|---|---|---|
| | 1 | 2 | 3 | 4 |
| DS | 0 | 0.12 | 0.37 | 0.49 |
| Breaking strength, g. | 3768 | 3002 | 2492 | 2622 |
| Ultimate elongation, % | 11.9 | 13.7 | 12.8 | 12.5 |
| Linear density, tex (g./1000 m.) | 178 | 197 | 217 | 241 |
| Tenacity, g./tex | 21.16 | 15.24 | 11.48 | 10.88 |
| Density, g./cm.$^3$ | 1.520 | 1.428 | 1.388 | 1.382 |
| Tenacity, g./cm.$^2 \times 10^{-6}$ | 32.16 | 21.76 | 15.93 | 15.04 |
| Energy to rupture (g./cm.$^2$) $\times 10^{-6}$ | 162 | 131 | 84 | 81 |

**TABLE VI. Mechanical Properties of Yarn Benzylated in Package Dyer**

| | Br. str., g. | Elongation, % | Linear density, tex | Tenacity, g./tex | Br. str., g., after 50% cycle |
|---|---|---|---|---|---|
| Scoured yarn | 535 | 9.5 | 40.0 | 13.4 | 567 |
| Control | 567 | 11.20 | 41.2 | 13.8 | 577 |
| Benzylated | 423 | 8.94 | 48.4 | 8.7 | 540 |

established that a high degree of rot resistance can be obtained through benzylation at relatively low add-ons. Yarns having a 12% weight gain retained over 90% of their strength after 24 weeks in a soil burial bed. An 80 × 80 fabric sample (6.0% weight gain) showed no signs of damage after 10 weeks of burial.

Sample dyeings of the benzylated yarns showed that of seven common acetate dyes tested, all dyed the benzylated cotton well. As expected, the benzylated cotton is resistant to direct dyes.

## Discussion

From a variety of experiments, some of which are reported here, has come the substantiation of an hypothesis that increased reagent solubility, coupled with control of the cellulose:sodacellulose equilibrium, can lead to essentially homogeneous cotton cellulose modifications. In addition, the realization has come that attendant effects such as changes in elongation, fiber strength, and polymer degradation may operate quite independently from the chemical modification.

A striking example of the latter may be illustrated as follows: if methanol, ethanol, and isopropanol are used in a series of experiments as described in Table III, the yields consistently decrease with increasing size of the alcohol; however, the polymer degradation as measured by loss of yarn strength remains low for all the alcohols. If now solvents such as dioxane or acetone are employed, the yields are improved over the controls, but very high strength losses are encountered.

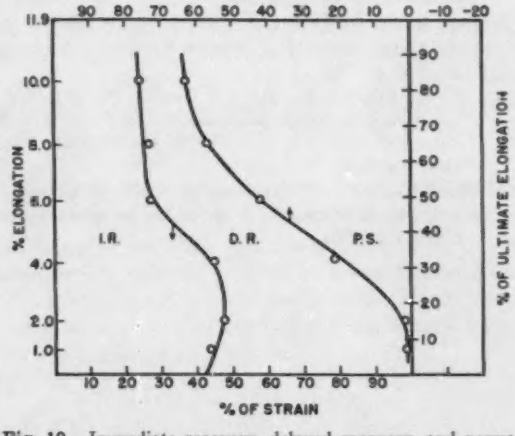


**Fig. 10.** Immediate recovery, delayed recovery, and permanent set of control yarn (No. 1, Table V).

Our experiments have led to the tentative conclusion that these mixed solvent systems facilitate cellulose reactions through their effect on the composition and properties of the aqueous phase about the fiber. This results in changes of reagent solubility in the aqueous phase, changes in the soda-cellulose:cellulose equilibria, and consequently to altered swelling power of the aqueous phase. The preferential absorption and solubility measurements support the first two ideas; the resulting swelling effect is more difficult to correlate, but is indicated by the ultimate elongation data. As mentioned previously, the ultimate elongation is not so much a function of the degree of substitution obtained as of the nature of the aque-

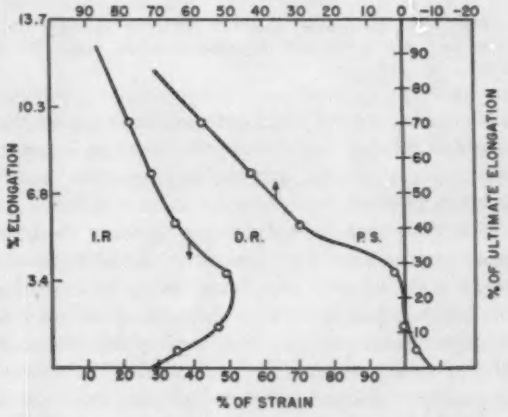


**Fig. 11.** Immediate recovery, delayed recovery, and permanent set of partially benzylated cotton yarn (No. 2, Table V).

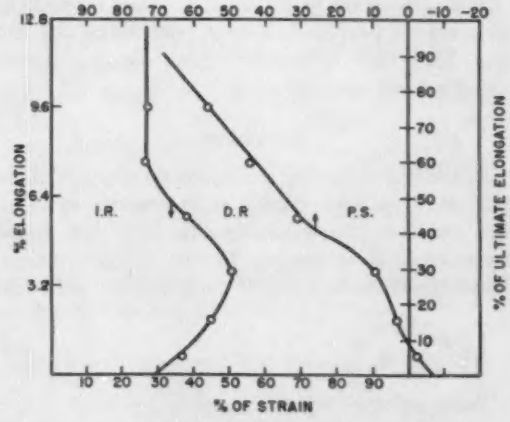


**Fig. 12.** Immediate recovery, delayed recovery, and permanent set of partially benzylated cotton yarn (No. 3, Table V).

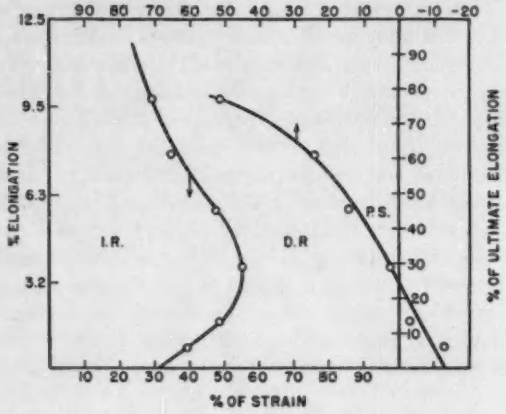


**Fig. 13.** Immediate recovery, delayed recovery, and permanent set of partially benzylated cotton yarn (No. 4, Table V).

ous solution on the fiber and the conditions of tension encountered. It also appears that the degree of reaction obtained is not highly dependent on the swelling allowed.

While several mixed solvent systems facilitate reaction, the protective action of the alcohols appears to be unique. Our initial thoughts were that the alcohols participated in and altered the alkaline depolymerization scheme described by Machell et al. [7] in such a manner as to terminate the depolymerization. However, viscosity measurements of samples heated in the presence of aqueous base in toluene, both with and without alcohol present, showed DP values of 1315 and 1526 respectively.

That the action of the alcohol is not through its reducing properties has been established by the negative action of several added reducing agents tested but not reported here.

## Summary

In addition to giving experimental support to the original hypothesis regarding heterogeneous cellulose reactions, these experiments have led to the preparation of interesting fibrous cellulose ethers. These ethers retain many of the desirable mechanical properties of the starting cotton and lead to increases in elastic recovery, decreased permanent set, substantivity to disperse dyes, microbiological resistance, and a high degree of thermoplasticity. Electron microscopy and x-ray evidence indicate that in the reaction system described the modification of the fiber is highly uniform.

## Acknowledgments

We would like to express our appreciation to the many members of this laboratory's service functions who aided immeasurably, through their skill and suggestions, in this investigation. We specially thank Messrs. Verne W. Tripp and Rollin Orr for stimulating discussions in addition to their particular skills in the microscopical and mechanical analysis.

## Literature Cited

1. Brown, Alexander, TEXTILE RESEARCH JOURNAL **25**, 891 (1955).
2. Creely, J. J., Stanonis, D. J., and Klein, E., to be published.
3. Dunhamel, J. and Laurent, P., *Compt. rend.* **234**, 2069 (1952).
4. Klein, Elias, Weaver, J. W., Webre, Beverly G., and Jurgens, Julian F., TEXTILE RESEARCH JOURNAL **27**, 50 (1957).
5. Kolthoff, I. M., *Pharmaceutisch Weekblad* **58**, 46 (1921).
6. Lorand, E. J. and Georgi, E. A., *J. Am. Chem. Soc.* **59**, 1166 (1937).
7. Machell, G., Richards, G. N., and Sephton, H. H., *Chem. & Ind. (London)* 467 (1957).
8. Okada, H., *Cellulosechemie* **12**, 11 (1931).
9. Orr, Rollin S., Burgis, Albert W., and Grant, James N., to be published.
10. Orr, Rollin S., Weiss, Louis C., Moore, Harry B., and Grant, James N., TEXTILE RESEARCH JOURNAL **25**, 592 (1955).
11. Ott, E., Spurlin, H. M., and Graffin, M. W., "Cellulose and Cellulose Derivatives," 3 Parts (High Polymers Vol. V), New York, Interscience Publishers (1954).
12. Worden, E. C., "Technology of Cellulose Ethers," Vol. III, Wilburn, N. J., Worden Laboratory and Library (1933).

*Manuscript received March 24, 1958.*

# Empirical Relations of Crease Recovery and Time

**P. R. Wilkinson and H. E. Stanley**

*E. I. du Pont de Nemours & Co., Inc., Textile Fibers Department, Wilmington, Delaware*

**Abstract**

A technique for measuring short-time crease recovery is described. Data from this method and from the standard Monsanto method were used to establish several empirical relationships between crease recovery and time which give linear plots and which permit extrapolation to very short and very long times. One of these relationships gives a linear plot over the time range of 5 sec. to several days. These relationships lead to several new parameters for characterizing fabric recovery: very short time crease recovery, rate of delayed recovery, and recovery after infinite time. These parameters depend primarily on fiber type and to a much lesser extent on fabric construction.

## Introduction

The ability of apparel fabrics to recover from unintentional creasing is commonly evaluated by use of a simple test, such as the Monsanto crease recovery test [1]. In such tests, a strip of fabric is creased for a specified time, released, and the degree of recovery measured, either in terms of an angle or as percent recovery. It is the purpose of this communication to report a modification of the Monsanto test which permits measurement of crease recoveries at very short times and to report methods for treating crease recovery data in order to obtain from it certain empirical descriptive constants for the behavior of a fabric.

Crease recovery data are normally obtained and reported at a specified time interval after the removal of the creasing load. This time interval usually is 5 min., but may be any other specified time. For several years crease recovery data have been obtained in our laboratory over the range of 15–300 sec. It has been customary to plot the 15–120 sec. data as a function of log time and to extrapolate such plots to 1 sec. to compute the short-time recovery of fabrics. These operations were made on the tacit assumption that crease recovery in percent (hereafter referred to by the letter $A$, with subscript to indicate specific recovery time) was related to time in the short time range by the following equation:

$$A_t = A_1 + b \log t \tag{1}$$

It has been observed, however, that plots of $A$ vs. $\log t$ deviate appreciably from linearity at times less than 15 sec. and greater than 120 sec. and that the magnitude of deviation varies from fabric to fabric. Hence, an improved function which would permit more accurate extrapolation and smoothing of data, not only in the short time range but also at extended periods of time, was quite desirable. Such a function should permit the calculation of more accurate parameters to represent the crease recovery behavior of fabrics over the entire time range.

Sommer [2] has reported equations for this purpose. The following equation was reported for the calculation of the recovery angle at a short time:

$$\alpha = \alpha_0(100\ t)^c \tag{2}$$

where $\alpha_0$ is the recovery angle at 0.01 min. and $c = \dfrac{\log (\alpha_2/\alpha_1)}{\log (t_2/t_1)}$. The use of recovery values at 60 min. and 5 min. was recommended for the calculation of $c$.

The equation:

$$\pi = \frac{\sqrt[c]{\dfrac{180}{\alpha_0}}}{6000} \tag{3}$$

where $\pi$ is the time in hours required for complete recovery, was also reported by Sommer.

## Experimental Procedure

The recovery of creased fabrics was measured at short times (2 sec.) and at long times (several days) to evaluate the agreement of available equations

**Fig. 1.** Modified crease recovery tester; A—specimen holder, B—specimen cover.

with experimental data and the usefulness of new equations for routine test procedures.

A standard Monsanto crease recovery tester was used to obtain crease recovery-time data for time periods greater than 10 sec. The ASTM procedure [1] was followed with the following exceptions:

1. A 1000-g. creasing load was used.
2. Crease recovery data were obtained at 10, 15, 30, 45, 60, 120, 180, and 300 sec. after removal of the load.

For obtaining crease recovery data at times less than 10 sec., the modified tester shown in Figure 1 was devised. It was shown that this modified tester could be used to obtain reproducible values at 2 sec. after removal of the creasing load. This modified tester differs from the standard tester as follows: the specimen holder (A) is removable from the face of the tester, and a cover of Lucite[1] (B), spring loaded so as to open automatically, replaces the plastic press normally used for creasing the specimen.

In the operation of this modified tester, a load is applied to the fabric specimen in the same manner as specified [1]. However, a few seconds before the end of the creasing period, the load is removed while the spring-loaded cover is held closed by hand. The holder is then attached to the face of the tester. At the end of the creasing period, pressure on the cover is released. This permits the spring-loaded cover to snap back from the specimen and allows a rapid reading to be made of the recovery. In the data reported below, at least five specimens were measured for each fabric sample.

Crease recovery data for fabrics of rayon, Dacron,[2] acetate, and wool are compared for the two methods in Table I. As shown, the results obtained with the modified tester are comparable to those from the standard tester at times greater than 10 sec.

Data for crease recoveries at longer times were obtained with both the modified and regular crease recovery testers, since both yield the same results. These data were obtained in a conditioned laboratory with the tester set in a box open only on the face. A door of Lucite was closed each time the specimens were allowed to stand for an extended period of time. This prevented the specimens from undergoing recovery due to air motion. Such long-time recovery data were collected over periods up to 15 days.

### Calculation of Short-Time Crease Recovery

Short-time data obtained with the modified tester are plotted as a function of log time (Equation 1) in Figure 2. As shown, the relation between $A$ and log $t$ is not linear; thus data obtained for short time recoveries by extrapolation are higher than the experimental data. The magnitude of the deviation varies from fabric to fabric. It is the greatest for those fabrics which show the largest crease recovery variations with time (nylon curve in Figure 2).

Calculated data for short-time recovery obtained from Equation 2, using the suggested times of 60 min. and 5 min., are higher than the experimental data. As shown in Table II, this is true over a range of crease recoveries. Crease recovery data at 60 min. differ from those at 5 min. by only 2 or 3% in most cases. This produces considerable inaccuracy in the calculations, since crease recovery data are reproducible to only $\pm 2\%$.

Data calculated from Equation 2 using $t_2/t_1$ as 300/10 sec. rather than 60/5 min. more nearly agree with experimental data (Table II). The calculated data vary with the choice of $t_2/t_1$.

From the comparisons of measured data with calculated values, it was concluded that the equations previously discussed are not entirely satisfactory for calculating crease recovery at short times.

Equation 1 can be corrected for curvature to yield the following equation which is linear over the

[1] Trademark for Du Pont's acrylic resin.

[2] Trademark for Du Pont's polyester fiber.

time range of 2–1000 sec. for crease recovery:

$$A_t = A_1 + b\frac{\log t}{t^d} \qquad (4)$$

This equation can be used to obtain $A_1$ by a plot of $A_t$ vs. $\log t/t^d$. The majority of the fabrics which we have investigated yield linear plots when $d = 0.05$. Representative curves of $A_t$ vs. $\log t/t^{-.05}$, extrapolated to 1 sec., are shown in Figure 3.

Equation 4 is used to obtain crease recovery data at times less than 2 sec. when such data are desired. Crease recovery data at times greater than 2 sec. are obtained with Equation 7 (discussed below).

### Calculation of Long-Time Crease Recovery

None of the equations previously discussed accurately express crease recovery at long periods of time. Crease recovery data calculated from Equations 1, 2, and 4 are higher than measured data. The time for complete recovery to occur ($\pi$), calculated from Equation 3, was reported by Sommer to be "hypothetical" since he found that the fabrics he tested had not exhibited complete recovery in the time calculated from Equation 3. This agrees with our experiences in that we have not found a fabric which, in the absence of external influences, has exhibited complete recovery in reasonable times (up to several days). We have postulated that this lack of recovery is caused by interfiber or interyarn friction, which prevents the recovery of creased fabrics. Since the Monsanto crease recovery procedure was designed to yield crease recovery data without external influence, it would be expected that few fabrics would exhibit complete recovery.

We have found that for the fabrics on which we have made long-time measurements the relation of crease recovery to time can be expressed by the following hyperbolic equation:

$$(A_\infty - A_t)(\log t) = S \qquad (5)$$

**TABLE I. Crease Recovery Data—Modified Tester vs. Regular Tester (65% RH, 70° F.)**

| Fabric | Crease recovery: 30-Sec. data, Modified tester | 30-Sec. data, Regular tester | 300-Sec. data, Modified tester | 300-Sec. data, Regular tester |
|---|---|---|---|---|
| Rayon shirting | 54 | 55 | 65 | 65 |
| Dacron shirting | 84 | 84 | 87 | 87 |
| Acetate shirting | 67 | 66 | 72 | 73 |
| Wool crepe | 84 | 83 | 88 | 88 |
| Wool tropical | 81 | 82 | 89 | 88 |

**TABLE II. Comparison of Calculated with Experimental Crease Recovery Data (65% RH, 70° F.)**

| Fabric | Measured data* $A_2$ | Calc. from equation 2: $A_2$† | $A_2$‡ |
|---|---|---|---|
| Acetate shirting | 59% | 60% | 70% |
| Dacron shirting | 78 | 76 | — |
| Nylon shirting | 49 | 50 | 64 |
| Wool crepe | 77 | 75 | 84 |
| Mohair/wool suiting | 80 | 78 | — |
| Wool suiting | 73 | 72 | — |

* Modified tester.
† Calculated with $t_2/t_1$ = 300 sec./10 sec.
‡ Calculated with $t_2/t_1$ = 60 min./5 min.

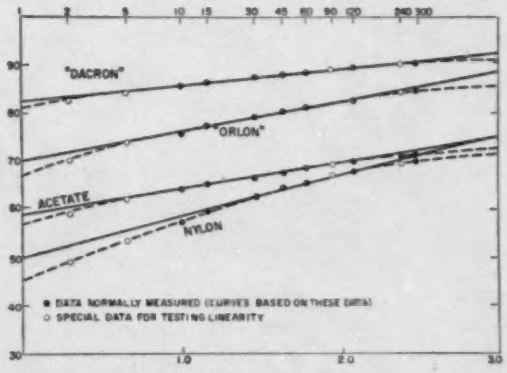


**Fig. 2.** Empirical relation of crease recovery to time; short time Equation 1; $A_t = A_1 + b \log t$. Scales: top, seconds; left, percent crease recovery; bottom, log time.

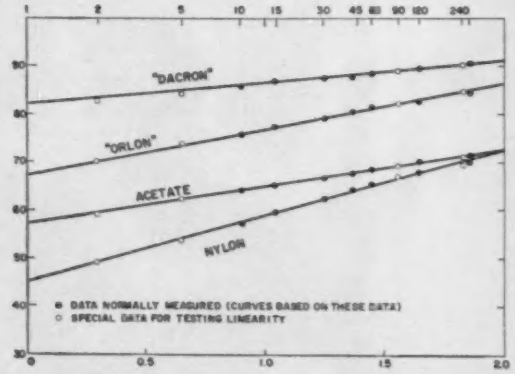


**Fig. 3.** Empirical relation of crease recovery to time; short time Equation 4; $A_t = A_1 + b \log t/t^{0.05}$. Scales: top, seconds; left, percent crease recovery; bottom, log $t/t^{0.05}$.

where $S$ is a characteristic delayed recovery constant, $A_t$ is crease recovery, and $A_\infty$ is the asymptote to the $A_t$ axis or $A_t$ at infinite time. This equation can be written as:

$$A_t = A_\infty - S/\log t \qquad (6)$$

which means that a plot of $A_t$ vs. $1/\log t$ should be linear, with intercept $A_\infty$ and slope $(-S)$.

Such a plot is shown in Figure 4 for two representative fabrics at several creasing conditions. The plots are linear from 60 sec. to several days. These plots can be extrapolated to infinite time. It should be noted that none of the plots when extrapolated to infinite time intersect the recovery axis at 100%. This indicates that some "permanent set"—"permanent" in the absence of external forces: gravity, flexing, etc.—is introduced into fabrics when they are creased. It should also be noted that the slope varies with the type of fiber and with the creasing conditions. The latter appear from these data to produce a decrease in the initial recovery and an equal increase in the delayed recovery, so that the net result is the same recovery at infinite time.

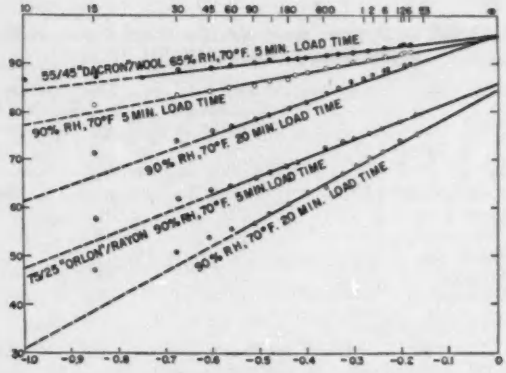
55/45 "DACRON"/WOOL 65% RH, 70°F. 5 MIN. LOAD TIME
90% RH, 70°F 5 MIN. LOAD TIME
90% RH, 70°F. 20 MIN. LOAD TIME
75/25 "ORLON"/RAYON 90% RH, 70°F. 5 MIN. LOAD TIME
90% RH, 70°F. 20 MIN. LOAD TIME

**Fig. 4.** Empirical relation of crease recovery to time; long time Equation 6; $A_t = A_\infty - S/\log t$. Scales: top, seconds, hours, days; left, percent crease recovery; bottom $-1/\log t$.

Equation 6 was modified as follows to extend the linearity to 5 sec. so that all of the collected experimental data could be used in defining the curve:

$$A_t = A_\infty - \frac{S}{\log (t + 11)} \qquad (7)$$

A plot of crease recovery vs. $1/\log (t + 11)$ is linear over the range of experimental data from 5 sec. to several days (Figure 5).

Equation 7 is simple to use even in routine test procedures. As shown in Figure 5, graph paper marked directly in time can be used. Since the correction factors applied to Equation 6 have little effect on the plot at times greater than 60 sec., Equation 6 can be used if short-time data are not desired.

The following properties of a fabric can be obtained from Equations 4 and 7 and crease recovery vs. time data collected over the time period of 10–300 sec.:

$A_1$—Crease recovery at 1 sec.; a measure of the "immediate" recovery of a fabric

$A_\infty$—Crease recovery at infinite time

$(100 - A_\infty)$—A measure of the permanent set in creasing

$(A_\infty - A_1)$—A measure of the delayed recovery from creasing

$S$—A constant which characterizes the rate of delayed recovery

The parameter $A_1$ when measured at both 65% RH and 90% RH generally ranks fabrics in the

**TABLE III. Crease Recovery Parameters for Fabrics of Various Fibers (Measured at 65% RH, 70° F.)**

| Fiber | $A_1$,* % | Limits,† % | $A_\infty$,‡ % | Limits,† % | $S$,‡ % log sec. | Limits,† % log sec. | No. of samples tested |
|---|---|---|---|---|---|---|---|
| Dacron | 79 | 3 | 90 | 3 | 10 | 1 | 4 |
| Wool | 72 | 2 | 96 | 1 | 18 | 2 | 7 |
| Orlon | 54 | 3 | 88 | 4 | 27 | 2 | 4 |
| Rayon—treated | 51 | 5 | 93 | 5 | 40 | 2 | 3 |
| Cotton—treated | 50 | 5 | 73 | 4 | 22 | 3 | 3 |
| Rayon—untreated | 33 | 4 | 72 | 4 | 36 | 2 | 2 |
| Cotton—untreated | 32 | 3 | 51 | 3 | 21 | 3 | 3 |

* From Equation 4.
† Fiducial limits at 90% confidence.
‡ From Equation 7.

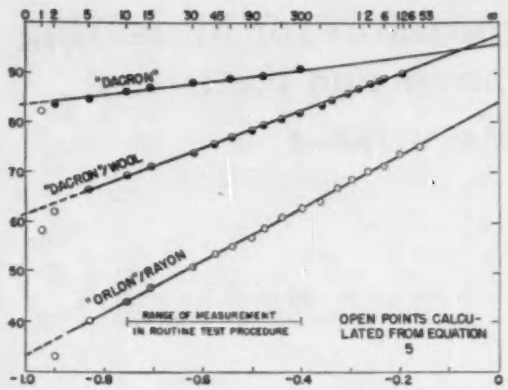
0 1 2 5 10 15 30 45 90 300 1 2 6 12 6 12 6 5 3 ∞
"DACRON"
"DACRON"/WOOL
"ORLON"/RAYON
RANGE OF MEASUREMENT IN ROUTINE TEST PROCEDURE
OPEN POINTS CALCULATED FROM EQUATION 5
-1.0 -0.8 -0.6 -0.4 -0.2 0

**Fig. 5.** Empirical relation of crease recovery to time over the time range 1 sec.–infinity; long time Equation 7; $A_t = A_\infty - S/\log\ (t + 11)$. Scales: top, seconds, hours, days; left, percent crease recovery; bottom, $-1/\log\ (t + 11)$.

**TABLE IV. Crease Recovery Parameters for Fabrics of Comparable Construction (65% RH, 70° F.)**

| Composition of fabric | $A_\infty$* | $S$* | $A_1$† |
|---|---|---|---|
| 100% Cotton | 48 | 23 | 30 |
| 70/30 Dacron/cotton | 77 | 14 | 60 |
| 85/15 Dacron/cotton | 85 | 10 | 74 |
| 100% Dacron | 86 | 9 | 76 |
| 85/15 Dacron/rayon | 84 | 14 | 68 |
| 70/30 Dacron/rayon | 82 | 21 | 58 |
| 55/45 Dacron/rayon | 81 | 27 | 45 |

* From Equation 8.
† From Equation 5.

same order as they are ranked during wear; the parameter $S$ generally ranks them in the same order as the magnitude of their overnight wrinkle recovery.

These parameters vary with fiber type, as shown in Table III. The type of fabric used in this study varied; e.g., the wool series included tropicals, crepes, worsteds, and sharkskins. The variation in crease recovery data with fabric type, however, was small compared to the differences between fiber type. Although it is certain that fabric structure influences recovery behavior, a discussion of this influence is outside the scope of this paper.

The main contribution of resin to cotton and rayon appears to be to increase $A_1$, the immediate recovery from wrinkling. There is little if any change in $S$, the rate of subsequent recovery.

As shown in Table IV and Figures 6 and 7, $A_1$, $A_\infty$, and $S$ vary linearly with composition for blend fabrics of comparable construction. In blends of Dacron with cotton and rayon, the Dacron fiber contributes a high immediate recovery to the fabric,

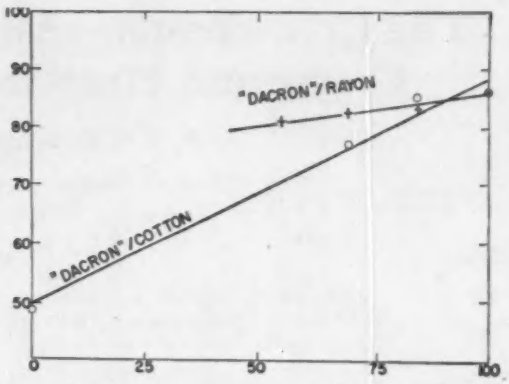


**Fig. 6.** Relation of percent recovery at infinite time (vertical scale) to blend composition (percent Dacron).

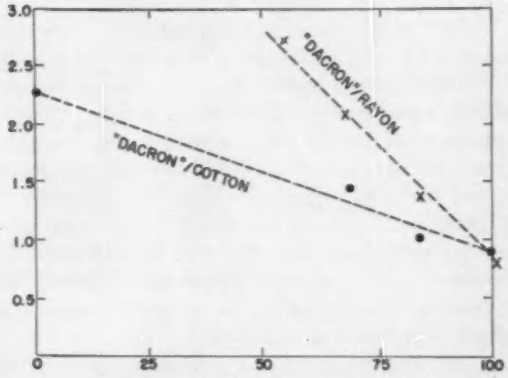


**Fig. 7.** Relation of delayed recovery constant (vertical scale) to blend composition (percent Dacron).

being reduced proportionately to the percent of cotton or rayon present. The reduction is reflected by a permanent loss of some recovery (see $A_\infty$, Table IV) and by a change of fast immediate recovery into a more delayed kind (see $A_1$ and $S$ of Table IV). The total recovery $A_\infty$ is not lowered as much by rayon as by cotton, as shown in Table IV and Figure 6. This is what would be expected on the basis of the data in Table III.

### Acknowledgment

The authors wish to express their appreciation to Drs. R. M. Hoffman and A. G. Scroggie for their assistance and guidance.

### Literature Cited

1. American Society for Testing Materials, "1955 Book of ASTM Standards," Part 7, Method D1295–53T (1955).
2. Sommer, H., *Melliand Textilber.* **33**, 201 (1952).

*Manuscript received March 17, 1958.*

# The Creasometer—An Apparatus for Measuring Crease and Pleat Sharpness and Retention

**P. R. Wilkinson and D. W. Ireland**

*E. I. du Pont de Nemours & Co., Inc., Textile Fibers Department, Wilmington, Delaware*

**Abstract**

This paper describes an instrument designed to measure the sharpness of a crease or pleat in a fabric specimen. Such data can be used to predict the behavior of garment creases during wear and after washing.

## Introduction

With the advent of hydrophobic fibers, new concepts of garment performance were introduced to the consumer and the textile industry. One of the outstanding properties of these fibers is their ability to retain an acceptable crease or pleat in a garment exposed to hot, humid conditions—conditions which would normally cause a complete loss of crease in a garment of natural fibers [2]. The wash-wear concept introduced new requisites for garments; for example, in addition to maintaining an unwrinkled appearance they must retain acceptable creases or pleats after washing and drying [3].

Laboratory fabric tests for evaluating the performance of creased fabrics in garments are desirable as quality control standards. Field testing is not only expensive and time-consuming, but often is of questionable value when too few subjects are used.

An instrument has been developed to characterize a crease after pressing and to measure the performance of creases after exposure to conditions simulating wear and after washing and drying. The term "crease" is defined as the deliberate fold in a fabric introduced by the application of heat, pressure, and/or moisture, and not as a fold produced inadvertently during wear. The work described herein refers only to the measurement of crease retention and not to the measurement of "wash and wear" in its entirety.

## Subjective Evaluation of Creases

The degree of sharpness of the crease affects the desirability of the garment for wear. In a study of the subjective evaluation of creases, almost all of a large number of evaluators chose sharper creases as more acceptable for wear. Crease sharpness, the term we have applied to this property of a creased fabric, depends on two geometrical factors: fabric thickness and crease angle. An ideal crease could be produced in an infinitely thin fabric with the adjacent sides parallel (angle = 0). As shown in Table I, increases in peak width (the width of a crease at 0.5 mm. from its tip, which is comparable to twice the fabric thickness) or increases in crease angle (the angle formed by the two sides of the crease) correlate with decreases in the sharpness, evaluated either subjectively or objectively.

Crease retention is the popular term denoting the effect of wear and/or washing on the appearance of creases in garments. Some ambiguity occurs, however, in interpreting crease retention data, because garment creases are frequently evaluated for crease sharpness after wear or washing, with no regard for the degree of sharpness of the original crease—an important factor in determining crease retention. Since most commercial fabrics accept a sharp crease when properly pressed, a fortuitous correlation exists between crease sharpness and crease retention. However, it is important to be able to distinguish clearly among the good retention of a sharp crease, the poor retention of a sharp crease, the good retention of a poor crease, and the poor retention of a poor crease, particularly in the evaluation of experimental fabrics.

In this paper we have used the following definitions which we recommend for use in both field testing and laboratory testing:

*Crease sharpness:* that property of a pressed-in crease which can be subjectively or objectively evaluated by the weighting of the factors—acuteness of crease angle and fabric thickness.

*Crease retention:* the relation of the crease in a subsequent state to the crease in the initial state.

### Principles and Design

The Creasometer is designed to obtain the optical profile of a crease in order that measurements can be made of its geometry. The design is based on the principle that a line on an uneven surface will profile the surface when the line is viewed at a very low angle from a point perpendicular to the line. This principle has been used in studies in various fields [1, 4].

The Creasometer has three major components: a light source and accessories for projecting a band of light onto the creased specimen, a mechanism for positioning the specimen, and an optical measuring system. The optical components are shown schematically in Figure 1 and in the full view photograph of the Creasometer in Figure 2. The mechanical component is shown in Figure 3.

A 300-watt, 35-mm. slide projector provides the source of illumination. For compactness, the beam of light is reflected from two first surface mirrors onto the creased specimen (Figure 1). A razor blade is mounted on the slide holder forming a baffle to produce a sharp profile line across the crease. The edge of the blade is brought into focus on the specimen so that the front third of the specimen is shaded.

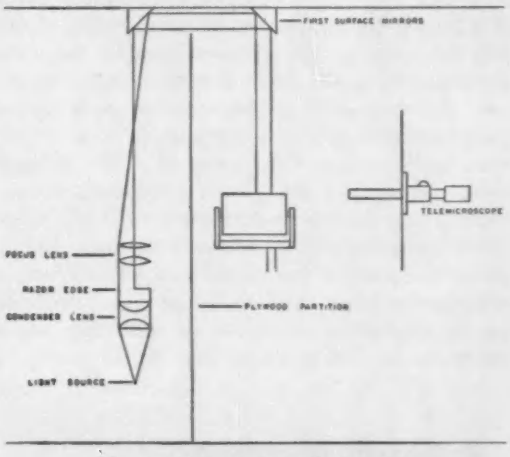


**Fig. 1.** Creasometer optical system.

**TABLE I. Correlation of Creasometer and Subjective Sharpness Data**

| Identification | Subjective sharpness, rank | Creasometer crease sharpness, % | Peak width, mm.† | Crease angle, ° |
|---|---|---|---|---|
| Brown gabardine | 2.1 * | 76 | 1.4 | 34 |
| Checked tweed | 2.3 * | 81 | 1.4 | 22 |
| Gray gabardine | 2.6 * | 73 | 1.7 | 37 |
| Brown gabardine | 3.8 | 61 | 1.7 | 55 |
| Gray gabardine | 4.4 | 65 | 1.9 | 48 |
| Gray gabardine | 5.8 | 57 | 2.4 | 53 |
| Gray tropical | 1.4 | 80 | 1.0 | 30 |
| Black gabardine | 2.5 * | 75 | 1.6 | 34 |
| Gray gabardine | 2.7 * | 78 | 1.0 | 35 |
| Blue flannel | 3.3 | 71 | 1.4 | 44 |
| Checked tweed | 1.9 | 81 | 1.2 | 24 |
| Tan gabardine | 1.9 | 79 | 1.3 | 28 |
| Blue tropical | 2.3 | 71 | 1.5 | 43 |
| Gray flannel | 4.0 | 43 | 3.1 | 70 |
| Black gabardine | 1.9 | 75 | 1.4 | 36 |
| Blue tropical | 1.9 | 76 | 1.3 | 35 |
| Gray gabardine | 2.6 | 73 | 1.4 | 38 |
| Brown gabardine | 3.8 | 71 | 1.5 | 41 |
| Checked tweed (A) | 1.8 * | 84 | 1.2 | 19 |
| Black gabardine | 1.9 * | 82 | 1.3 | 25 |
| Blue striped tropical | 3.0 | 78 | 1.2 | 33 |
| Checked tweed (B) | 3.4 | 74 | 1.4 | 50 |

* Not a statistically significant difference.
† Width at 0.5 mm. from tip of crease.

A plastic cylinder 3 in. in diameter and 6 in. in length holds the specimen horizontally on the positioning mechanism. This cylinder permits the creased fabric to assume a shape which is very similar to that occurring in wear.

Three separate movements of the specimen are necessary to position it properly for measurement. The positioning mechanism must be capable of raising and lowering the specimen to place the crease apex tangent to the 2-mm. line in the eyepiece reticle. Rotation of the plastic cylinder about its axis permits alignment of the crease apex with the vertical reticle scale so that crease width can be measured. Rotation of the cylinder horizontally about a vertical axis passing through the crease apex where the illumination and shadow meet in sharp contrast allows alignment of the crease axis with the axis of the telemicroscope, so that a true profile of the crease can be measured. Provisions for these three movements can be seen in Figure 3.

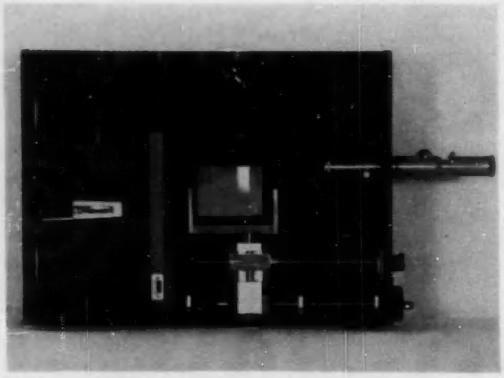

**Fig. 2.** Creasometer (side view).

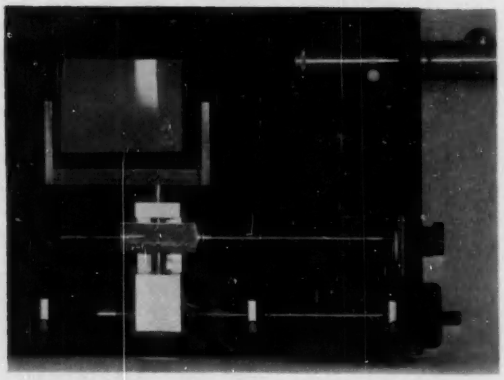

**Fig. 3.** Detail of positioning mechanism.

A telemicroscope, equipped with wide-field eyepiece and adjusted to produce a 15-power magnification, permits measurement of crease width. When the specimen is correctly positioned, the crease line is a continuation of the axis of the telemicroscope; hence, this axis is perpendicular to the profile line.

Crease sharpness is calculated from a measurement of crease width. In addition to yielding a satisfactory measurement of crease sharpness, crease width data can be plotted to obtain a pictorial record of the specimen.

The reticle used in the telemicroscope for the measurement of crease width was fabricated in our laboratory, since the desired scales were not stock items available through commercial sources. As shown in Figure 4, the horizontal scale is divided into 240 equal parts with major divisions every 10 units. Each major division represents 0.5 mm. at 15-power magnification. The vertical scale has major divisions at 0.05, 0.2, 0.5, 1, 2, and 3 mm. below the horizontal scale. Crease width is measured at the 2.0-mm. division. The other divisions of the vertical scale are used for an accurate plot, if pictorial data are required.

## Experimental Procedure

Three specimens, 4-in. warp by 8-in. filling, are cut from each fabric sample. The specimens are folded to 4-in. squares and pressed on a commercial Hoffman trouser press. To reproduce commercial pressing conditions on our press, a steam pressure of 75 lb./sq. in. was necessary for a 3 sec. head steaming period followed by 3 sec. of vacuum. The specimens are placed flat on a table top and condi-

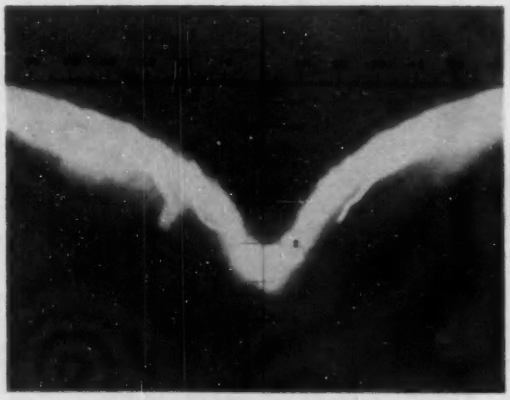

**Fig. 4.** Telemicroscope reticle.

tioned for 24 hr. at 70° F., 65% RH, then exposed to 80° F. and 80% RH during crease removal for a period of 5 hr. The specimens are opened and placed apex downward on a uniformly smooth surface, such as tempered Masonite, for the first 2 hr. A load of 15 g. per linear inch of crease is applied for the remaining 3 hr.

The load is applied by a strip of brass, 4 × 0.85 × 0.125 in., weighing 60 g. After having been pressed for 3 hr., the specimens are hung by one end to recover for 24 hr. at 70° F., 65% RH and then measured as follows.

With the crease apex pointing outward, one end of the specimen is attached to the narrow strip of sandpaper on the surface of the specimen holder. As the holder is rotated by the positioning knob, the specimen is "rolled" onto the cylinder with the crease under the tension of one-half the weight of the specimen. To accommodate fabrics exhibiting a smooth surface, double-faced pressure-sensitive tape may be applied to the cylinder in place of the sandpaper.

The cylinder is rotated until the crease apex is in line with the axis of the telemicroscope. Final adjustments are made by viewing the crease through the telemicroscope. When correctly adjusted, the crease should appear as in Figure 4. Final adjustments include vertical alignment of the crease, equalizing the halo of light below the crease, and positioning the crease apex on the 2.0-mm. line of the vertical scale. When positioned as specified above, the crease width is read directly on the horizontal scale.

Crease removal during washing is simulated by agitating the specimens for 10 min. in an automatic washer. Before the spin cycle occurs, the specimens are removed and hung by one end to dry. After a 16-hr. drying period, they are measured with the Creasometer as described previously.

The crease sharpness of any crease can be expressed as a percentage of the crease width limits (zero reading for an ideal crease; infinite reading for a flat fabric with no crease) by the following relation:

$$\% \text{ crease sharpness} = 100/K^{(\text{Creasometer Reading})}$$

or

$$\text{Log } (\% \text{ crease sharpness}) = 2 - (\text{Creasometer Reading}) \log K$$

This equation can be written as:

$$\text{Log } A = 2 - 0.002R$$

where $A = \%$ crease sharpness, $R =$ Creasometer width reading at 2.0-mm. from the tip of the crease, and $0.002 = \log K$. The constant $K$ was chosen so that a crease of 50% sharpness would result from a Creasometer width reading of 150, that value which appears to represent a crease of borderline acceptability after five days of wear.

A semilog plot of percent crease sharpness vs. $R$ is linear and passes through the points 100% at 0 reading, 50% at 150 reading, and 0% at an infinite reading.

Crease retention is expressed by the following equation:

$$\% \text{ crease retention} = 100 \times \frac{\% \text{ crease sharpness (final state)}}{\% \text{ crease sharpness as pressed}}$$

This instrument is applicable for the measurement of crease sharpness as commercially pressed, crease sharpness as hand pressed, crease sharpness as worn, crease sharpness after washing, and crease retention.

## Discussion of Results

As shown by Table I, crease sharpness data obtained with the Creasometer rank creases in the same order as they are ranked by subjective evaluation. Each subjective rank is the average of the data obtained using 20 subjects. The subjects were asked to rank the creases in each series and to indicate the basis for their decision. Ninety-five per cent indicated that the appearance of pointedness or sharpness of the crease was the decisive factor and that this appearance was governed by the width of the crease line and by the curvature of the crease. For the most part, an increase in crease width or crease angle results in a decrease in both objective and subjective crease sharpness (Table I).

The subjective data were found to be somewhat dependent on the color and pattern of the fabric and on past experiences of the raters. Patterns, especially checks and stripes, tend to decrease the crease sharpness rating by breaking up the continuous nature of the shadows cast by a crease and the light reflected from the crease (see checked tweed in Table I). Some fabrics were rated better in crease sharpness than would have been expected for the shape of the crease. For example, in the case of flannel fabrics, raters appeared to be basing their ratings in part on what a flannel fabric crease would normally be expected to look like. Since creases in these fabrics

**TABLE II. Comparison of Laboratory and Field Data**

| Fabric | Laboratory | | | Field* | |
|---|---|---|---|---|---|
| | Initial | Sim. wear | Wash | Wear | Wash |
| Dacron, filament-spun | 81% | 76% | 70 | 1 | 2 |
| Dacron | 76 | 69 | — | 2 | — |
| 65/35 Dacron/rayon | 75 | 67 | — | 2 | — |
| 65/35 Dacron/rayon | 78 | 67 | 62 | 2 | 2 |
| 70/30 Orlon/wool | 78 | 63 | 53 | 2 | 2 |
| Wool | 80 | 62 | 10 | 2 | 5 |
| Dacron/Orlon, filament-spun | 82 | 59 | 58 | 2 | 2 |
| 75/25 Dacron/rayon | 73 | 57 | 55 | 2 | 2 |
| 55/45 Dacron/wool | 73 | 57 | 54 | 2 | 2 |
| 55/45 Dacron/wool | 73 | 56 | — | 2 | — |
| 70/30 Wool/Dacron | 73 | 55 | 15 | 2 | 5 |
| 50/50 Dacron/wool | 75 | 52 | — | 2 | — |
| 65/35 Dacron/rayon | 71 | 50 | 49 | 2 | 2 |
| 75/25 Wool/Dacron | 74 | 49 | 10 | 3 | 5 |
| 65/35 Dacron/cotton | 72 | 47 | — | 2 | — |
| 50/50 Dacron/cotton | 71 | 47 | 41 | 3 | 3 |
| 75/25 Wool/Dacron | 70 | 39 | 30 | 4 | 5 |
| 80/20 Rayon/Dacron | 79 | 39 | 10 | 4 | 5 |
| Rayon/acetate | 78 | 33 | 10 | 5 | 5 |
| Cotton | 63 | 23 | 10 | 5 | 5 |

* 1—Perfect; 2—satisfactory change; 3—borderline for wear; 4—unsatisfactory change; 5—bad change.

are not normally sharp, a less sharp crease in a flannel was in some cases rated as better than a sharper crease in a fabric such as a gabardine. The effect was not as noticeable in this test where the creases were directly compared as it would be in a test where an absolute rating is given to a fabric without comparative standards.

The data in Table I show a direct comparison between the subjective and the objective measurement of crease properties. The creases which were studied to obtain these data were in the initial state; e.g., representative of fabric creases before wearing. With the exception of one crease, they were all satisfactory, and in most cases would be considered excellent creases.

The relation between crease sharpness after wearing and washing as measured by the Creasometer technique and as evaluated from field testing is shown in Table II. Field data were obtained subjectively from fabrics in commercial use.

As shown in Table II, a satisfactory prediction of the retention of creases after wearing or washing can be made from the laboratory data. Significant differences in crease properties are obtained with the laboratory test for fabrics that are not significantly different in wear because of the variability of the wear rating.

Suiting fabrics containing 100% cotton or nylon show an initial crease sharpness which is lower than that obtained with fabrics containing 100% wool, Dacron,[1] Orlon,[2] rayon, or combinations of these fibers. Steam-pressed fabrics of wool, Dacron, Orlon, or rayon contain sharp creases and show differences in initial crease sharpness (Table II), primarily because of differences in fabric thickness.

In these studies, fabrics of 100% wool generally exhibited satisfactory creases after simulated wear removal of the crease but unsatisfactory creases after washing. Fabrics of 100% Dacron, 100% Orlon, and blends containing majority percentages of these fibers usually exhibited satisfactory creases after both simulated wear removal and washing.

## Summary

Laboratory tests for predicting the performance of fabrics in field use are desirable as replacements for the more expensive and time-consuming procedure of wear testing. The Creasometer test meets part of these requirements, that of predicting the retention of pressed creases in fabrics after wearing and after laundering.

[1] Du Pont's trademark for its polyester fiber.
[2] Du Pont's trademark for its acrylic fiber.

The Creasometer is used to measure the geometry of a crease. This measurement, made on a pressed fabric which has been given a simulated wear and/or washing, can be converted to percent crease sharpness or crease retention and used to predict field performance. In addition, a measurement can be obtained of the ability of a fabric to be creased by any of the available pressing methods.

Crease sharpness data, as obtained objectively with the Creasometer procedure, correlates satisfactorily with wear and with the subjective rating of pressed fabrics.

**Acknowledgment**

The authors wish to express their appreciation to Drs. R. M. Hoffman, A. G. Scroggie, and H. E. Stanley for their assistance and guidance.

**Literature Cited**

1. Finzel, T. G. and Fok, S. M., *Modern Textiles* **37**, 39 (1956).
2. Quig, J. B. and Dennison, R. W., *Ind. Eng. Chem.* **44**, 2176 (1952).
3. Rawlings, G. D., Stanley, H. E., and Wilkinson, P. R., TEXTILE RESEARCH JOURNAL **26**, 974 (1956).
4. Tolansky, S., *Scientific American* **191**, 54 (1954).

*Manuscript received March 7, 1958.*

# The Mothproofing of Wool with Dieldrin

**M. Lipson and J. R. McPhee**

*Wool Textile Research Laboratories, C.S.I.R.O., Geelong, Victoria, Australia*

**Abstract**

Dieldrin does not react with wool but, during treatment in aqueous emulsions, some of the insecticide penetrates the fibers. This small amount, sufficient to mothproof the wool, is not removed by the usual drycleaning solvents which do not cause swelling, but can be extracted completely by hot methanol or acetone. Dieldrin is gradually lost when treated wool is washed in soap solutions, but an initial application of 0.05% on the weight of wool gives a mothproofing effect which withstands machine washing for 3 hr. ASTM Standard Tests have been applied to wool containing 0.05% Dieldrin, and the insectproofing effect found to be fast (Class 3) to laundering, dry and wet cleaning, hot pressing, sea water, acid and alkaline perspiration, light, and rubbing.

Dieldrin has been applied to large amounts of wool at various stages of processing; the results of these industrial trials are given. Treatment should preferably be in the final wet process, since some of the insecticide is removed by subsequent dyeing, bleaching, or milling. Application is preferred from the dyebath when dyeing is the final wet process.

## Introduction

Dieldrin is highly toxic to larvae of the common clothes moth (*Tineola bisselliella* Humm.), the furniture carpet beetle (*Anthrenus flavipes* Le Conte), and the Australian carpet beetle (*Anthrenocerus australis* Hope) [8, 10, 11]. In preliminary work on its use as an industrial mothproofing agent, Lipson and Hope [10, 11] found that the insectproofing effect was unexpectedly fast to washing and drycleaning and suggested that this may be due to chemical combination of Dieldrin with reactive sidechains in the wool.

This paper describes an investigation into the possibility of reaction between wool and Dieldrin and presents further studies on its use in mothproofing, including results of mill trials.

## Experimental

### *Materials*

The fabric for laboratory work was a commercial all-wool flannel made from carbonized Merino pieces.

Unless otherwise stated, the aqueous emulsions used were made from a concentrate in organic solvent of 15% Dieldrin and 6% commercial anionic emulsi-

**TABLE I. Mortality Rates of Moth Larvae on Dieldrin Treated Wool**

| Dieldrin, % on wt. of wool | % Mortality (mean ± standard error of 10 observations) after | | |
|---|---|---|---|
| | 5 days | 6 days | 7 days |
| 0.0001 | 38 ± 4 | 41 ± 4 | 49 ± 5 |
| 0.0005 | 47 ± 4 | 70 ± 4 | 78 ± 4 |
| 0.001 | 50 ± 4 | 78 ± 4 | 89 ± 3 |
| 0.005 | 86 ± 4 | 95 ± 3 | 100 |
| 0.01 | 91 ± 3 | 97 ± 2 | 99 |
| 0.02 | 96 ± 2 | 97 ± 2 | 100 |

fier dispersed in cold water. The emulsifier had no adverse effect on insect larvae at concentrations up to 1% on the weight of wool.

For solid insecticide, technical flake Dieldrin (97%), which had been recrystallized 6 times from ethanol, was used (M.P. 176–177° C.).

All other chemicals used were commercial quality.

### *Methods*

*Application of Dieldrin to wool.* Dieldrin was applied to 8-in. fabric squares by allowing them to take up their own weight of a solution in petroleum ether or ethanol. Alternatively, the fabric was wet out in an aqueous emulsion of Dieldrin and squeezed to leave an amount of liquor equal to the weight of the fabric. The solvent or water was then allowed to evaporate at room temperature. In some experiments, a strip of fabric weighing 70 g. was treated in a small winch dyeing machine containing 3 l. of acidified emulsion until the disperse phase was exhausted.

*Moth and carpet beetle testing.* Tests were made with 21-day-old *Tineola* larvae, or 8-week-old *Anthrenus* larvae, as previously described [9].

*Washing tests.* The method has been previously described [9].

*Bioassay test for estimating Dieldrin on wool.* Varying amounts of Dieldrin were applied to wool from alcoholic or petroleum ether solutions. Five circular samples (1½ in. diameter) were cut from each treated fabric and subjected to the usual moth test. Each sample was tested with four batches of larvae, the numbers alive being counted on the 5th, 6th, and 7th days of the test period. The results, summarized in Table I, show that it is possible to obtain an estimate of the amount of Dieldrin on wool if counts are taken on each of the three days. This method was used in following loss of Dieldrin from wool during washing and drycleaning.

*Drycleaning tests.* White spirit containing 0.1% drycleaning emulsion and 0.025% commercial drycleaning detergent was used. Each drycleaning involved shaking a fabric for 15 min. in the drycleaning liquor, centrifuging for 2 min., drying for 10 min. at 75° C. in a tumble drier, and finally steam pressing for 2 min.

*Extraction and paper chromatography.* Wool was dissolved in boiling 1 *N* sodium hydroxide, the Dieldrin extracted with ethyl acetate, the extract dried with anhydrous sodium sulfate, concentrated and transferred quantitatively to filter paper for chromatography by the method of Mitchell and Patterson [12]. It was possible to detect 0.001% Dieldrin on a 1-g. sample of wool.

*Rates of absorption of Dieldrin from emulsions.* Samples of conditioned fabric (1 g.) were wet out *in vacuo* in various buffer solutions and allowed to stand overnight. The wool, in buffer, and 100 ml. of a 0.02% Dieldrin emulsion in similar buffer were each brought separately to the required temperature. The wool was removed, attached immediately to a stainless steel gauze frame connected to a rod from a stirrer motor, and immersed in the emulsion. The frame was rotated at 25 rpm. Dieldrin concentrations were determined turbidimetrically with a Spekker absorptiometer on samples of emulsion withdrawn at measured time intervals.

*Dyeing.* Strips of fabric (70 g.) were dyed in the laboratory winch dyeing machine according to manufacturers' directions for each dye.

*Bleaching.* Strips of fabric (70 g.) were bleached in the winch dyeing machine for 2 hr. at 50° C. in 3 l. of 3 vol. hydrogen peroxide at pH 9.2 (0.05 *M* borate). The fabrics were rinsed in three changes of water and air-dried.

*Piece scouring.* Strips of fabric (70 g.) were scoured for 30 min. in 5% soap solution at 50° C. in the laboratory winch machine. The fabrics were washed off for 30 min. (3 changes of water) at 40–50° C.

## Results and Discussion

### *Possible Reaction of Dieldrin with Wool*

Previous work on the fastness properties [11] suggested the possibility of chemical combination of Dieldrin with wool; also, from the chemistry of simple epoxides it appeared that Dieldrin might react with amino, phenolic, or carboxyl side chains [6].

Dieldrin was found not to react with the thiol

groups of cysteine or thioglycollic acid either from alcoholic solutions at the boil or from aqueous emulsions at 50° C. Since thiol groups generally react more readily with epoxides than the other functional groups mentioned above [6], it is unlikely that reaction could take place with wool. The extraction and chromatographic method showed that treated wool retained small amounts of Dieldrin after 30 extractions with hot benzene, although no residual Dieldrin could be detected after the wool had been washed in 20 changes of alcohol and acetone (1:1) mixtures, a procedure which would not have broken any new covalent bonds. Thus, there is no reaction between Dieldrin and wool, the fastness properties of the treatment to solvent extraction being due to small amounts of insecticide which penetrate the wool fibers and can be removed only by solvents capable of swelling the fibers.

*Rates of Absorption of Dieldrin from Emulsions*

The initial rates of absorption, estimated graphically, are given in Table II. As drop size varied slightly with pH and temperature, calibration curves had to be determined separately in each instance. Further, the emulsions were affected by stirring so that a control, stirred in the absence of wool, had to be included for each experiment.

It is unlikely that the increase in rate of absorption with decreasing pH is due to a small change in drop size observed. This increased rate is almost certainly due to the wool, positively charged in acid solution, strongly attracting the negatively charged emulsion drops.

*Amounts of Dieldrin Required for Protection of Wool*

Varying amounts of Dieldrin were applied to fabrics from alcoholic or petroleum ether solutions of different concentrations. Results of moth tests are given in Table III.

In the absence of yeast extract, 0.0005% Dieldrin protects wool against moth larval attack, but 0.005% is necessary for protection from carpet beetle larvae or from moth larvae when yeast extract is added. When the Dieldrin concentration was 0.005% or greater, all the carpet beetle larvae died in 3–4 weeks without eating any more wool than indicated in Table III. These concentrations are much lower than the amounts of other insecticides needed to prevent attack [5]. The resistance of different strains of insects to Dieldrin can vary considerably [1], so it is possible that the minimum effective concentrations found could differ between laboratories.

As newly hatched larvae are usually involved in any attack on wool, moths and beetles were allowed to lay eggs for 1 day on Dieldrin-treated fabrics. The eggs were not destroyed; larvae hatched out in the usual time. With 0.02% Dieldrin on the weight of wool, all died within 12–24 hr. Even 0.0001% Dieldrin killed newly hatched moth larvae in about 24 hr.

*Drycleaning Fastness*

Fabrics containing 0.02% Dieldrin (applied from emulsion at pH 7) were Soxhlet-extracted for 3 days with methanol or acetone, or for 4 days with benzene. The mothproofing effect of Dieldrin was removed by methanol and acetone, but 0.0005% Dieldrin, which still protected the wool from moth larval attack, remained after the benzene extraction. Since the solubilities of Dieldrin in methanol, acetone, and benzene are 5, 54, and 75 g./100 ml. respectively [4], the results must mean that solvents which cannot penetrate the wool will not completely remove

**TABLE II. Rates of Absorption of Dieldrin from Emulsions**

| Temp., °C. | pH | Initial rate of absorption, μmole/g. wool/min. |
|---|---|---|
| 20 | 2.8 | 2.1 |
| 30 | 2.8 | 3.1 |
| 40 | 2.8 | 4.7 |
| 20 | 5.0 | 0.6 |
| 20 | 7.0 | nil |
| 20 | 9.1 | nil |

**TABLE III. Protection of Wool against Insect Attack by Dieldrin at Low Concentrations**

| | Moth test on unbaited fabric | | Moth test on baited fabric* | | Carpet beetle test on unbaited fabric | |
|---|---|---|---|---|---|---|
| Dieldrin, % on wt. of wool | Wt. loss, mg. | Mortality, % | Wt. loss, mg. | Mortality, % | Wt. loss, mg. | Mortality, % |
| — | 49 | 20 | 99 | 5 | 71 | 5 |
| 0.0001 | 13 | 90 | 40 | 50 | 57 | 0 |
| 0.0005 | 3 | 90 | 20 | 75 | 26 | 5 |
| 0.001 | 6 | 90 | 12 | 85 | 25 | 5 |
| 0.005 | 2 | 100 | 5 | 95 | 5 | 35 |
| 0.01 | 1 | 100 | 3 | 100 | 3 | 60 |
| 0.02 | 1 | 100 | 3 | 100 | 1 | 80 |

* Fabrics were baited with an aqueous yeast extract [13].

the insecticide, the small amount remaining being sufficient to mothproof the wool. However, solvents which penetrate the fibers remove the final traces of Dieldrin.

Fabrics treated as indicated in Table IV were drycleaned with white spirit, trichlorethylene, or perchlorethylene.

It can be seen from Table IV that the mothproofing effect of Dieldrin is fast to the three commonly used drycleaning solvents. Perchloroethylene and trichlorethylene extraction imparted a certain degree of moth resistance to untreated fabrics.

There is a striking difference in drycleaning fastness of Dieldrin when applied from petroleum ether solution or aqueous emulsion. In the former, Dieldrin is simply deposited on the outside of the fibers, and 0.4% on the weight of wool can be completely removed by 5–10 dry cleanings. However, when applied from aqueous emulsion, a small amount of Dieldrin is absorbed into the fibers and is not extracted by the drycleaning solvents. Thus, initial application of as little as 0.04% Dieldrin gives a mothproofing which persists for at least 30 drycleanings. The pH of application does not affect the amount of Dieldrin resisting drycleaning.

The resistance of treated wool to carpet beetle larvae is lost after 5 or 6 drycleanings, since the amounts of Dieldrin inside the fibers are not sufficient to protect the wool.

*Washfastness*

The rate of removal of Dieldrin from treated wool depends on the detergent power of the washing liquor (Table V). Similar results have been found with DDT [7].

With 1% soap, the mothproofing effect was lost after 4–8 quarter-hour washes, but with 0.2% soap, it resisted almost 20 washes. The protection given by 0.1% Dieldrin against carpet beetle larvae was removed after 4 washes in 0.5% soap.

The proprietary soap powder was not as effective as pure soap at the same concentration, whereas Lissapol N and soap were similar. The results did not show whether Teepol removed Dieldrin from wool or not, since enough Teepol had been absorbed by an untreated sample during a 3-hr. washing to render it mothproof [9]. In washing mothproofed goods, it would probably be desirable to use an anionic synthetic detergent to obtain the added effect of such compounds.

**TABLE IV. Drycleaning Fastness Tests on Dieldrin Treated Wool**

| Method of application of Dieldrin | Initial Dieldrin concn., % | Drycleaning solvent | Number of dry cleanings | Moth test | | |
|---|---|---|---|---|---|---|
| | | | | Final Dieldrin concn.,* % | Wt. loss, mg. | Mortality, % |
| From petroleum ether solution | 0.02 | white spirit | 2 | 0.0005 | 9 | 90 |
| | | | 4 | 0.0001 | 15 | 75 |
| From petroleum ether solution | 0.1 | white spirit | 5 | nil | 12 | 75 |
| From petroleum ether solution | 0.4 | white spirit | 5 | 0.0001 | 6 | 95 |
| | | | 10 | nil | 12 | 85 |
| From anionic aqueous emulsion at pH2 | 0.05 | white spirit | 20 | 0.001 | 2 | 100 |
| | | | 30 | 0.001 | 2 | 100 |
| From anionic aqueous emulsion at pH 2 | 0.1 | white spirit | 20 | 0.002 | 1 | 100 |
| | | | 30 | 0.001 | 1 | 100 |
| From anionic aqueous emulsion at pH 2 | 0.1 | trichlorethylene | 10 | 0.002 | 1 | 100 |
| | | | 30 | 0.001 | 1 | 100 |
| From anionic aqueous emulsion at pH 2 | 0.1 | perchlorethylene | 10 | 0.002 | 1 | 100 |
| | | | 30 | 0.002 | 1 | 100 |
| From anionic aqueous emulsion at pH 7 | *c* 0.005 | white spirit | 12 | 0.001 | 2 | 100 |
| From anionic aqueous emulsion at pH 7 | *c* 0.02 | white spirit | 12 | 0.001 | 2 | 100 |
| From anionic aqueous emulsion at pH 9 | *c* 0.01 | white spirit | 12 | 0.001 | 1 | 100 |
| Treated in emulsifier only | nil | white spirit | 20 | nil | 48 | 10 |
| Treated in emulsifier only | nil | trichlorethylene | 30 | nil | 12 | 85 |
| Treated in emulsifier only | nil | perchlorethylene | 30 | nil | 15 | 85 |

* From bioassay test.

As reported earlier [11], Dieldrin applied from an emulsion shows greater washfastness than when applied from petroleum ether solution. This was confirmed in the present work.

Bioassay tests showed that with an anionic emulsion at pH 7, more Dieldrin was taken up than calculated from liquor uptake, but at pH 9, much less was taken up than calculated, due to repulsion between the negatively charged fibers and negatively charged emulsion drops. Using a cationic emulsion at pH 9, more Dieldrin went onto the wool, but complete exhaustion did not occur. The cationic emulsion at pH 9 was not as good as the anionic in acid solution.

*Effect of Subsequent Wet Processing*

Dieldrin (0.05% by weight) was applied to wool from aqueous emulsions at pH 2. The fabrics were then dyed with Naphthalene Scarlet 4RS or Neolan Green BL, or bleached with peroxide.

Bioassay tests indicated that dyeing or bleaching reduced the Dieldrin concentration to about 0.001%. This residual Dieldrin was removed by 4 quarter-hour washes in 0.5% soap but not by 12 drycleanings.

These results, together with those in Table V, showed that goods should preferably not be treated prior to dyeing, bleaching, or milling.

*Insect Tests on Wool taken from Sheep Dipped in Dieldrin*

It has been reported [11] that wool taken from sheep 3 months after dipping in Dieldrin emulsions was mothproof both in the greasy and scoured state.

It has now been found that greasy wool from sheep dipped 6 months previously in 0.1% or 0.01% (wt./vol.) emulsions is mothproof, residual Dieldrin from the more concentrated emulsion protecting the wool from carpet beetle larvae also. The mothproofing effect from the stronger solution also persisted after scouring, but that of the weaker was removed. Thus, although dipping or jetting with Dieldrin could give some degree of protection later, mill treatment is essential for a satisfactory result.

*Persistence of Mothproofness*

Dieldrin-treated fabrics have shown no significant loss in resistance to insect attack over periods of up to four years. A sample of carpet exposed to the weather for two years was still protected, although the color had faded beyond recognition. Earlier experiments [11] showed that the treatment was still effective after four months' outdoor exposure. These tests were continued for seven months, by which time the samples had deteriorated to such an extent that further tests were impossible. Despite this degradation, the wool was still resistant to insects.

It is likely, therefore, that the mothproofing effect of Dieldrin should persist over long periods and afford protection for the normal life of garments which are not frequently washed.

*Evaluation of Treatment by Standards of the American Society for Testing Materials*

Wool was treated with Dieldrin by immersion in an emulsion at pH 2 (sulfuric acid) containing 0.05% Dieldrin on the weight of wool, raising the temperature to the boiling point over 15 min., and boiling for a further 5 min. After being rinsed in water, the fabric was air-dried.

Insect testing was carried out according to ASTM designation D582–54 [2], except that larvae of *Anthrenus flavipes* were used in place of *Attagenus piceus* (Oliv.) for carpet beetle testing. The performance of treated fabrics in service tests was evaluated by the standard tests of ASTM designation D627–54 [3].

The insectproofing effect of Dieldrin passed all tests, being fast to laundering, dry and wet cleaning, hot pressing (damp and dry), sea water, acid and alkaline perspiration, light, and rubbing. Although some Dieldrin was removed, the wool was still unattacked by either clothes moth or carpet beetle larvae after the most severe of the fastness tests. On ASTM Standards, therefore, Dieldrin treatment for insectproofing wool is Class 3.

*Application of Dieldrin in Processing*

Experiments were carried out to ascertain the most suitable stages for large scale application.

*During acid-dyeing.* Fabrics were dyed with Naphthalene Scarlet 4 RS at pH 2.2; 0.05% Dieldrin on the weight of wool is added either at the start of the dyeing or at various times up to within 10 min. of boiling being discontinued. In all instances, washfastness of the treatment was better than when the same amount of Dieldrin was applied to undyed wool from acidified aqueous emulsions (Table VI).

*After dyeing.* Fabrics were dyed with Naphthalene Scarlet 4 RS, rinsed, and 0.05% Dieldrin

applied by emulsion-exhaustion to the wool from the rinse liquor at 25–30° and pH 3.1 for 15 min. After treatment, the wool was rinsed, squeezed, and air-dried. The washfastness of this treatment (Table VI) was slightly better than when Dieldrin was similarly applied to undyed wool, but was not as good as when applied during dyeing.

*After peroxide bleaching.* Bleached wool, treated in an anionic emulsion at pH 9.1 for 15 min. at 25–30° C., gave similar results to unbleached wool. Application from a 0.1% (wt./vol.) Dieldrin emulsion at pH 9 provided sufficient Dieldrin for the mothproofing effect to withstand 12 washes, but very little Dieldrin was taken up from more dilute emulsions.

More Dieldrin went onto the wool when a cationic emulsion was used at pH 9 but, as with unbleached wool, complete exhaustion was not obtained.

The most satisfactory method was to acidify the rinse liquor after bleaching and apply Dieldrin from an anionic emulsion (Table VI).

*After piece-scouring or milling.* The results were similar to those described in the previous section; the most satisfactory and economical method of application involved rinsing thoroughly, reducing the pH to 5 or less with sulfuric acid, and allowing the emulsion to exhaust onto wool.

**TABLE V. Effect of Washing on Dieldrin Treatment ***

| Wash liquor | pH of wash | No. of washes | Dieldrin,† % | Moth test: Wt. loss, mg. | Moth test: Mortality, % |
|---|---|---|---|---|---|
| — | — | — | 0.1 | 1 | 100 |
| 0.2% Soap | 10.0 | 12 | 0.002 | 3 | 100 |
| | | 20 | 0.0001 | 12 | 90 |
| 0.5% Soap | 10.1 | 8 | 0.001 | 5 | 100 |
| | | 10 | 0.0005 | 8 | 90 |
| | | 12 | 0.0001 | 13 | 80 |
| 1% Soap | 10.3 | 4 | 0.001 | 6 | 95 |
| | | 8 | nil | 17 | 80 |
| 0.5% Teepol 610 | 8.0 | 12 | Untreated control | 5 | 90 |
| | | 8 | —‡ | 4 | 100 |
| | | 12 | —‡ | 5 | 100 |
| 0.5% Lissapol N | 7.8 | 12 | Untreated control | 12 | 90 |
| | | 8 | 0.001 | 7 | 95 |
| | | 12 | 0.0001 | 15 | 80 |
| 0.5% Proprietary soap powder | 10.5 | 12 | Untreated control | 27 | 75 |
| | | 8 | 0.001 | 5 | 100 |
| | | 12 | 0.0005 | 7 | 100 |

* Initial Dieldrin concentration was 0.1% on wt. of wool, applied from aqueous emulsion; all washing was done at 50° C.
† From bioassay test.
‡ No estimate could be made because of the effect of Teepol itself.

## Mill Trials

Details of treatment conditions are given in Table VII.

### *Treatment of Pieces*

Dieldrin was applied to pieces in five different mills at various stages of processing. Samples for testing were taken after the pieces had been finished; blankets, for example, had been hydro-extracted, tentered, and raised. Table VII shows that satisfactory mothproofing can be obtained during dyeing or in rinse liquors after dyeing, bleaching, or milling. Larval testing of piece goods indicated clearly that Dieldrin was applied evenly during these treatments.

### *Treatment of Tops*

Dieldrin was applied to tops during dyeing or in the rinse liquor after dyeing (Table VII). The mothproofing effect on knitted fabric made from these treated samples resisted a 2-hr. washing and 20 dry cleanings, indicating that the treatment was satisfactory from the point of view of the finished article. For application during backwashing, 0.1% (wt./vol.) Dieldrin emulsion was made up in the second bowl of a two-bowl unit, capacity 55 gal., temperature 45° C., and roller expression 50%.

**TABLE VI. Fastness Properties of 0.05% Dieldrin Applied in Processing**

| Method of application | No. of washes | No. of dry cleanings | Dieldrin,* % | Moth test: Wt. loss, mg. | Moth test: Mortality, % |
|---|---|---|---|---|---|
| During acid dyeing, pH 2.2 | — | — | 0.05 | 1 | 100 |
| | 8 | | 0.002 | 2 | 100 |
| | 10 | | 0.001 | 1 | 100 |
| | 12 | | 0.0005 | 6 | 85 |
| | | 30 | 0.001 | 4 | 100 |
| In rinse liquor after acid dyeing, pH 3.1 | — | — | 0.05 | 0 | 100 |
| | 8 | | 0.001 | 1 | 100 |
| | 10 | | 0.0005 | 3 | 100 |
| | 12 | | 0.0001 | 11 | 70 |
| | | 30 | 0.001 | 3 | 100 |
| In acidified rinse liquor after peroxide bleaching (anionic emulsion), pH 1.9 | — | — | 0.05 | 1 | 100 |
| | 8 | | 0.001 | 1 | 100 |
| | 10 | | 0.0005 | 4 | 95 |
| | 12 | | nil | 32 | 35 |
| | | 30 | 0.001 | 5 | 100 |

* From bioassay test.

**TABLE VII. Summary of Mill Trials**

Unless otherwise indicated, 15% Dieldrin concentrate was added to liquor to give 0.05% Dieldrin on the weight of wool. (The mothproofing effects of all the Dieldrin treated samples were fast to 20 drycleanings.)

| Type of goods | Stage of processing at which Dieldrin was applied | Weight of wool, lb. | Volume of liquor, gal. | pH of treatment | Time of treatment, min. | Temperature of treatment, °C. | Dieldrin,* % | Moth test | | Moth test on goods after 8 × ¼-hr. washes | | |
|---|---|---|---|---|---|---|---|---|---|---|---|---|
| | | | | | | | | Wt. loss, mg. | Mortality, % | Dieldrin,* % | Wt. loss, mg. | Mortality, % |
| Piece | During acid dyeing | 80 | 150 | 2.6 | 60 | 100 | 0.05 | 2 | 100 | 0.001 | 5 | 100 |
| Piece | Liquor after acid dyeing | 80 | 100 | 5.0 | 15 | 25 | 0.05 | 1 | 100 | 0.0005 | 8 | 90 |
| Piece | In normal rinse liquor after milling | 180 | 60 | 8.1 | 15 | 20 | 0.05 | 2 | 100 | 0.0005 | 7 | 85 |
| Piece | In acidified rinse liquor after milling | 180 | 60 | 4.8 | 15 | 20 | 0.05 | 0 | 100 | 0.0005 | 6 | 90 |
| Piece | In acidified rinse liquors after peroxide bleaching | 90 | 100 | 3.0 | 15 | 25 | 0.05 | 1 | 100 | 0.0005 | 9 | 95 |
| Tops | During neutral dyeing | 180 | 500 | 6.8 | 60 | 100 | 0.05 | 0 | 100 | nil | 30 | 25 |
| | | | | | | | 0.05† | 1 | 100 | 0.0005† | 8 | 95 |
| Tops | In rinse liquor after acid dyeing | 360 | 1000 | 4.1 | 15 | 30 | 0.05 | 3 | 100 | nil | 28 | 30 |
| | | | | | | | 0.05† | 2 | 100 | 0.0005† | 7 | 100 |
| Tops | Backwashing | | | See text | | | | | | See text | | |
| | | | | | | | 0.05† | 4 | 100 | 0.0005† | 9 | 85 |
| Yarn on cones | In rinse liquor after neutral dyeing | 90 | 300 | 6.5 | 15 | 30 | 0.05† | 3 | 100 | 0.0005† | 8 | 90 |
| Yarn in hanks | In rinse liquor after acid dyeing | 250 | 900 | 5.1 | 15 | 25 | 0.05 | 2 | 100 | 0.0005 | 7 | 95 |
| Yarn in hanks‡ | During tape scouring | | | See text | | | | | | See text | | |
| Untreated | Controls | | | | | | nil | 30–40 | 0–10 | nil | 30–40 | 0–10 |

* From bioassay test.
† Moth tests carried out on the finished knitted pieces.
‡ Trial designed to give 0.02% Dieldrin on the weight of wool.

Samples of sliver were taken for mothtesting at the start, half way through, and at the end of the run. All were mothproof, bioassay tests indicating that more than 0.05% Dieldrin was on the first sample and about 0.02–0.05% on later samples. The treated wool was mill-processed and the final knitted fabric tested. From bioassay tests, this appeared to contain about 0.05% Dieldrin, the mothproofing effect being fast to drycleanings and to a 2-hr. washing.

*Treatment of Yarn*

Treatment of yarn on cones or in hanks in the rinse liquors after dyeing in their respective dyeing machines was satisfactory (Table VII).

For application during hank scouring, 0.04% (wt./vol.) Dieldrin emulsion was made up in the third bowl of a tape scouring machine. Dieldrin could not be put in the 4th (rinse) bowl, since the liquor was being changed continually. The pH of the third bowl was 9.4, the temperature 40° C., and the rollers between third and fourth bowls gave 50% expression; 1200 lb. of wool was scoured in about 2 hr. Hanks were taken at the start of the run and then at 200-lb. intervals. Moth larval tests indicated that 0.02% Dieldrin was applied initially, but this dropped to about 0.005% on the final samples. The mothproofing effect on the first sample withstood a 1-hr. washing, but all the Dieldrin was removed from the later samples in a 0.5-hr. washing. Better results could be obtained from more concentrated Dieldrin emulsions, but it may be necessary to top up with Dieldrin during the scouring.

*Use of Nonionic Dieldrin Emulsions*

Industrial trials also have been carried out using Dieldrin emulsions containing a nonionic emulsifier.

When Dieldrin was applied from the dyebath, results were similar to anionic emulsions, but when applied from rinse liquors, especially at liquor ratios greater than 20:1, the results were not as good as with anionic emulsions at pH $< 5$.

## Conclusions

When Dieldrin is applied to wool from organic solvents, surface deposition only is obtained, the amount taken up depending on the uptake of liquor.

However, the disperse phase of anionic emulsions of Dieldrin does have an affinity for wool in acid solutions, since the fiber is then positively charged. The drops of dilute aqueous emulsions therefore can be exhausted onto wool from acid solutions. Some Dieldrin actually penetrates the fibers from emulsions, although most probably is deposited on the surface. This small amount of absorbed Dieldrin is not removed by drycleaning solvents and is sufficient to prevent attack by moth larvae. Thus, the mothproofing effect on wool treated with aqueous Dieldrin emulsions is fast to drycleaning.

Dieldrin is gradually removed from wool by washing in soap solutions, the rate depending on the detergent power of the washing liquor. Processed wool containing 0.05% Dieldrin is still mothproof after a 2-hr. washing in a wash-wheel with 0.5% soap solution at 50° C., since this Dieldrin content is a large excess over the minimum effective amount.

Wet-finishing processes, such as dyeing, bleaching, or milling, considerably lower the concentration of Dieldrin on treated wool. It is not removed completely by these treatments, the wool still being resistant to moth larvae, but the residual Dieldrin is removed by soap solution in a short time.

To obtain the most satisfactory mothproofing of finished goods, it is therefore desirable to apply Dieldrin as the last wet process.

## Acknowledgments

Industrial tests were made possible by the ready cooperation of numerous Australian mills. We are indebted to the local industry for its willing support in undertaking such trials.

We acknowledge with thanks the assistance of Mr. T. Bath and Miss L. Boardman in carrying out the larval tests.

Mr. J. P. Phillips of Shell Chemicals (Aust.) Pty. Ltd. has kindly provided all samples of Dieldrin used in the experiments.

## Literature Cited

1. Ascher, K. R. S., *Riv. parassitol.* **16**, 31 (1955).
2. ASTM Committee D-13, "ASTM Standards on Textile Materials," American Society for Testing Materials, Philadelphia, 119 (1956).
3. ASTM Committee D-13, "ASTM Standards on Textile Materials," American Society for Testing Materials, Philadelphia, 125 (1956).
4. Brown, A. W. A., "Insect Control by Chemicals," New York, Wiley, 3 (1951).
5. Brown, A. W. A., "Insect Control by Chemicals," New York, Wiley, 702 (1951).
6. Fraenkel-Conrat, H., *J. Biol. Chem.* **154**, 227 (1944).
7. Goodall, F. L., Gorton, T. F., and Summersgill, J. V., *J. Soc. Dyers Colourists* **62**, 189 (1946).
8. Kearns, C. W., Weinman, C. J., and Decker, G. C., *J. Econ. Entomol.* **42**, 127 (1949).
9. Lipson, M., *Proc. Int. Wool Text. Res. Conf. Austr. 1955* **E**, 514 (1956).
10. Lipson, M. and Hope, R. J., *Nature* **175**, 599 (1955).
11. Lipson, M. and Hope, R. J., *Proc. Int. Wool Text. Res. Conf. Austr 1955* **E**, 523 (1956).
12. Mitchell, L. C. and Patterson, W. I., *J. Assoc. Offic. Agr. Chemists* **36**, 553 (1953).
13. Swiss Association for Testing Material, Draft Specifications 25/A 3001, 3002 (1949).

*Manuscript received March 7, 1958.*

# Evaluation of Formaldehyde Pretreatment for Wool Bleaching

**J. E. Moore[1] and R. A. O'Connell**

*Western Utilization Research and Development Division, Agricultural Research Service, U. S. Department of Agriculture, Albany 10, California*

**Abstract**

The formaldehyde treatment of wool fibers and fabric prior to bleaching by hot alkaline peroxide solutions has been investigated. Although pretreated fabrics exhibit lower alkali solubility and better handle after bleaching, characteristic degradation, shown by various single-fiber as well as fabric properties, is not retarded by the pretreatment. Formaldehyde pretreatment alone, under the conditions used, lowers the breaking stress and breaking extension of single fibers, but this degradation may not be severe enough to cause concern for many fabric uses. Other experiments, without formaldehyde pretreatment, fail to support the claim that wool fibers possess increased susceptibility to damage when strained prior to bleaching.

## Introduction

Formaldehyde treatment of wool to increase its resistance to solubilization in hot alkaline solutions is the subject of patents as early as 1903 [6]. More recently, there has been renewed interest in the use of formaldehyde to protect wool against solubilization during exposure to the rather vigorous chemical treatments of dyeing [3], carbonizing [4], and bleaching [11]. Damage in these instances commonly is evaluated by the alkali solubility test of Harris and Smith [8], since this requires little specialized technique or equipment. However, the results of this test are not always satisfactorily related to the physical properties of the chemically treated fibers. For example, wool treated with formaldehyde, either before or after exposure to acid, is reported to show decreased damage as determined by decreased solubility in hot alkali, but fails to exhibit corresponding improvement in several single-fiber properties [5].

The literature concerning the reactions of formaldehyde with proteins is extensive, the large number of possible reactions having been limited and clarified in recent years by Fraenkel-Conrat [7]. The elastic properties of formaldehyde treated wool have been examined by Speakman [13] and others [12, 15]. However, it appears that little attention has been paid to the relation of the Harris alkali solubility test to single-fiber and fabric properties of wool treated with formaldehyde prior to peroxide bleaching. Accordingly, this study has been undertaken to evaluate the use of formaldehyde as a protective pretreatment for wool fibers and fabric subjected to hot alkaline peroxide bleach solutions. A second objective is to examine the possibility [9] that wool fibers may exhibit increased susceptibility to damage when strained prior to bleaching.

[1] Now with California Spray-Chemical Corporation, Richmond, California.

## Materials and Methods

An 11-oz. unbleached gabardine of 64s quality Australian wool in the ready-to-dye state was chosen for these studies. The wool was given a preliminary scour with 0.05% Triton X-100, a nonionic detergent, at 120° F. for 30 min., followed by thorough rinsing. Scouring, formaldehyde pretreatment, and bleaching were carried out in a laboratory package dyeing machine to ensure uniformity of treatment. The fabric was first cut into 6½ by 58-in. strips to allow wrapping about the cloth carrier (a perforated dye tube constructed with flanged ends).

### *Formaldehyde Pretreatment*

Half of the gabardine strips were treated at 130° F. for 0.5 hr. by circulating an aqueous solution containing 0.45% formaldehyde (on weight of fabric) adjusted to pH 5.0 as needed with acetic acid. The wool was finally rinsed thoroughly. An uptake of approximately 0.5% was obtained.

*Bleaching Procedure*

The fabric was bleached in two volumes (0.6%) of hydrogen peroxide containing 0.2% tetrasodium pyrophosphate and 0.025% ethylenediamine tetraacetic acid, tetrasodium salt, liquor–wool ratio, 80:1. The pH of the bath was adjusted initially to 9.6 with sodium hydroxide. The temperature was maintained at 150° F.

*Methods of Testing*

1. Alkali solubility was determined from weight decrease following immersion of 400 mg. of the cloth in 40 ml. of 0.1 *M* NaOH for 1 hr. at 65° C. according to the method of Harris and Smith [8]. Prior to treatment with alkali, the samples were unraveled and cut into small pieces to facilitate penetration of the reagent.

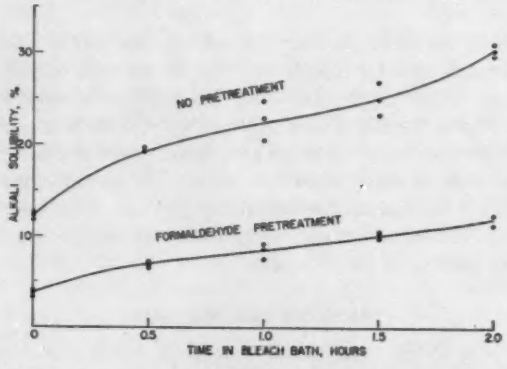


**Fig. 1.** Influence of formaldehyde pretreatment on alkali solubility of peroxide-bleached wool.

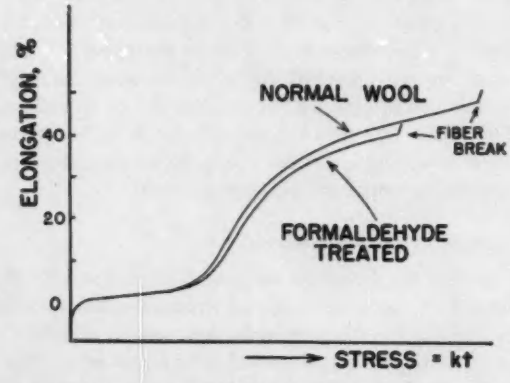


**Fig. 2.** Typical wet stress–strain response of formaldehyde treated vs. normal wool.

2. Force–extension data were obtained from single fibers submerged in water after removal from the treated fabric samples. Testing was carried out at a constant rate of loading of 20 g./tex/min. based on the average tex of the untreated fiber. Measurements were made on 18 warp fibers from each fabric sample. Fibers suitable for calibration were obtained from a sample of Columbia wool that had been thoroughly solvent scoured and washed well with distilled water. For investigation of excessive peroxide damage attributable to prestretching, a series of fibers was vibroscoped and calibrated by stretching 0, 3, 15, and 30% in water. Recovery was allowed to continue overnight in water, the 0% fibers being soaked but not stretched. Six fibers from each class were sewn to a 5 × 5 flannel swatch. The swatches were then subjected to 0.1 *M* buffered solutions at pH 8.0 (boric acid–borax) and 10.0 (sodium bicarbonate–sodium hydroxide) for 1.5 hr. at 150° F. Half the solutions contained hydrogen peroxide at 3 vol. (0.9%) concentration, liquor–wool ratio, 25:1. After being washed well in distilled water, the single fibers were recovered and the stress–strain curves rerun in water. Reduction in work to stretch was calculated for the 30% and 15% stretched fibers in the conventional manner. For the 3% and 0% stretched fibers, ratios of work to stretch 30% after treatment to an average value for the wool under study were used.

3. Fabric properties were determined on samples taken from strips cut from the bolt along the fill. To allow for variation in the cloth, samples for fabric testing were taken from the strips in such a manner that the same warp yarns appeared in any one test.

a. Fabric stiffness was determined by the cantilever method according to ASTM specifications [1]. It is considered that differences in flexural rigidity of about 10% can just be detected subjectively.

b. Breaking strengths were determined on cut strips with the Instron Tester. Wet tests were performed with the samples submerged in water.

c. Tear resistance was obtained by the Elmendorf falling pendulum method [2].

d. Accelerotor abrasion resistance was obtained by abrading the fabric in an Accelerotor at 3000 r.p.m. with 180-grit abrasive [14].

4. Color differences were measured with the Gardner Automatic Color Difference Meter. This instrument expresses color in terms of three parameters: *Rd*, which measures light reflectance or bright-

**TABLE I. Comparison of Wet Single-Fiber Properties of Fibers Removed from Bleached Fabrics ***

| Property | Pretreatment | Hours in bleach bath 0 | ½ | 1 | 1½ | 2 |
|---|---|---|---|---|---|---|
| Stress at 30% extension, g./tex† | None | 4.4 ± 0.6 | 4.0 ± 0.2 | 3.9 ± 0.2 | 3.9 ± 0.2 | 3.8 ± 0.3 |
| | Formaldehyde | 4.8 ± 0.3 | 4.4 ± 0.6 | 4.2 ± 0.2 | 4.2 ± 0.3 | 4.1 ± 0.6 |
| Young's modulus, g./tex | None | 84 ± 10 | 66 ± 6 | 58 ± 6 | 61 ± 4 | 61 ± 8 |
| | Formaldehyde | 82 ± 7 | 74 ± 8 | 79 ± 6 | 73 ± 6 | 67 ± 8 |
| Stress at break, g./tex | None | 8.0 ± 1.3 | 7.7 ± 0.8 | 6.9 ± 0.6 | 6.5 ± 1.1 | 7.0 ± 0.9 |
| | Formaldehyde | 6.7 ± 0.8 | 6.1 ± 1.0 | 5.7 ± 0.7 | 5.9 ± 0.7 | 6.0 ± 0.9 |
| Extension at break, % | None | 46 ± 3 | 47 ± 3 | 47 ± 3 | 43 ± 5 | 47 ± 4 |
| | Formaldehyde | 37 ± 4 | 36 ± 5 | 37 ± 3 | 39 ± 3 | 41 ± 3 |

* Values are the averages of 18 determinations and are given in terms of 95% confidence limits.
† Weight in grams of 1000 m. of fiber.

ness; *a*, a numerical measure of redness when plus and greenness when minus; and *b*, a numerical measure of yellowness when plus and blueness when minus.

## Results and Conclusions

The effects of formaldehyde pretreatment on the alkali solubility of bleached fabrics are shown in Figure 1. It is apparent that the pretreatment offers significant protection against solubilization in hot sodium hydroxide. Moreover, the handle of the unprotected bleached fabrics was noticeably less full and considerably more "slippery" than that of the pretreated bleached fabrics.

The typical effects of formaldehyde treatment on the force–extension curve of single wool fibers tested wet are shown in Figure 2. The curve is displaced along the stress axis to such an extent that 5–10% more work is required to stretch the treated fiber than to stretch the untreated control. Also, the breaking stress and breaking extension are significantly lower for the treated fibers. The recovery behavior following elongation is not significantly changed. Although these effects may be interpreted as reflection of the formation of additional cross-links between the peptide chains, there is no observable change in the degree of supercontraction in hot bisulfite solution—as is the case, for example, after treatment of wool with difunctional isocyanates [10].

A comparison of several wet single-fiber properties of fibers taken from bleached fabrics is given in Table I. All the single-fiber properties measured are seen to decrease with time in the bleach bath, though the decreases are not so large as might be inferred from the 30% alkali solubilities of fabrics bleached 2 hr. Formaldehyde produced a moderate improvement in the values of stress at 30% extension and Young's modulus. Breaking stress and breaking extension, however, are appreciably lowered by formaldehyde alone. The magnitude of the changes may cause little concern in fabric uses where the applied forces are normally small. For other applications, as in papermaker's felts, in which the fabric may be subjected to forces of considerable magnitude

**TABLE II. Properties of Bleached Fabrics**

| Property | Pretreatment | Hours in bleach bath 0 | 1½ | 3 |
|---|---|---|---|---|
| Cantilever stiffness bending length, cm. | None | 1.68 | 1.78 | 2.01 |
| | Formaldehyde | 1.68 | 1.74 | 2.00 |
| Flexural rigidity, mg.-cm. | None | 102 | 123 | 175 |
| | Formaldehyde | 102 | 115 | 173 |
| Breaking strength, lb. (dry) | None | 48.0 | 45.6 | 46.6 |
| | Formaldehyde | 46.3 | 45.9 | 45.7 |
| Breaking elongation, % (dry) | None | 46 | 42 | 41 |
| | Formaldehyde | 43 | 41 | 41 |
| Breaking strength, lb. (wet) | None | 34.0 | 26.6 | 27.0 |
| | Formaldehyde | 28.8 | 26.1 | 25.4 |
| Breaking elongation, % (wet) | None | 71 | 72 | 74 |
| | Formaldehyde | 63 | 70 | 67 |
| Abrasion weight loss, % | None | 5.0 | 6.4 | 6.9 |
| | Formaldehyde | 5.6 | 6.8 | 6.7 |
| Tear resistance, g. | None | 2880 | 2420 | 2200 |
| | Formaldehyde | 2720 | 2250 | 1960 |

**TABLE III. Color Differences of Bleached Fabrics**

| Hours in bleach bath | Pretreatment | Color measurements | | |
|---|---|---|---|---|
| | | *Rd* | *a* | *b* |
| 0 | None | 61.1 | 2.3 | 13.5 |
| | Formaldehyde | 61.3 | 3.1 | 12.0 |
| 1.5 | None | 69.9 | 1.0 | 9.6 |
| | Formaldehyde | 68.6 | 1.5 | 9.6 |
| 3.0 | None | 69.4 | 1.0 | 9.6 |
| | Formaldehyde | 70.8 | 1.4 | 9.6 |

**TABLE IV. Reduction in Work to Stretch for Prestretched Fibers Subjected to Peroxide Bleach**

| Degree of prestretch, % | Treatment | |
|---|---|---|
| | Peroxide | Buffer |
| | pH 8.0 | |
| 0 | 78 ± 4 | 90 ± 6 |
| 3 | 80 ± 4 | 98 ± 1 |
| 15 | 81 ± 2 | 96 ± 1 |
| 30 | 76 ± 5 | 90 ± 1 |
| | pH 10.0 | |
| 0 | 79 ± 6 | 79 ± 2 |
| 3 | 80 ± 2 | 85 ± 1 |
| 15 | 81 ± 1 | 83 ± 1 |
| 30 | 82 ± 1 | 85 ± 0 |

Values are the results of measurements determined for six fibers and are given in terms of 95% confidence limits.

while wet, the lowering of breaking stress and breaking extension may be important.

Some properties of the bleached fabrics are given in Table II. Impairment of most fabric properties occurs progressively as the bleaching treatment is lengthened; significantly, formaldehyde appears to furnish little protection. The fabrics are somewhat stiffened. Wet breaking strength and tear resistance are lowered. Abrasion weight loss is greater. Above all, the formaldehyde treatment gave no significant protection.

The color differences of bleached fabrics are given in Table III. The best white appears to have been obtained under our conditions at or before 1.5 hr. The formaldehyde treatment had little effect on the whiteness of fabrics obtained in these instances. It should be noted that bleaching of wool results in an increase in reflectance, accompanying a decrease in yellowness.

Kirby and Rutherford [9] have reported increased susceptibility of wool fibers to peroxide damage when the fibers had been strained 30% before treatment. To test this observation further, fibers were stretched varying lengths, allowed to recover, and exposed to peroxide. The results of this experiment are given in Table IV. There appears to be no correlation between degree of stretch and fiber damage under our conditions, as determined by reduction in work to stretch. However, the authors have noted a high degree of variability in the attack of peroxide on single fibers from bleached cloths. This variability may be related to Kirby and Rutherford's observations.

## Acknowledgments

The authors express appreciation to W. Fong for performing the bleaching experiments and color measurements and to Mrs. L. Brown, Mrs. E. Johnson, and Mrs. H. Kivela for performing the physical measurements.

## Literature Cited

1. ASTM Method D 1388–55 T, *ASTM Standards on Textile Materials*, 655 ff. (1956).
2. ASTM Method D 1424–56 T, *ASTM Standards on Textile Materials*, 250 (1956).
3. Bauer, J., *Am. Dyestuff Reptr.* **45**, 253 (1956).
4. Bauer, J., private communication.
5. Dusenbury, J. H., Mercer, E. H., and Wakelin, J. H., TEXTILE RESEARCH JOURNAL **24**, 890 (1954).
6. Brit. Pat. 3492, A. M. Clark (1903).
7. Fraenkel-Conrat, H., Cooper, M., and Olcott, H. S., *J. Am. Chem. Soc.* **67**, 950 (1945).
8. Harris, M. and Smith, A. L., *J. Research Nat. Bur. Standards* **17**, 577 (1936).
9. Kirby, Rosa D. and Rutherford, H. A., TEXTILE RESEARCH JOURNAL **25**, 569 (1955).
10. Moore, J. E. and O'Connell, R. A., TEXTILE RESEARCH JOURNAL **27**, 783 (1957).
11. Peroxygen Products Bulletin No. P 59–652, Electrochemical Department, E. I. du Pont de Nemours and Co., Wilmington, Delaware.
12. Richards, H. R. and Speakman, J. B., *J. Soc. Dyers Colourists* **71**, 537 (1955).
13. Speakman, J. B. and Peill, P. L. D., *J. Textile Inst.* **34**, 70T (1943).
14. Stiegler, H. W., Glidden, H. E., Mandikos, G. J., and Thompson, G. R., *Am. Dyestuff Reptr.* **45**, 685 (1956).
15. Stoves, J. L., *Trans. Faraday Soc.* **39**, 294 (1943).

*Manuscript received March 14, 1958.*

# Findings and Recommendations on the Use of the Vibroscope

**D. H. Patt**

*American Cyanamid Company, Stamford Laboratories, Research Division, Stamford, Conn.*

**Abstract**

The vibroscope method of determining linear density of fibers is based on the principle of the vibrating string, wherein the linear density is directly determined by tension and length of a fiber vibrating at resonance. In establishing a standard ASTM method for use of an instrument operating on this principle, the effect of three factors inherent in fibers had to be determined. These are (a) shape of fiber cross section, (b) area of cross section, and (c) Young's modulus. This paper is a report of the cooperative test program under ASTM auspices. Results indicated that equipment and procedure used without corrections for the effect of the various factors involved furnish reliable linear density measurements within about 5% of the denier value obtained.

## Introduction

With the recent sharp increase in interest in determining physical properties of single fibers, it became apparent that the methods which had been in use for determining linear density [1] of short lengths of fine filaments were not adequate in a number of respects. Direct weighing was a tedious, time-consuming procedure requiring an exceedingly sensitive balance. Calculation from specific gravity and microscopically determined area of cross section was subject to error in the measurement of both of these characteristics. Here also, procedures were frequently tedious, and use of the same fiber for subsequent tests was impossible.

Four years ago it was suggested that the Fibers Subcommittee in ASTM Committee D-13 (Textiles) might profitably look into the development of a quicker, more reliable method for the determination of linear density. Accordingly a task group was formed to investigate possible approaches to the problem. The goal of the group's work was to be the proving and writing of a standard method capable of furnishing data of reasonable precision and accuracy.

The work of Gonsalves [3] in Holland, and later Dart and Peterson [2] and Voong and Montgomery [4] in this country, suggested the use of the principle of the vibrating string as the basis for a method. The principle states that the weight per unit length of a completely flexible string (fiber) can be calculated directly if the natural frequency of transverse vibration is determined when a measured length is held under a known tension. For such a fiber the linear density, $m_1$, is exactly given by

$$m_1 = T/4L^2f_1^2$$

in C.G.S. units, where $f_1$ is the fundamental resonant frequency, $L$ is the free length of the fiber in cm., and $T$ is the tension in dynes.

Several instruments utilizing this principle were already in use among members of the task group, giving added impetus to the decision to draft such a method. The name, "vibroscope," was first applied by Gonsalves.

## Operating Characteristics

Vibroscopes in use have used several means for causing a predetermined length of fiber under known tension to vibrate at an assigned frequency and for detecting resonance. In general, the upper end of a fiber can receive the vibration mechanically, such as from a loudspeaker coil or phonograph cutting head, or an alternating electrostatic impulse can be applied near its center via small, closely spaced electrodes placed on either side of the fiber. The length of the fiber is sometimes its total length, or it may be defined and limited by having the fiber pass over

[1] Usually measured as denier (g./9000 m.) or tex (g./1000 m.).

a fret analogous to that on a banjo. Tension may be applied by a small hanging weight of known mass or by means of an adjustable chain weight. At the correct combination of frequency, tension, and length the fiber will vibrate laterally in its fundamental mode; resonance may be detected by observing a maximum in amplitude of vibration through a low-power microscope or other magnifying means. Figures 1 and 2 illustrate the foregoing description for one type of vibroscope, the so-called electromechanical, or American Viscose, design [2]. The electrostatic, or Textile Research Institute, design has been described elsewhere [1, 4].

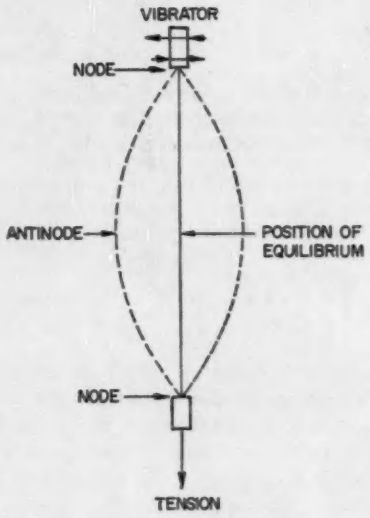


**Fig. 1.** Electromechanical vibroscope.

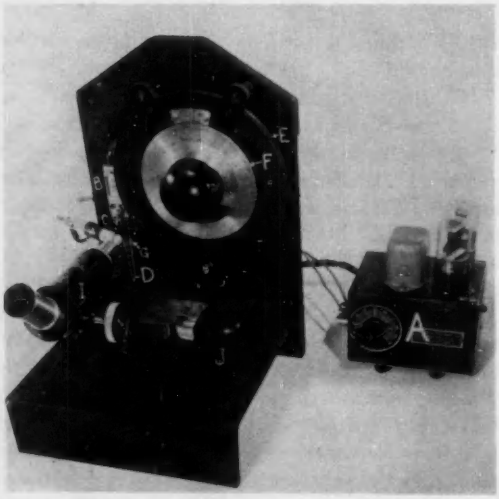


**Fig. 2.** American Viscose type vibroscope. A—oscillator, B—phonograph cutting head, C—fiber, D—chain for applying load to fiber, E—drum, F—dial calibrated in denier units for direct reading, G—fret to give constant fiber length, H—light for illuminating fiber, and J—jig for clamping fiber.

In utilizing the vibrating string principle for fiber measurements, any or all of the terms of the equation may be varied. In actual practice it is usual to maintain two of the three factors constant and find $m_1$ in terms of the remaining variable. Reduction to one variable simplifies the test and improves precision. Choice of this variable depends on the particular situation and is influenced by fiber characteristics, handling and mounting problems, and interest in carrying out subsequent tests on the same fiber. Similarly, the selection of values for the free length of the fiber, the tension to be applied, the frequency of vibration, and the range needed to be covered by any of these will be determined by the particular situation. In this respect the two instruments mentioned above fall into two classifications: the American Viscose (AV) type holds frequency and test length constant and varies tension by means of a chain weight; the Textile Research Institute (TRI) type holds tension and test length constant and varies frequency output from a calibrated variable-frequency oscillator.

## Standardization of a General Method

Of necessity a method written to cover such a wide diversity of possible instrument types and test conditions would be quite general. However, it was felt that a standardized procedure for use in measuring linear density on any one of the possible combinations of the elements making up a vibroscope system could be provided. In addition, a discussion of the various possible means of vibrating the fiber, observing its vibration at its natural frequency, applying a known tension, and measuring and fixing the test length could be furnished, with suggestions for combining these elements into a workable instrument. This method is currently published as a proposed method in the ASTM manual [1]. Details of the technique for reliable measurements are described in this method. This includes guides to assembly of an instrument, calibration, warnings pertaining to sources of error, etc.

The use of the simple equation

$$m_1 = T/4L^2f_1^2$$

assumes a perfectly flexible fiber of essentially circular cross section. However, in practice a fiber is not perfectly flexible. Its stiffness tends to raise the natural frequency of vibration over that for the perfectly flexible case. A correction factor in terms of Young's modulus of the fiber material and the moment of inertia of the fiber about the neutral axis can be added to the original equation to correct for this deviation from perfect flexibility. In addition, if the plane of vibration of the fiber is not controlled, deviations of the fiber from a circular cross section introduce an uncertainty in this correction factor. These deviations increase with increasing denier of the fiber. Another contributor to spurious increase in denier is the crimp found in many fibers. Inasmuch as a crimped fiber would be longer when straightened, this "added" weight appears as an increase in linear density.

It was hoped that the method might give adequate precision on the linear density values obtained without use of this correction term. Accordingly, an interlaboratory test program was statistically designed to test the effect of variations in fiber denier, stiffness, and shape of cross section on the precision of the results obtained. Crimp was omitted by including only uncrimped fibers.

## Statistical Plan

A factorial experimental design was set up for us by Cyanamid's Mathematical Analysis Group. Eight types of fibers representing all possible combinations of round and flat cross section, high and low denier, and high and low modulus were to be vibroscoped by eight different laboratories. It was realized that, although intercomparison of vibroscopes in different laboratories would resolve the question of interlaboratory reproducibility, there was no direct guarantee as to the ability of these instruments to provide accurate absolute data. Consequently, a "referee" was set up in the form of direct weighings of the test fibers. Because of known difficulties experienced even in the use of the referee method, it was agreed that means for checking the accuracy and precision of weighings should be provided. Three laboratories were selected to weigh successively all of the fibers used prior to vibroscoping. Participating laboratories for vibroscoping would be chosen so as to have at least two of the commoner types of vibroscopes represented. Conditions of 65% relative humidity and 70° F. were chosen for all the work.

**TABLE I. Code System for Vibroscope Round Robin Fiber Identification**

| Denier | Modulus | Shape of cross section | Identification |
|---|---|---|---|
| L | L | F | Dinitrile A |
| L | H | F | Orlon* fil., 75–30–0.32 81 |
| L | L | R | Nylon—du Pont |
| L | H | R | Rayon—Am. Viscose |
| H | L | F | Acetate, bright—du Pont |
| H | H | F | Rayon, dull—du Pont |
| H | L | R | Nylon—du Pont |
| H | H | R | Rayon—Am. Viscose |

Thus HLF would refer to bright acetate fibers (High denier, Low modulus, Flat cross section).

* du Pont trademark.

## Experimental

In collecting the fibers, low denier was considered approximately three, high denier ten or more. Less than 20 g./den. was specified for low modulus, more than 50 g./den. for high. An attempt was made to keep the cross section shape as near to the ideal as possible. In practice, round fibers included some crenulated ones and flat fibers varied from barely flattened to broad ribbon-like shapes. Table I describes the fibers and their characteristics, and Figure 3 shows the diversity of cross sections.

Ten-centimeter lengths of the fibers were prepared for weighing in bundles of five for high denier and fifteen for low denier. This was necessary to keep the bundle weights approximately equal and in a workable range of 150 $\mu$g. or more. A bundle of each type of fiber was prepared for each participating laboratory, making 64 fiber bundles to be weighed.[2] Fibers were coded and packaged in corked glass tubes, and the entire lot was shipped in succession to the three laboratories for weighing. Weighings were performed on balances with at least 0.003 mg. sensitivity.

Upon receipt of all the weight data, they were submitted to statistical analysis. Two laboratories furnished weighings in duplicate, one only a single weighing.

An analysis of variance showed that differences in the fiber weighings from the three laboratories were

[2] Actually ten sets of fibers were prepared and weighed and ten laboratories participated. Besides giving interested laboratories in excess of the eight necessary for the factorial experimental plan an opportunity to test their instruments, this gave reasonable assurance of having eight valid sets of measurements at the end of the experiment.

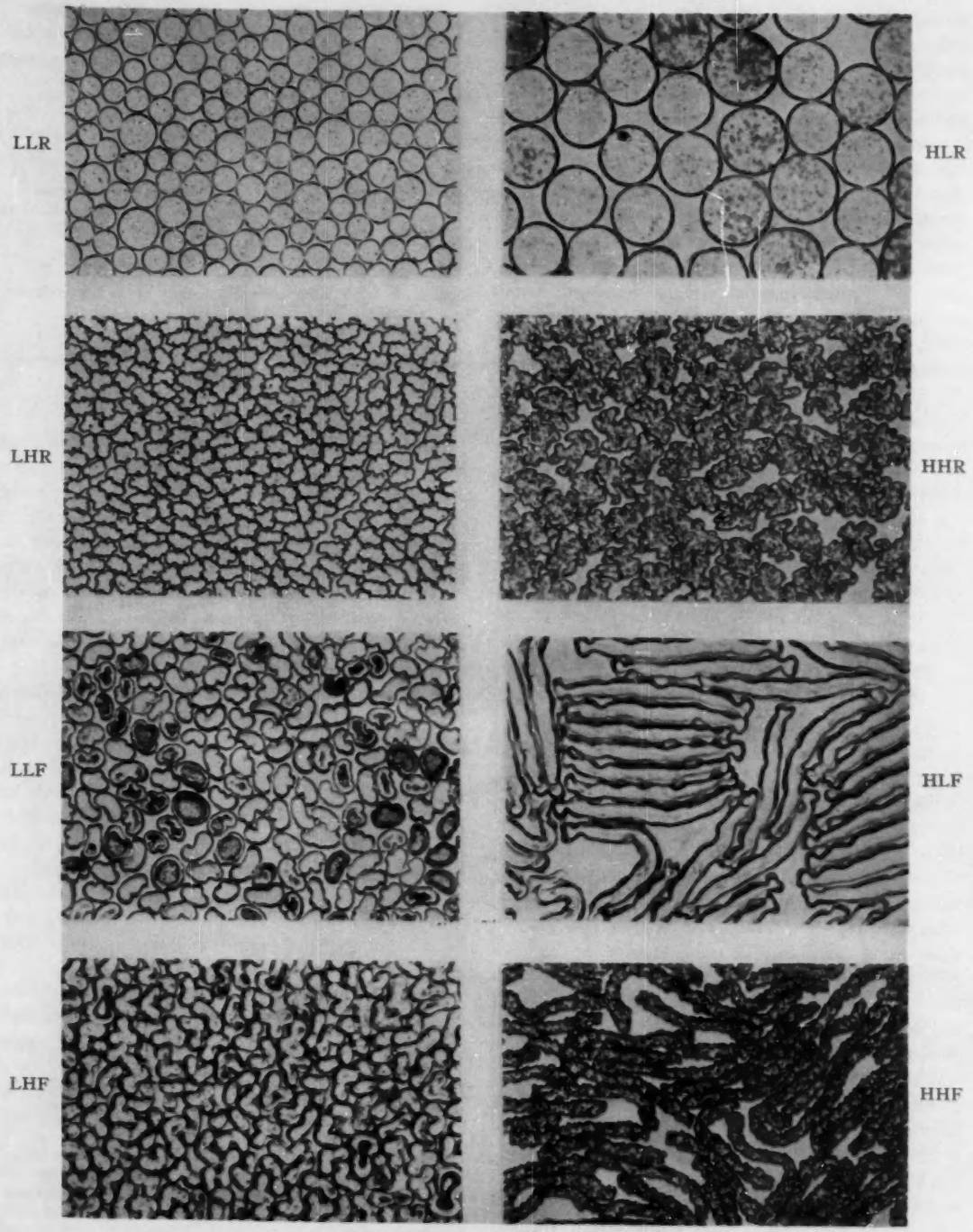


**Fig. 3.** Photomicrographs of fiber cross sections (250×).

not significant. For a single weighing of any fiber type by one laboratory, the standard error was found to be 34.7 μg. and the 95% confidence limits to be ±68 μg. on weights in the range 275–900 μg. This indicated that an average of the three weights on each bundle could be used to calculate a primary denier value with which to compare the average denier for the same bundle obtained with the vibroscope. This denier was calculated for each bundle and is recorded in Table II along with average weight from each laboratory and the average for the three laboratories.

Each participating laboratory was to vibroscope five fibers of each type. This necessitated selecting five out of each fifteen low denier fibers. To eliminate all possibility of bias toward heavier fibers in this choice, the members of each bundle were laid out in numbered positions. Corresponding numbers were then drawn at random until five fibers had been chosen. Only if a fiber had been badly damaged

**TABLE II. Weight of Fiber Bundles and Calculated Average Denier of Individual Fibers**

| Fiber type 5/bundle | Lab no. | Bundle wt., mg.* Lab B | Lab A | Lab C | Av. wt. | Single fiber denier calc. from wt. | Fiber type 15/bundle | Lab no. | Bundle wt., mg. Lab B | Lab A | Lab C | Av. wt. | Single fiber denier calc. from wt. |
|---|---|---|---|---|---|---|---|---|---|---|---|---|---|
| HLR | 1 | .846 | .805 | .813 | .821 | 14.78 | LLR | 1 | .436 | .434 | .438 | .436 | 2.62 |
| | 2 | .832 | .835 | .846 | .838 | 15.08 | | 2 | .503 | .508 | .511 | .507 | 3.04 |
| | 3 | .869 | .869 | .875 | .871 | 15.70 | | 3 | .486 | .489 | .495 | .490 | 2.94 |
| | 4 | .686 | .686 | .690 | .687 | 12.37 | | 4 | .499 | .506 | .512 | .506 | 3.04 |
| | 5 | .778 | .792 | .789 | .786 | 14.15 | | 5 | .531 | .522 | .534 | .529 | 3.19 |
| | 6 | .913 | .928 | .940 | .927 | 16.86 | | 6 | .485 | .491 | .492 | .490 | 2.93 |
| | 7 | .739 | .746 | .749 | .745 | 13.40 | | 7 | .457 | .454 | .463 | .458 | 2.75 |
| | 8 | .753 | .765 | .768 | .762 | 12.32 | | 8 | .419 | .423 | .426 | .422 | 2.53 |
| | 9 | .813 | .822 | .834 | .823 | 14.81 | | 9 | .413 | .416 | .416 | .415 | 2.49 |
| | 10 | .898 | .901 | .910 | .903 | 16.25 | | 10 | .494 | .494 | .489 | .492 | 2.95 |
| HLF | 1 | .815 | .824 | .829 | .823 | 14.81 | LLF | 1 | .435 | .443 | .448 | .442 | 2.65 |
| | 2 | .772 | .792 | .691 | .752 | 13.54 | | 2 | .365 | .382 | .381 | .376 | 2.26 |
| | 3 | .788 | .790 | .796 | .791 | 14.20 | | 3 | .412 | .422 | .413 | .417 | 2.50 |
| | 4 | .820 | .832 | .841 | .831 | 14.96 | | 4 | .363 | .374 | .368 | .368 | 2.21 |
| | 5 | .736 | .808 | .790 | .778 | 14.00 | | 5 | .372 | .382 | .380 | .378 | 2.27 |
| | 6 | .803 | .809 | .815 | .809 | 14.56 | | 6 | .391 | .406 | .399 | .399 | 2.41 |
| | 7 | .775 | .770 | .775 | .773 | 13.91 | | 7 | .411 | .407 | .409 | .409 | 2.45 |
| | 8 | .834 | .832 | .846 | .837 | 15.01 | | 8 | .364 | .366 | .364 | .365 | 2.19 |
| | 9 | .808 | .804 | .808 | .807 | 15.03 | | 9 | .386 | .391 | .393 | .390 | 2.20 |
| | 10 | .807 | .803 | .812 | .807 | 14.53 | | 10 | .405 | .406 | .409 | .407 | 2.44 |
| HHR | 1 | .408 | .414 | .419 | .414 | 7.45 | LHR | 1 | .277 | .308 | .286 | .290 | 1.74 |
| | 2 | .402 | .411 | .411 | .408 | 7.34 | | 2 | .326 | .325 | .329 | .327 | 1.96 |
| | 3 | .432 | .442 | .449 | .441 | 7.94 | | 3 | .278 | .275 | .291 | .281 | 1.69 |
| | 4 | .399 | .416 | .414 | .410 | 7.38 | | 4 | .304 | .314 | .313 | .310 | 1.86 |
| | 5 | .408 | .420 | .425 | .418 | 7.52 | | 5 | .283 | .292 | .292 | .289 | 1.75 |
| | 6 | .379 | .378 | .399 | .385 | 6.93 | | 6 | .290 | .293 | .287 | .290 | 1.74 |
| | 7 | .404 | .415 | .416 | .412 | 7.42 | | 7 | .292 | .296 | .294 | .294 | 1.76 |
| | 8 | .381 | .395 | .397 | .391 | 7.04 | | 8 | .297 | .304 | .302 | .301 | 1.81 |
| | 9 | .433 | .443 | .462 | .446 | 7.15 | | 9 | .287 | .301 | .296 | .295 | 1.77 |
| | 10 | | .421 | .417 | .418 | 7.52 | | 10 | .299 | .300 | .308 | .302 | 1.81 |
| HHF | 1 | .553 | .567 | .573 | .564 | 10.15 | LHF | 1 | .432 | .442 | .446 | .440 | 2.64 |
| | 2 | .546 | .560 | .565 | .557 | 10.03 | | 2 | .445 | .444 | .457 | .449 | 2.69 |
| | 3 | .563 | .569 | .575 | .569 | 10.30 | | 3 | .440 | .438 | .445 | .441 | 2.65 |
| | 4 | .572 | .575 | .527 | .558 | 10.04 | | 4 | .442 | .441 | .457 | .447 | 2.68 |
| | 5 | .548 | .550 | .574 | .557 | 10.01 | | 5 | .435 | .433 | .437 | .435 | 2.61 |
| | 6 | .561 | .566 | .576 | .568 | 10.22 | | 6 | .425 | .422 | .423 | .423 | 2.54 |
| | 7 | .562 | .571 | .586 | .573 | 10.31 | | 7 | .424 | .424 | .428 | .425 | 2.55 |
| | 8 | .553 | .561 | .566 | .566 | 10.16 | | 8 | .428 | .430 | .431 | .430 | 2.58 |
| | 9 | .577 | .579 | .587 | .581 | 10.46 | | 9 | .433 | .432 | .430 | .432 | 2.59 |
| | 10 | .554 | .566 | .560 | .560 | 10.08 | | 10 | .453 | .449 | .466 | .456 | 2.74 |

* Lab A = Celanese, Lab B = American Cyanamid, Lab C = Textile Research Institute.

in the handling during weighing was it eliminated and a replacement drawn.

At this point, each participating laboratory received its own set of fibers, with instructions for testing. A set consisted of the eight fiber types, five fibers each. The instructions, important to the statistical plan, were to be followed exactly using the method as tentatively written. No corrections were to be made for stiffness or shape of cross section. It was suggested that a single operator perform all the measurements on one vibroscope. True duplicate measurements were to be obtained, that is, each fiber was to be removed from the instrument and replaced for the second determination. Duplicate individual vibroscope denier for each fiber and the average of the ten measurements on each fiber type are recorded in Table III.

## Analysis

At the suggestion of our statisticians, a ratio of average vibroscope denier to average weight denier was chosen as the basis of comparison in the analy-

**TABLE III. Individual Fiber Vibroscope Data**

| | | Lab 1 | | | Lab 2 | | | Lab 3 | | | Lab 4 | | | Lab 5 | | |
|---|---|---|---|---|---|---|---|---|---|---|---|---|---|---|---|---|
| Fiber type | Fiber no. | 1st Meas. | 2nd Meas. | Av. 10* | 1st Meas. | 2nd Meas. | Av. 10 | 1st Meas. | 2nd Meas. | Av. 10 | 1st Meas. | 2nd Meas. | Av. 10 | 1st Meas. | 2nd Meas. | Av. 10 |
| HLR | 1 | 12.42 | — | | 11.92 | 11.92 | | 18.9 | 18.4 | | 12.7 | 12.8 | | 12.93 | 12.82 | |
| | 2 | 10.92 | — | | 18.36 | 18.36 | | 15.9 | 14.6 | | 11.9 | 11.9 | | 13.46 | 13.47 | |
| | 3 | 10.71 | — | | 10.88 | 10.88 | | 13.3 | 16.7 | | 10.2 | 10.1 | | 13.62 | 13.60 | |
| | 4 | 12.15 | — | | 11.65 | 11.65 | | 9.7 | 15.9 | | 11.7 | 11.9 | | 13.37 | 13.36 | |
| | 5 | 13.28 | — | | 14.57 | 14.57 | | 15.2 | 10.5 | | 12.1 | 12.4 | | 15.41 | 15.34 | |
| | | | | 11.90 | | | 13.48 | | | 14.91 | | | 11.77 | | | 13.74 |
| HLF | 1 | 12.15 | — | | 12.24 | 12.45 | | 12.8 | 11.8 | | 14.3 | 14.1 | | 14.20 | 14.10 | |
| | 2 | 12.42 | — | | 15.40 | 14.31 | | 12.3 | 13.3 | | 14.4 | 14.5 | | 15.56 | 12.20 | |
| | 3 | 13.89 | — | | 14.06 | 13.57 | | 15.9 | 13.3 | | 15.4 | 15.5 | | 14.53 | 14.13 | |
| | 4 | 15.67 | — | | 15.12 | 14.84 | | 13.3 | 15.9 | | 15.6 | 15.6 | | 14.02 | 14.29 | |
| | 5 | 14.92 | — | | 12.24 | 12.45 | | 15.2 | 11.3 | | 14.7 | 14.7 | | 12.36 | 15.51 | |
| | | | | 13.81 | | | 13.67 | | | 13.51 | | | 14.88 | | | 14.09 |
| HHR | 1 | 7.77 | — | | 7.16 | 7.16 | | 6.57 | 7.92 | | 7.49 | 7.58 | | 7.81 | 7.83 | |
| | 2 | 7.64 | — | | 5.83 | 5.83 | | 7.92 | 7.92 | | 7.09 | 7.14 | | 7.69 | 7.87 | |
| | 3 | 6.37 | — | | 5.92 | 5.92 | | 7.67 | 6.77 | | 6.65 | 6.81 | | 7.00 | 7.04 | |
| | 4 | 7.26 | — | | 6.78 | 6.90 | | 8.76 | 8.76 | | 7.78 | 7.84 | | 6.42 | 6.53 | |
| | 5 | 6.47 | — | | 6.78 | 6.78 | | 7.67 | 7.92 | | 6.30 | 6.39 | | 7.34 | 7.66 | |
| | | | | 7.10 | | | 6.50 | | | 7.79 | | | 7.11 | | | 7.32 |
| HHF | 1 | 9.50 | — | | 9.00 | 10.19 | | 9.4 | 10.5 | | 9.99 | 10.04 | | 9.44 | 9.55 | |
| | 2 | 9.69 | — | | 9.57 | 9.37 | | 10.1 | 10.5 | | 10.57 | 10.67 | | 9.46 | 9.74 | |
| | 3 | 9.32 | — | | 9.37 | 9.18 | | 12.3 | 10.1 | | 10.36 | 10.36 | | 10.03 | 10.10 | |
| | 4 | 9.69 | — | | 9.57 | 9.18 | | 10.5 | 9.7 | | 10.57 | 10.57 | | 9.42 | 9.62 | |
| | 5 | 9.32 | — | | 10.19 | 10.19 | | 10.9 | 10.1 | | 10.21 | 10.67 | | 10.13 | 10.23 | |
| | | | | 9.50 | | | 9.59 | | | 10.41 | | | 10.40 | | | 9.78 |
| LLR | 1 | 3.24 | — | | 4.00 | 4.00 | | 3.07 | 3.81 | | 2.88 | 2.67 | | 2.63 | 2.75 | |
| | 2 | 3.05 | — | | 2.20 | 2.16 | | 4.28 | 2.19 | | 2.35 | 2.30 | | 3.28 | 3.43 | |
| | 3 | 2.52 | — | | 3.45 | 3.15 | | 2.83 | 2.89 | | 3.80 | 4.05 | | 2.51 | 2.55 | |
| | 4 | 2.14 | — | | 3.51 | 3.15 | | 2.15 | 4.08 | | 2.24 | 2.11 | | 3.31 | 3.40 | |
| | 5 | 2.09 | — | | 3.06 | 3.06 | | 3.81 | 2.95 | | 3.48 | 3.40 | | 2.62 | 2.71 | |
| | | | | 2.61 | | | 3.18 | | | 3.21 | | | 2.93 | | | 2.92 |
| LLF | 1 | 3.00 | — | | 1.70 | 1.73 | | 2.57 | 2.83 | | 1.99 | 1.89 | | 3.06 | 3.20 | |
| | 2 | 2.35 | — | | 2.29 | 2.29 | | 2.62 | 2.19 | | 2.04 | 1.96 | | 2.14 | 2.13 | |
| | 3 | 3.35 | — | | 2.00 | 2.04 | | 2.53 | 2.73 | | 2.22 | 2.33 | | 2.40 | 2.28 | |
| | 4 | 2.74 | — | | 2.29 | 2.34 | | 2.62 | 2.67 | | 1.99 | 2.08 | | 1.85 | 1.67 | |
| | 5 | 3.23 | — | | 1.82 | 1.82 | | 2.57 | 2.73 | | 1.97 | 2.01 | | 2.28 | 2.42 | |
| | | | | 2.93 | | | 2.13 | | | 2.61 | | | 2.05 | | | 2.35 |
| LHR | 1 | 1.70 | — | | 1.79 | 1.79 | | 1.69 | 1.69 | | 1.98 | 1.93 | | 1.95 | 1.99 | |
| | 2 | 1.89 | — | | 1.96 | 2.00 | | 1.72 | 1.86 | | 1.82 | 1.80 | | 1.99 | 2.06 | |
| | 3 | 1.74 | — | | 1.73 | 1.70 | | 1.86 | 1.83 | | 1.87 | 1.81 | | 1.87 | 1.90 | |
| | 4 | 1.68 | — | | 1.89 | 1.89 | | 1.80 | 1.95 | | 1.85 | 1.84 | | 1.88 | 1.87 | |
| | 5 | 1.76 | — | | 1.89 | 1.86 | | — | — | | 1.86 | 1.84 | | 1.95 | 1.95 | |
| | | | | 1.75 | | | 1.85 | | | 1.80 | | | 1.86 | | | 1.94 |
| LHF | 1 | 2.45 | — | | 2.60 | 2.55 | | 2.53 | 2.67 | | 2.66 | 2.54 | | 2.45 | 2.47 | |
| | 2 | 2.83 | — | | 2.60 | 2.66 | | 2.62 | 2.83 | | 2.52 | 2.36 | | 2.73 | 2.99 | |
| | 3 | 2.78 | — | | 2.49 | 2.49 | | 2.57 | 2.57 | | 2.55 | 2.65 | | 2.62 | 2.52 | |
| | 4 | 2.48 | — | | 2.60 | 2.60 | | 2.73 | 2.57 | | 2.57 | 2.75 | | 2.50 | 2.55 | |
| | 5 | 2.45 | — | | 2.60 | 2.66 | | 2.57 | 2.53 | | 2.45 | 2.51 | | 2.75 | 2.80 | |
| | | | | 2.60 | | | 2.58 | | | 2.62 | | | 2.56 | | | 2.64 |

* Average of five—no duplicate measurements.

sis. Theoretically, this value should be 1. Deviations from unity in this ratio could be ascribed to taking a subsample of the weighed bundle of low denier fibers for vibroscoping or to experimental error. Ratios and pertinent data are recorded in Table IV.

The statistical analysis performed on the ratios indicated the following:

1. An analysis of variance showed (a) that of denier, cross section, and Young's modulus, denier had the only significant influence on the relation between weighings and vibroscope measurements, (b) that there was a highly significant difference between laboratories, and (c) that the denier × laboratory interaction was significant.

2. In general, high deniers gave ratios of vibroscope deniers to average weight deniers lower than 1.0 and low deniers gave ratios higher than 1.0.

3. Laboratory 9 obtained significantly higher results than Laboratories 6, 2, 10, and 1; Laboratory 6 obtained significantly lower results than Laboratories 8 and 9. In order to check the possibility of consistent instrument bias, average denier for each fiber type was plotted versus the $D_v/D_w$ ratio for

**TABLE III (continued)**

| | | Lab 6 | | | Lab 8 | | | Lab 9 | | | Lab 10 | | |
|---|---|---|---|---|---|---|---|---|---|---|---|---|---|
| Fiber type | Fiber no. | 1st Meas. | 2nd Meas. | Av. 10 | 1st Meas. | 2nd Meas. | Av. 10 | 1st Meas. | 2nd Meas. | Av. 10 | 1st Meas. | 2nd Meas. | Av. 10 |
| HLR | 1 | 17.78 | 17.82 | | 12.50 | 12.48 | | 15.50 | 15.99 | | 10.7 | 10.4 | |
| | 2 | 13.65 | 13.81 | | 13.68 | 13.66 | | 14.16 | 14.16 | | 21.3 | 16.8 | |
| | 3 | 12.75 | 12.75 | | 11.44 | 11.48 | | 15.74 | 18.50 | | 12.7 | 13.5 | |
| | 4 | 13.91 | 13.94 | | 15.50 | 15.52 | | 12.81 | 12.99 | | 11.0 | 11.0 | |
| | 5 | 15.58 | 15.80 | | 16.01 | 16.05 | | 18.19 | 17.89 | | 11.6 | 11.0 | |
| | | | | 14.78 | | | 13.84 | | | 15.60 | | | 13.00 |
| HLF | 1 | 11.75 | 11.67 | | 16.88 | 16.86 | | 15.74 | 16.77 | | 14.0 | 14.4 | |
| | 2 | 11.63 | 11.67 | | 14.54 | 14.66 | | 15.27 | 15.27 | | 12.3 | 12.7 | |
| | 3 | 15.72 | 15.95 | | 14.08 | 14.15 | | 15.27 | 15.74 | | 13.1 | 15.4 | |
| | 4 | 12.50 | 12.79 | | 12.84 | 12.79 | | 15.74 | 15.74 | | 14.4 | 14.4 | |
| | 5 | 12.54 | 12.67 | | 14.53 | 14.52 | | 13.56 | 13.18 | | 13.5 | 14.0 | |
| | | | | 12.89 | | | 14.58 | | | 15.23 | | | 13.82 |
| HHR | 1 | 5.72 | 5.73 | | 7.96 | 8.08 | | 8.55 | 8.65 | | 6.1 | 6.2 | |
| | 2 | 7.35 | 7.10 | | 6.70 | 6.75 | | 8.18 | 9.06 | | 6.9 | 7.5 | |
| | 3 | 6.05 | 6.01 | | 6.32 | 6.35 | | 8.96 | 8.36 | | 6.4 | 6.2 | |
| | 4 | 5.98 | 5.91 | | 6.80 | 6.91 | | 8.65 | 8.65 | | 7.0 | 7.2 | |
| | 5 | 6.58 | 6.34 | | 7.93 | 7.94 | | 8.18 | 8.27 | | 7.9 | 7.3 | |
| | | | | 6.28 | | | 7.18 | | | 8.55 | | | 6.87 |
| HHF | 1 | 9.75 | 9.83 | | 9.71 | 9.72 | | 10.76 | 11.34 | | 8.9 | 9.1 | |
| | 2 | 9.70 | 9.79 | | 10.25 | 10.31 | | 11.19 | 11.49 | | 9.4 | 9.1 | |
| | 3 | 9.22 | 9.43 | | 10.54 | 10.58 | | 11.19 | 11.19 | | 9.4 | 9.9 | |
| | 4 | 9.93 | 9.84 | | 10.22 | 10.23 | | 11.19 | 11.34 | | 9.1 | 9.6 | |
| | 5 | 9.15 | 9.23 | | 9.87 | 9.83 | | 10.49 | 11.05 | | 9.9 | 9.4 | |
| | | | | 9.58 | | | 10.13 | | | 11.12 | | | 9.38 |
| LLR | 1 | 4.63 | 4.64 | | 2.00 | 2.00 | | 2.12 | 2.12 | | 4.05 | 4.20 | |
| | 2 | 2.75 | 2.82 | | 3.38 | 3.43 | | 2.63 | 2.56 | | 2.25 | 2.11 | |
| | 3 | 3.08 | 3.20 | | 2.24 | 2.31 | | 2.68 | 2.66 | | 3.28 | 3.18 | |
| | 4 | 2.09 | 2.19 | | 3.08 | 3.07 | | 2.12 | 2.19 | | 2.79 | 2.87 | |
| | 5 | 1.84 | 1.78 | | 2.36 | 2.37 | | 3.62 | 3.58 | | 2.56 | 2.60 | |
| | | | | 2.90 | | | 2.62 | | | 2.62 | | | 2.99 |
| LLF | 1 | 1.85 | 1.80 | | 6.56 | 6.56 | | 1.98 | 1.98 | | 2.06 | 2.11 | |
| | 2 | 3.18 | 3.12 | | 2.12 | 2.18 | | 2.14 | 2.11 | | 2.47 | 2.40 | |
| | 3 | 1.88 | 1.81 | | 2.14 | 2.14 | | 2.33 | 2.33 | | 3.04 | 2.53 | |
| | 4 | 3.10 | 3.21 | | 2.38 | 2.41 | | 2.41 | 2.73 | | 2.31 | 2.17 | |
| | 5 | 2.52 | 2.39 | | 2.18 | 2.17 | | 2.41 | 2.66 | | 2.56 | 2.91 | |
| | | | | 2.49 | | | 2.22 | | | 2.30 | | | 2.46 |
| LHR | 1 | 1.75 | 1.72 | | 1.89 | 1.86 | | 1.85 | 1.98 | | 2.04 | 2.06 | |
| | 2 | 1.62 | 1.69 | | 1.87 | 1.89 | | 1.95 | 1.58 | | 1.81 | 1.81 | |
| | 3 | 1.50 | 1.54 | | 1.84 | 1.84 | | 1.60 | 1.97 | | 1.71 | 1.71 | |
| | 4 | 1.51 | 1.57 | | 1.74 | 1.76 | | 1.98 | 1.82 | | 2.14 | 2.06 | |
| | 5 | 1.62 | 1.71 | | 1.97 | 2.01 | | 1.75 | 1.73 | | 1.97 | 2.01 | |
| | | | | 1.62 | | | 1.86 | | | 1.82 | | | 1.93 |
| LHF | 1 | 2.19 | 2.28 | | 2.61 | 2.63 | | 2.34 | 2.43 | | 2.83 | 2.71 | |
| | 2 | 2.16 | 2.28 | | 2.82 | 2.83 | | 2.58 | 2.66 | | 2.68 | 2.64 | |
| | 3 | 2.13 | 2.22 | | 2.67 | 2.67 | | 2.63 | 2.66 | | 2.40 | 2.47 | |
| | 4 | 2.26 | 2.33 | | 2.60 | 2.63 | | 2.78 | 2.78 | | 2.53 | 2.50 | |
| | 5 | 2.18 | 2.23 | | 2.38 | 2.40 | | 2.78 | 2.81 | | 2.87 | 2.64 | |
| | | | | 2.22 | | | 2.62 | | | 2.64 | | | 2.63 |

**TABLE IV. Denier Ratios Used in the Statistical Analysis**

| Fiber type | Lab 1 | | | Lab 2 | | | Lab 3 | | | Lab 4 | | | Lab 5 | | |
|---|---|---|---|---|---|---|---|---|---|---|---|---|---|---|---|
| | Wt. den. | Av. vib. den. | $\frac{D_v}{D_w}$ | Wt. den. | Av. vib. den. | $\frac{D_v}{D_w}$ | Wt. den. | Av. vib. den. | $\frac{D_v}{D_w}$ | Wt. den. | Av. vib. den. | $\frac{D_v}{D_w}$ | Wt. den. | Av. vib. den. | $\frac{D_v}{D_w}$ |
| HLR | 14.78 | 11.90 | 0.805 | 15.08 | 13.48 | 0.894 | 15.7 | 14.91 | 0.950 | 12.37 | 11.77 | 0.951 | 14.15 | 13.74 | 0.971 |
| HLF | 14.81 | 13.81 | 0.932 | 13.54 | 13.67 | 1.010 | 14.2 | 13.51 | 0.951 | 14.96 | 14.88 | 0.995 | 14.00 | 14.09 | 1.006 |
| HHR | 7.45 | 7.10 | 0.953 | 7.34 | 6.50 | 0.886 | 7.94 | 7.79 | 0.981 | 7.38 | 7.11 | 0.963 | 7.52 | 7.32 | 0.973 |
| HHF | 10.15 | 9.50 | 0.936 | 10.03 | 9.59 | 0.956 | 10.3 | 10.41 | 1.011 | 10.04 | 10.40 | 1.036 | 10.01 | 9.78 | 0.977 |
| LLR | 2.62 | 2.61 | 0.996 | 3.04 | 3.18 | 1.046 | 2.94 | 3.21 | 1.092 | 3.04 | 2.93 | 0.964 | 3.19 | 2.92 | 0.915 |
| LLF | 2.65 | 2.93 | 1.106 | 2.26 | 2.13 | 0.942 | 2.50 | 2.61 | 1.044 | 2.21 | 2.05 | 0.928 | 2.27 | 2.35 | 1.035 |
| LHR | 1.74 | 1.75 | 1.006 | 1.96 | 1.85 | 0.944 | 1.69 | 1.80 | 1.065 | 1.86 | 1.86 | 1.000 | 1.75 | 1.94 | 1.109 |
| LHF | 2.64 | 2.60 | 0.985 | 2.69 | 2.58 | 0.959 | 2.65 | 2.62 | 0.989 | 2.68 | 2.56 | 0.955 | 2.61 | 2.64 | 1.011 |

| Fiber type | Lab 6 | | | Lab 8 | | | Lab 9 | | | Lab 10 | | |
|---|---|---|---|---|---|---|---|---|---|---|---|---|
| | Wt. den. | Av. vib. den. | $\frac{D_v}{D_w}$ | Wt. den. | Av. vib. den. | $\frac{D_v}{D_w}$ | Wt. den. | Av. vib. den. | $\frac{D_v}{D_w}$ | Wt. den. | Av. vib. den. | $\frac{D_v}{D_w}$ |
| HLR | 16.86 | 14.78 | 0.877 | 12.32 | 13.84 | 1.123 | 14.81 | 15.60 | 1.053 | 16.25 | 13.00 | 0.800 |
| HLF | 14.56 | 12.89 | 0.885 | 15.01 | 14.58 | 0.971 | 15.03 | 15.23 | 1.013 | 14.53 | 13.82 | 0.951 |
| HHR | 6.93 | 6.28 | 0.906 | 7.04 | 7.18 | 1.020 | 7.15 | 8.55 | 1.196 | 7.52 | 6.87 | 0.914 |
| HHF | 10.22 | 9.58 | 0.937 | 10.16 | 10.13 | 0.997 | 10.46 | 11.12 | 1.063 | 10.08 | 9.38 | 0.913 |
| LLR | 2.93 | 2.90 | 0.990 | 2.53 | 2.62 | 1.036 | 2.49 | 2.62 | 1.052 | 2.95 | 2.99 | 1.014 |
| LLF | 2.41 | 2.49 | 1.033 | 2.19 | 2.22 | 1.014 | 2.20 | 2.50 | 1.045 | 2.44 | 2.46 | 1.008 |
| LHR | 1.74 | 1.62 | 0.931 | 1.81 | 1.86 | 1.028 | 1.17 | 1.82 | 1.028 | 1.81 | 1.93 | 1.066 |
| LHF | 2.54 | 2.22 | 0.874 | 2.58 | 2.62 | 1.016 | 2.59 | 2.64 | 1.019 | 2.74 | 2.63 | 0.960 |

that fiber for each laboratory. However, this plot was completely random in respect to individual laboratory position. Laboratory 10 could not be considered different in any respect despite different humidity conditions. No significant differences could be shown for type of vibroscope used.

4. It is probable that the denier × laboratory interaction is caused by the high denier effect on the ratios in Laboratories 1, 3, and 10.

5. The standard error for a single ratio was found to be 0.0529, giving 95% confidence limits on a single ratio of ±0.108. (Single ratio means the ratio of the average of ten vibroscope deniers by one laboratory on one fiber type:the average weight deniers of the same bundle of fibers.)

6. The precision of vibroscope measurements obtained from the duplicate determinations was consistently fairly high in some laboratories and low in others, even though interlaboratory agreement was reasonably good. Consequently, in view of the fact that the standard error of a single measurement varied from a low of 0.03 in the most precise laboratory to a high of 1.21 in the least, a pooled estimate of precision overall would not have been meaningful. In general, the standard errors increased with increase in denier.

7. Since experimental error increases with denier even where no subsampling is performed, it would seem probable that denier is a more influential factor in the error of the ratio than subsampling.

Details of the statistical procedures can be found in the Appendix. From these and the foregoing it can be concluded that the equipment and procedure as described in the method furnished reliable linear density measurements within about 5%.

### Acknowledgments

This work was done cooperatively with a number of laboratories. People who have participated in the work are as follows: G. F. Bush, G. F. Bush Associates; J. H. Dusenbury, Textile Research Institute; D. Engle, Carbide and Carbon Company; G. M. Hart, Dow Chemical Company; E. W. Lothrop, American Viscose Company; F. B. Lutz, Chemstrand Corporation; H. Mereness, Institute of Textile Technology; R. S. Morgan, B. F. Goodrich Company; A. G. Scroggie, du Pont; G. L. Shertz, Hercules Powder Company; B. S. Sprague, Celanese Corporation of America; C. R. Stock, American Cyanamid Company; R. L. Stultz, Carbide and Carbon Chemical Company; H. Wakeham, Textile Research Institute; and L. M. Wise, Hercules Powder Company.

## Appendix

Detailed statistical data are included in this section. Table I gives the data used for the statistical analysis. Table II shows the analysis of variance for nine laboratories. The analysis of variance was also calculated for the first eight laboratories, excluding Laboratory 10 because of differing humidity conditions. No significant difference was noted for the two analyses, so the analysis including Laboratory 10 was reproduced.

Table III gives the average weight and vibroscope denier and corresponding average ratio of $D_v/D_w$ for each fiber type.

Since the analysis of variance showed that the laboratories differed, a Studentized Range Test was performed to see which laboratories could be considered different from others. Table V ranks the laboratories by their average ratios. Laboratories connected by a line cannot be considered different; those not connected can be considered different. Laboratories which are 0.088 or more ratio units away can be considered significantly different. This procedure assures that the probability of all contrasts being correct is 95%.

Table V also shows that no significant differences can be attributed to Vibroscope type.

**TABLE I. Denier Data* for Statistical Analysis**

| Fiber type† | | HLR | HLF | HHR | HHF | LLR | LLF | LHR | LHF |
|---|---|---|---|---|---|---|---|---|---|
| Lab 1‡ | Wt. den. | 14.78 | 14.81 | 7.45 | 10.15 | 2.62 | 2.65 | 1.74 | 2.64 |
| | Vib. den. | 11.90 | 13.81 | 7.10 | 9.50 | 2.61 | 2.93 | 1.75 | 2.60 |
| | $D_v/D_w$ | 0.805 | 0.932 | 0.953 | 0.936 | 0.996 | 1.106 | 1.006 | 0.985 |
| Lab 2 | Wt. den. | 15.08 | 13.54 | 7.34 | 10.03 | 3.04 | 2.26 | 1.96 | 2.69 |
| | Vib. den. | 13.48 | 13.67 | 6.50 | 9.59 | 3.18 | 2.13 | 1.85 | 2.58 |
| | $D_v/D_w$ | 0.894 | 1.010 | 0.886 | 0.956 | 1.046 | 0.942 | 0.944 | 0.959 |
| Lab 3 | Wt. den. | 15.7 | 14.2 | 7.94 | 10.3 | 2.94 | 2.50 | 1.69 | 2.65 |
| | Vib. den. | 14.91 | 13.51 | 7.79 | 10.41 | 3.21 | 2.61 | 1.80** | 2.62 |
| | $D_v/D_w$ | 0.950 | 0.951 | 0.981 | 1.011 | 1.092 | 1.044 | 1.065 | 0.989 |
| Lab 4 | Wt. den. | 12.37 | 14.96 | 7.38 | 10.04 | 3.04 | 2.21 | 1.86 | 2.68 |
| | Vib. den. | 11.77 | 14.88 | 7.11 | 10.40 | 2.93 | 2.05 | 1.86 | 2.56 |
| | $D_v/D_w$ | 0.951 | 0.995 | 0.963 | 1.036 | 0.964 | 0.928 | 1.000 | 0.955 |
| Lab 5 | Wt. den. | 14.15 | 14.00 | 7.52 | 10.01 | 3.19 | 2.27 | 1.75 | 2.61 |
| | Vib. den. | 13.74 | 14.09 | 7.32 | 9.78 | 2.92 | 2.35 | 1.94 | 2.64 |
| | $D_v/D_w$ | 0.971 | 1.006 | 0.973 | 0.977 | 0.915 | 1.035 | 1.109 | 1.011 |
| Lab 6 | Wt. den. | 16.86 | 14.56 | 6.93 | 10.22 | 2.93 | 2.41 | 1.74 | 2.54 |
| | Vib. den. | 14.78 | 12.89 | 6.28 | 9.58 | 2.90 | 2.49 | 1.62 | 2.22 |
| | $D_v/D_w$ | 0.877 | 0.885 | 0.906 | 0.937 | 0.990 | 1.033 | 0.931 | 0.874 |
| Lab 8 | Wt. den. | 12.32 | 15.01 | 7.04 | 10.16 | 2.53 | 2.19 | 1.81 | 2.58 |
| | Vib. den. | 13.84 | 14.58 | 7.18 | 10.13 | 2.62 | 2.22** | 1.86 | 2.62 |
| | $D_v/D_w$ | 1.123 | 0.971 | 1.020 | 0.997 | 1.036 | 1.014 | 1.028 | 1.016 |
| Lab 9 | Wt. den. | 14.81 | 15.03 | 7.15 | 10.46 | 2.49 | 2.20 | 1.77 | 2.59 |
| | Vib. den. | 15.60 | 15.23 | 8.55 | 11.12 | 2.62 | 2.30 | 1.82 | 2.67 |
| | $D_v/D_w$ | 1.053 | 1.013 | 1.196 | 1.063 | 1.052 | 1.045 | 1.028 | 1.019 |
| Lab 10 | Wt. den. | 16.25 | 14.53 | 7.52 | 10.08 | 2.95 | 2.44 | 1.81 | 2.74 |
| | Vib. den. | 13.00 | 13.82 | 6.87 | 9.38 | 2.99 | 2.46 | 1.93 | 2.63 |
| | $D_v/D_w$ | 0.800 | 0.951 | 0.914 | 0.931 | 1.014 | 1.008 | 1.066 | 0.960 |

* The weight deniers are the average results of weighings by each of three laboratories of bundles of fifteen fibers for the low denier types and of bundles of five fibers for the high denier types. The vibroscope deniers are the average results of duplicate measurements by a laboratory of five fibers—for low denier fibers these were chosen randomly from the fifteen.

† Factor 1 is denier; factor 2 is modulus; factor 3 is cross section.

‡ Average vibroscope denier for Laboratory 1 is the average of single measurements on five fibers. No correction was made in the analysis because it was felt to be too small to justify the additional time required.

** This is the average of duplicate weighings of four fibers. No correction was made for the reason stated above (‡).

**TABLE II. Analysis of Variance**

| Source of variation | Sums of squares | Degrees of freedom | Mean square | Variance ratio | |
|---|---|---|---|---|---|
| *Main effects* | | | | | |
| Denier | .028441 | 1 | .028441 | 10.16 | ** |
| Modulus | .000465 | 1 | .000465 | <1 | NS |
| Cross section | .000004 | 1 | .000004 | <1 | NS |
| Laboratories | .106910 | 8 | .013364 | 4.78 | *** |
| *Interactions* | | | | | |
| Den. × mod. | .009181 | 1 | .009181 | 3.28 | NS |
| Den. × C.S. | .006826 | 1 | .006826 | 2.44 | NS |
| Den. × labs | .052116 | 8 | .052116 | 2.32 | * |
| Mod. × C.S. | .006748 | 1 | .006748 | 2.41 | NS |
| Mod. × labs | .013659 | 8 | .001707 | <1 | NS |
| C.S. × labs | .018226 | 8 | .002278 | <1 | NS |
| Den. × mod. × C.S. | .000676 | 1 | .000676 | <1 | NS |
| Residual (error) | .089521 | 32 | .002798 | | |
| Total (corr.) | .332773 | 71 | | | |

* Significant at 5% probability level.
** Significant at 0.5% probability level.
*** Significant at 0.1% probability level.
NS Not significant at 5% probability level or less.

**TABLE III**

| Fiber type | Av. denier By wt. | Av. denier By vib. | $D_v/D_w$ av.* |
|---|---|---|---|
| HLR | 14.51 | 13.83 | .953 |
| HLF | 14.51 | 14.07 | .970 |
| HHR | 7.34 | 7.23 | .985 |
| HHF | 10.17 | 10.06 | .989 |
| LLR | 2.85 | 2.88 | 1.011 |
| LLF | 2.34 | 2.38 | 1.018 |
| LHR | 1.79 | 1.82 | 1.014 |
| LHF | 2.62 | 2.55 | .974 |

* Average for eight laboratories—Laboratory 10 was excluded before computations were made. However, the inclusion of Laboratory 10 would have only reinforced the trend.

Table IV gives the standard error of a single vibroscope reading over all fiber types for each laboratory.

**TABLE IV**

| Laboratory | Standard error |
|---|---|
| 1 | — |
| 2 | 0.16 |
| 3 | 1.21 |
| 4 | 0.10 |
| 5 | 0.52 |
| 6 | 0.08 |
| 8 | 0.03 |
| 9 | 0.23 |
| 10 | 0.60 |

**TABLE V**

| Type of Vibroscope | AV | TRI | TRI | TRI | AV | AV | AV | TRI | TRI |
|---|---|---|---|---|---|---|---|---|---|
| Laboratory | 6 | 2 | 10 | 1 | 4 | 5 | 3 | 8 | 9 |
| Av. $D_v/D_w$ | .929 | .955 | .956 | .965 | .974 | 1.000 | 1.010 | 1.026 | 1.059 |

## Literature Cited

1. ASTM Manual on Textile Materials, 710–718 (Nov. 1956).
2. Dart, S. L. and Peterson, L. E., TEXTILE RESEARCH JOURNAL **19**, 89–93 (1949); **22**, 819–822 (1952).
3. Gonsalves, V. E., TEXTILE RESEARCH JOURNAL **17**, 369–375 (1947).
4. Voong, E. T. L and Montgomery, D. J., TEXTILE RESEARCH JOURNAL **23**, 821–830 (1953).

*Manuscript received January 14, 1958.*

# Responses to Environmental Changes and an Equation of State for Nylon Yarn

**Bernard H. Eckstein[1], Earl H. Olson[2], and William F. Ames[3]**

*E. I. du Pont de Nemours and Company, Inc., Wilmington, Delaware*

**Abstract**

Nylon yarn at constant temperature was exposed to changes in relative humidity. It was found that, at constant length, the tension in the yarn is inversely proportional to the logarithm of the relative humidity; at constant tension, the logarithm of the length is proportional to the relative humidity. At low strains, stress is proportional to strain. Then over a limited range a linear relation exists between log stress and log strain. "Equations of state" were derived relating these variables, and the constants therein were evaluated for a nylon textile yarn. Different equations apply in different regions of the stress–strain curve. A similar equation was derived for the case of varying temperature, but the constants were not evaluated.

## Experimental

### *Introduction*

As part of a general program on the physical behavior of 66 nylon yarns under various conditions, the changes which such yarns undergo with changes in relative humidity, extension, and temperature have been studied. The initial aim had been to predict the responses in tension and/or length changes of the yarns when they were subjected to various states of tension, extension, relative humidity, or temperature during normal handling.

The responses described here are not necessarily the initial ones but represent the quasi-equilibrium states attained after the yarns have been conditioned beyond the extremes of temperature and humidity which they encountered during the experiments. The behavior of the moisture-sensitive, semicrystalline polyhexamethylene adipamide yarns was found to obey some general relationships which had been derived principally for cross-linked materials, assuming no particularly detailed internal structure for the filaments.

It can be concluded that, over certain limited ranges, the elastic behavior of nylon is similar to that of a cross-linked material. Quasi-static stress–strain measurements were made at 74° F. at selected relative humidities. From these measurements and the thermodynamic theory of Treloar [6], semi-empirical expressions were obtained relating moisture content at fixed relative humidity to the tension. Equations of state were derived, but it was found that different equations apply in different regions of the stress–strain curve.

### *Description of Materials*

Data were obtained on two yarns: 70–34 and 210–34 nylon yarns. The first was a 70-den., 34-filament textile yarn containing ½ turn/in. Z-twist, made from a polymer with a number-average molecular weight about 13,000 and containing 0.3% of finely dispersed $TiO_2$. It had a specific birefringence of 0.050, an X-ray orientation as measured by half angles of 13° (both inner and outer arcs), tenacity of 4.9 g./den.,[4] and an elongation of 20.4% with an initial elastic modulus of 31.5 g./den. and a maximum elastic modulus of 68 g./den. The second yarn was a 210-den., 34-filament industrial high-tenacity yarn made from a polymer of number-average molecular weight 14,000, but containing only 0.02% of finely dispersed $TiO_2$. Its specific birefringence was 0.062; the X-ray orientation as measured by half angles was 11.2° for the inner arc and 10.4° for the outer arc. This yarn displayed a tenacity of 7.4 g./den., an elongation of 14.6%, an initial modulus of 31, and a maximum modulus of 109 g./den.

[1] Present address: National Carbon Co. Division of Union Carbide Corporation, Research Laboratories, P. O. Box 6116, Cleveland 1, Ohio.

[2] Textile Fibers Department, Carothers Research Laboratory.

[3] Engineering Department, Engineering Service Division.

[4] 1 g./den. = $1.03 \times 10^9$ dynes/cm.$^2$ for 66 nylon.

Experiments on another 70–34 yarn which contained 2% $TiO_2$ showed it to be almost indistinguishable from the first 70–34 yarn described above; i.e., there was no effect due to changing the filler content.

*Stress–Strain Behavior*

Information about the changes in tension with changes in length is conveniently derived from experiments on an Instron tester. This is a constant-rate-of-elongation device and, of course, the results obtained depend not only on the environmental conditions but also on the rates of elongation.

The experiments here described were carried out on 10-in. samples at 72% relative humidity and 74° F. using a rate of extension of 60%/min. Each stress–strain curve shown in Figure 1 is an average of 10 measurements. The total force was read from the Instron charts at intervals of 0.3% elongation and all 10 readings per degree of elongation were averaged to plot the curves. Figure 1 shows both the conventional stress–strain curve (the lower curve), in which the total force is divided by the initial denier, and the true stress–strain curve (the upper curve), in which the total force at a given strain is divided by the actual denier at that elongation. Only the latter is used in the mathematical section.

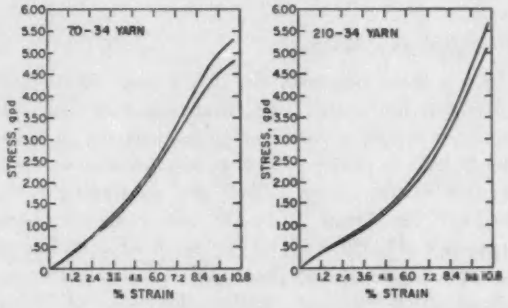


**Fig. 1.** Stress–strain curves for nylon yarns (upper curve, true stress; lower curve, conventional stress–strain diagram).

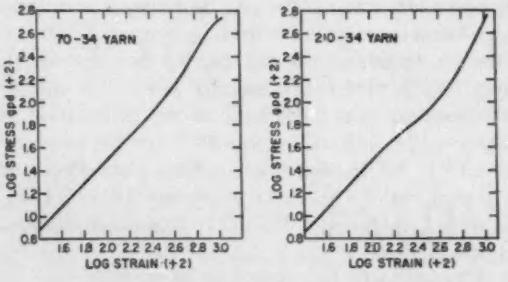


**Fig. 2.** Log stress vs. log % strain for nylon yarn.

The viscoelastic theory underlying the interpretation of experiments at constant rates of elongation has been discussed by Smith [5]. Insofar as can be told from the presently available data, nylon textile yarn seems to obey Smith's theory over certain intervals. Figure 2 shows that for a moderate range of extension a linear plot is obtained in a log true stress vs. log strain diagram. More extensive Instron data would have permitted extrapolation to an infinitely slow rate of loading or the determination of the temperature dependence of the elastic properties of nylon. The other yarn studied, the high-tenacity industrial 210–34 yarn, shows a somewhat different stress–strain curve and does not agree as well with Smith's theory. This poorer agreement is to be expected for a medium of high molecular orientation.

*Length–Relative Humidity Relations at Constant Tension and Temperature*

Barkas [1] has worked out the fundamental thermodynamic theory of the relation between the liquid content of a gel and stresses to which the gel may be subjected. Treloar [6] has modified this for the case of a general cylindrical system under an axial stress. A semicrystalline polymer may be considered as a cross-linked system. From Treloar's theory it may be shown that the logarithm of length should be a linear function of the relative humidity for a sample under constant load. This is illustrated by data in Figure 3.

Treloar presents his results in the form

$$\frac{(\partial q)}{(\partial X)p} = \frac{1+q}{\rho_m v p_0} \cdot \frac{1}{l}\left[\frac{\partial l}{\partial (p/p_0)}\right]_X$$

which may be written as

$$\frac{1}{l}\left[\frac{\partial l}{\partial (p/p_0)}\right]_X = \left[\frac{\partial (\ln l)}{\partial (p/p_0)}\right]_X = \frac{\rho_m v p_0}{1+q}\left[\frac{\partial q}{\partial X}\right]_p$$

where $l$ = length of sample, $p$ = actual vapor pressure of water, $p_0$ = equilibrium pressure of water at the temperature of the experiment, $\rho_m$ is the density of the swollen state, $v$ is the volume occupied by 1 g. of vapor at the pressure $p$, $q$ is the weight of water per gram of dry material, and $X$ is the force in the axial direction. Of course, $100(p/p_0)$ = RH, the relative humidity. As the theory would

predict, the length dependence on relative humidity decreases with increasing tension, and the moisture absorption of a sample under high tension is less than that of a sample under low tension. Because of the low moisture uptake by nylon, a plot of length vs. relative humidity is also almost linear, as shown in Figure 4.

The length–humidity behavior of nylon yarns depends to some extent on age. The samples here described were well aged and had to be conditioned at the extremes of the ranges studied before any reproducible measurements could be obtained. The length dependence on humidity for very freshly drawn yarns is less than that for aged yarns. There appears to be little, if any, difference between the 70–34 and 210–34 yarns, as shown in Figure 3. The same theoretical treatment was verified experimentally for undrawn yarns also, but they show a greater sensitivity to moisture.

### *Tension–Relative Humidity Behavior at Constant Length and Temperature*

Consider a yarn or filament held at a constant length under a certain tension $t_a$. This tension is proportional to the free energy of the sample, which, in turn, depends upon the chemical potential $\mu_a$.

$$t_a \propto F_a = \mathrm{RT} \ln \mu_a$$

Consider the filament as a system of two components, the polymer and water vapor. The water vapor may be considered a dilute gas which is in equilibrium with the water vapor in the surrounding atmosphere. When the relative humidity is changed, the concentration of this dilute component is changed. The chemical potential of the system may be replaced by the activity or the partial pressure of the gas. Therefore, when the partial pressure of the water vapor $p_a$ changes to a new state $p_b$, and hence, the tension of the system goes from $t_a$ to $t_b$, the following relation holds:

$$t_a - t_b \propto \Delta F = \mathrm{RT} \ln \frac{p_a}{p_b} = \mathrm{RT} \ln \frac{p_a/p_0}{p_b/p_0}$$

Figure 5 shows that indeed the tension in a yarn at constant length does depend upon the logarithm of the relative humidity. However, the slopes of the lines do not seem to depend on the tension level until fairly high tensions are reached. At the lower tension levels, for aged yarns which have been relaxed once, the change in tension is approximately 0.30 g./den./decade change in relative humidity for

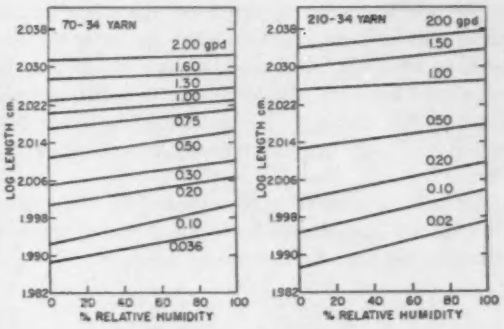


**Fig. 3.** Log length vs. % relative humidity for nylon yarns, aged, conditioned, and once relaxed briefly.

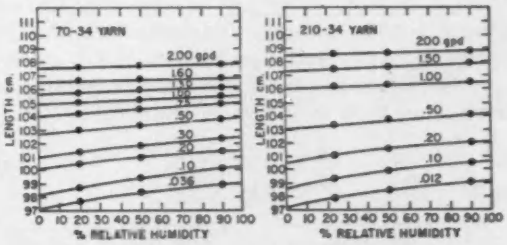


**Fig. 4.** Length–moisture relationship in nylon yarns which have been aged, once relaxed briefly, then strung up under the loads indicated at 50% RH (length = 100 cm.), then conditioned.

70–34 yarns and about 0.26 g./den./decade for the 210–34 yarns. For fresh 70–34 yarn which had never experienced zero tension, a change of 0.34 g./den. was found. Qualitatively similar behavior was shown by low orientation undrawn yarns, but the slopes of the curves were much steeper.

### *Force–Temperature Measurements*

Force–temperature measurements on nylon yarns have been reported by Bryant [2] and Roseveare [4], whose work was much more careful and painstaking than that of the present authors. The results obtained in this study are included merely because they were obtained on items which were otherwise studied in great detail. The crude data obtained may be represented conveniently by one straight line over the full range of temperature studied (25–140° C.), but more painstaking work, such as that of Roseveare, would show a small change in slope for the line at each transition point.

The total force $f_T$ can be expressed as two terms, $f_T = f_E + f_S$, where $f_E$ is the energy contribution to the retractive force and $f_S$ is the entropy contri-

bution. This latter is given by the slope of the curve and remains constant over the interval covered, so that the total force at any point may be calculated knowing the force at one point and the slope of the curve. The necessary data are presented in Table I and a typical curve is shown in Figure 6.

Actually, according to Roseveare [3], "The thermodynamic equation of state for a material under tensile stress may be written as follows:

$$f = \frac{(\partial E)}{(\partial l)_T} - T\frac{(\partial S)}{(\partial l)_T} \quad (1)$$

$$= f_E + f_S \quad (2)$$

where $f$, $E$, $l$, $S$, and $T$ are tensile force, internal energy, length, entropy, and temperature. The change in energy and entropy with length cannot be measured readily, but the entropy coefficient can be obtained from the following relationship:

$$\frac{(\partial S)}{(\partial l)_T} = -\frac{(\partial f)}{(\partial T)_l} \quad (3)$$

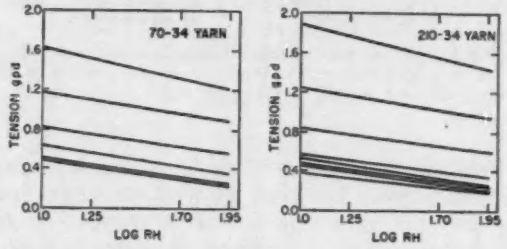


**Fig. 5.** Tension vs. log (% relative humidity) for nylon yarns at various tension levels. The yarns were aged, once relaxed, and conditioned.

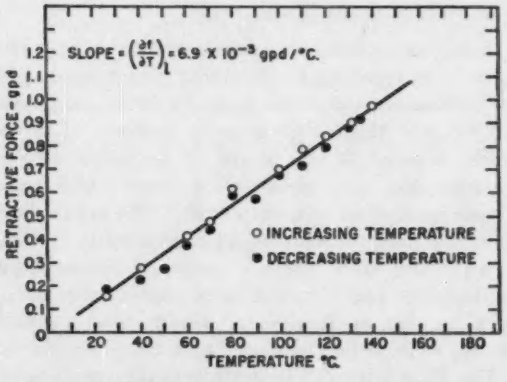


**Fig. 6.** Typical force–temperature curve for 70–34 nylon. The sample was strung up at 0.05 g./den. initial load, annealed at 145° C., and run in dry nitrogen.

For each of the drawn yarns studied, samples were strung up at the nominal tension indicated and then annealed for ½ hr. at 145° C. After the yarns were annealed the runs were reproducible. After the first annealing process, the samples at higher tension exhibited a stress decay proportional to the nominal initial tension, but the samples strung up at very low tensions became virtually indistinguishable. However, their general tension level rose. The amount of stress decay depends directly on the temperature, as shown by Roseveare, but not on the time of heating.

Consider Table I. One would expect that the greater the degree of the order of the system, hence the lower the entropy of the system, the greater will be the entropy contribution. This is borne out by the data obtained. The slope, i.e., the entropy contribution for a given yarn, rises slightly with increasing starting tension; that is, with increasing order in the yarn. The slopes for the 210–34 yarn at any given starting tension are greater than the slopes for the textile yarns. At the moment it is not quite clear why the substitution of 100% RH for 0% RH should make so little difference unless one assumes that the sorption of the small amount of moisture does not change the internal order of the polymer appreciably and hence does not affect the entropy of the system markedly.

**TABLE I. Results of Force–Temperature Measurements on Nylon Yarns**

| Yarn | Atmosphere | Nominal tension, 25° C., g./den. | Actual tension, 25° C., $f_T$, g./den. | Slope $\left(\frac{\partial f}{\partial T}\right)_l$ or $\frac{f_S}{T}$ at 25–140° C., g./den./° C. |
|---|---|---|---|---|
| 70–34 | Dry $N_2$ | 0.05 | .165 | $6.9 \times 10^{-3}$ |
| | | 0.10 | .190 | 7.3 |
| | | 0.20 | .175 | 6.6 |
| | | 0.50 | .225 | 7.8 |
| | | 1.00 | .485 | 8.4 |
| | | 2.00 | .825 | 9.2 |
| 70–34 | Steam (100% RH) | 0.05 | .240 | 6.6 |
| | | 0.10 | .220 | 6.2 |
| | | 0.20 | .270 | 6.4 |
| | | 0.50 | .325 | 6.6 |
| | | 1.00 | .515 | 8.2 |
| | | 2.00 | .960 | 7.1 |
| 210–34 | Dry $N_2$ | 0.05 | .230 | 7.6 |
| | | 0.10 | .260 | 6.1 |
| | | 0.20 | .280 | 7.6 |
| | | 0.50 | .385 | 8.0 |
| | | 1.00 | .650 | 9.2 |
| | | 2.00 | 1.20 | 10.3 |

### Mathematical

Because each of the theoretical relations was readily verified experimentally, the Technical Computations Group of the Engineering Department derived equations to describe the observed behavior. The functional relationships based on the observed phenomena are shown in the derivations below. These are carried out for the type 70–34 nylon yarn to illustrate the method.

*Derivation: At Constant Temperature $T$, for the Tension Range 0.3 g./den. $\leqslant t \leqslant$ 2.1 g./den. (True Stress)*

Let $T$ = temperature, °C.; $l$ = length in cm.; $t$ = tension in g./den.; and $R$ = % relative humidity. Figure 3 illustrates that

$$\frac{\partial \ln l}{\partial R} = K_1(t) \qquad \text{I-1}$$

This derivative is independent of $l$ and $R$ but may (and does) depend upon $t$. Integration of I-1 yields

$$l = K_2(t)e^{K_1(t)R} \qquad \text{I-2}$$

where $K_2$ and $K_1$ are functions of tension whose form is to be determined. Figure 2 shows that

$$\frac{\partial \ln l}{\partial \ln t} = K_6(R) \qquad \text{I-3}$$

$$l = K_7(R)t^{K_6(R)} \qquad \text{I-4}$$

Now I-2 and I-4 must be compatible. Hence, taking logarithms

$$\ln l = \ln K_2(t) + K_1(t)R \qquad \text{I-5}$$

$$\ln l = \ln K_7(R) + K_6(R) \ln t \qquad \text{I-6}$$

Differentiating I-6 with respect to $R$ yields

$$\frac{\partial \ln l}{\partial R} = \frac{1}{K_7}\frac{dK_7}{dR} + \frac{dK_6}{dR}\ln t = K_1(t) \qquad \text{I-7}$$

But since $K_1$ is a function only of $t$, and since $K_6$ and $K_7$ are functions of $R$ only, I-7 can be true only if

$$\frac{1}{K_7}\frac{dK_7}{dR} = C_1$$

or

$$K_7 = C_2^* e^{C_1 R} \quad (C_2^* = e^{C_2}) \qquad \text{I-8}$$

and

$$\frac{dK_6}{dR} = C_3$$

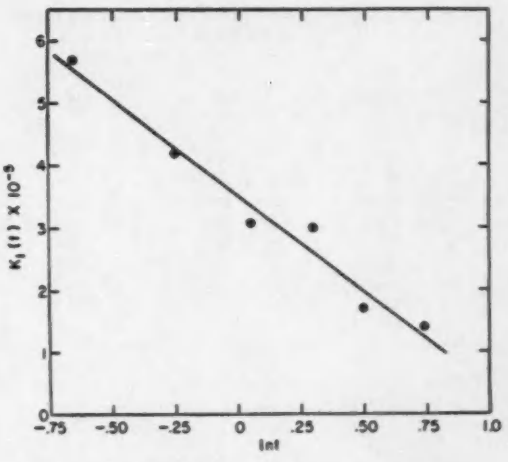


**Fig. 7.** The slope of $K_1(t)$ as a function of tension ($K_1(t) = \partial(\ln l)/\partial R = 3.538 \times 10^{-5} - 3.086 \times 10^{-5} \ln t$).

or

$$K_6 = C_3R + C_4 \qquad \text{I-9}$$

Hence $K_1$ is predicted theoretically to be

$$K_1(t) = C_1 + C_3 \ln t \qquad \text{I-10}$$

Substitution of I-8 and I-9 in I-4 yields the "equation of state" as

$$l = C_2^* e^{C_1 R} t^{C_3 R + C_4} \qquad \text{I-11}$$

or (using the reduced variable $\phi = l/l_0$)

$$\phi = \frac{l}{l_0} = C_2 e^{C_1 R} t^{C_3 R + C_4} \qquad \text{I-12}$$

where $l_0$ is the initial length measured under some set of conditions and used to evaluate the other constants.

An alternative procedure can be used. If I-5 is differentiated with respect to $\ln t$, the same result (I-11) is obtained.

The necessary constants are easily evaluated. A least squares fit to the data for 70–34 yarn in Figure 3 (see Table II) verifies that with tensions from 0.3 g./den. to 2.1 g./den. the form $C_1 + C_3 \ln t$ for $K_1(t)$, predicted theoretically, is excellent.

Figure 7 shows the plot of $K_1(t)$ vs. $\ln t$. The equation is

$$K_1(t) = 3.538 \times 10^{-5} - 3.086 \times 10^{-5} \ln t \qquad \text{I-13}$$

where $C_1 = 3.538 \times 10^{-5}$ and $C_3 = -3.086 \times 10^{-5}$.

**TABLE II. Stresses at 72% RH and Slopes for Figure 3, for 70–34 Nylon Yarn**

| $t$ (true stress) | $\ln t$ | $K_1(t) = \frac{\partial \ln l}{\partial R} \times 10^{-5}$ |
|---|---|---|
| 2.1 | .742 | 1.4 |
| 1.65 | .501 | 1.7 |
| 1.35 | .300 | 3.0 |
| 1.05 | .049 | 3.1 |
| .78 | −.248 | 4.2 |
| .52 | −.654 | 5.7 |
| .30 | — | 5.3 |
| .20 | — | 6.0 |
| .10 | — | 8.7 |
| .036 | — | 7.2 |

**TABLE III. Comparison of Calculated and Experimental Results from Figure 3, for 70–34 Nylon Yarn**

| $t$, g./den. | $R$, % | $\log l$, Formulae | $\log l$, Figure 3 |
|---|---|---|---|
| 2.1 | 10 | 2.0314 | 2.0317 |
| 1.65 | 80 | 2.0285 | 2.0288 |
| 1.35 | 50 | 2.0251 | 2.0245 |
| 1.05 | 100 | 2.0227 | 2.0229 |
| 0.52 | 20 | 2.0115 | 2.0122 |

To determine $C_4$, the data from Figure 2 are utilized; one finds that $C_4 = 0.0339$ at $t = 1.05$ and $R = 72\%$.

Figure 3 yields $C_5 = 0.9958$, which is obtained at $t = 1.05$ g./den. (true stress), and $R = 72\%$. This results in

$$\phi = \frac{l}{l_0} = 0.9958\, e^{3.538\times10^{-5}R[0.0339-3.086\times10^{-5}R} \qquad \text{I-14}$$

Table III shows some comparisons; i.e., checks of the equation against the experimental results. For convenience of comparison these are shown in logarithmic (base 10) form.

*Derivation: At Constant Temperature, for the Range $0 \leqslant t \leqslant 0.3$ g./den. (True Stress)*

Figure 3 again illustrates that

$$\frac{\partial \ln l}{\partial R} = u_1(t) \qquad \text{II-1}$$

but the function $u_1$ is different from $K_1$. By integration this yields

$$l = u_2(t)e^{u_1(t)R} \qquad \text{II-2}$$

Figure 1 shows

$$\frac{\partial l}{\partial t} = f_1(R)$$

or

$$l = f_1(R)t + f_2(R) \qquad \text{II-3}$$

Therefore

$$f_1(R)t + f_2(R) = u_2(t)e^{u_1(t)R} \qquad \text{II-4}$$

Differentiating II-4 with respect to $t$, we have

$$f_1(R) = e^{u_1(t)R}\left\{\frac{du_2}{dt} + u_2\frac{du_1}{dt}R\right\} \qquad \text{II-5}$$

Relation II-5 is true in the class of all differentiable functions only if

$$\frac{du_2}{dt} = b$$

or

$$u_2(t) = a + bt$$
$$u_1(t) = C \qquad \text{II-6}$$

Hence

$$l/l_0 = e^{CR}[A + Bt]$$
$$A = a/l_0 \qquad B = b/l_0 \qquad \text{II-7}$$

The observation II-6—$u_1(t) = C$ (constant)—predicts some discrepancy between the experimental observations and the theoretical equation. On the one hand, Table II shows that there is a variation in $\partial(\ln l)/\partial R$ in the low tension range ($0 \leqslant t \leqslant 0.3$ g./den.), even though this is definitely erratic, and on the other hand, the theory says that mathematical consistency requires that $\partial \ln l/\partial R$ be constant. In these low ranges of tension, theory and experiment disagree, probably because the stress–strain curve may not be really linear or, more likely, because the experimental error is large at these low tensions.

The constants in this equation can be evaluated using the data obtained from Figures 1 and 3. Table II gives an approximate value of $C$. Disregarding the value 8.7, one estimates $C$ to be $6.17 \times 10^{-5}$. From Figure 1, at $t = 0$ g./den., $l/l_0 = 1.0012$, so that $1.0012 = Ae^{6.17\times10^{-5}\times72}$ or $A = 0.99675$. $B$ is then found to be $+0.00125$. The "equation of state" for the low tension range is

$$\phi = l/l_0 = [.99675 + .00125\,t]e^{6.17\times10^{-5}R} \qquad \text{II-8}$$

*Derivation: At Variable Temperature, $0 \leqslant t \leqslant 0.3$ g./den.*

The present data are inadequate for an evaluation of the constants in the equation here derived. Nonetheless, the derivation of the equation of state, suggested by the experimental results, is shown.

Assume $t = F(l, T, R)$ and consider $l$, $T$, $R$ as independent variables. From Figures 1, 5, and 6 it is seen that

$$\frac{\partial t}{\partial \ln R} = W_1(l, T) \qquad \text{III-1}$$

$$\frac{\partial t}{\partial l} = W_2(T, R) \qquad \text{III-2}$$

$$\frac{\partial t}{\partial T} = W_3(l, R) \qquad \text{III-3}$$

Integration yields

$$t = W_1(l, T) \ln R + W_4(l, T) \qquad \text{III-4}$$

$$t = W_2(T, R)l + W_5(T, R) \qquad \text{III-5}$$

$$t = W_3(l, R)T + W_6(l, R) \qquad \text{III-6}$$

Of course, these must all be compatible. Differentiating III-4 and III-6 with respect to $T$, one obtains

$$\frac{\partial W_1(l, T)}{\partial T} \ln R + \frac{\partial W_4(l, T)}{\partial T} = W_3(l, R) \qquad \text{III-7}$$

So the left-hand side of III-7 must be such that

$$W_1(l, T) = f_1(l)T + f_1^*(l) \qquad \text{III-8}$$
$$W_4(l, T) = f_2(l)T + f_2^*(l)$$

since $T$ must be eliminated by differentiating.[5]

Also, differentiating III-4 and III-6 with respect to $R$, one finds

$$W_1(l, T) = R\frac{\partial W_3(l, R)}{\partial R}T + R\frac{\partial W_6(l, R)}{\partial R} \qquad \text{III-9}$$

Hence

$$R\frac{\partial W_3}{\partial R}(l, R) = f_3(l) \qquad \text{III-10}$$

$$R\frac{\partial W_6}{\partial R}(l, R) = f_4(l)$$

[5] $f^*(l)$ refers to "constant" function of integration.

or

$$W_3(l, R) = f_3(l) \ln R + f_3^*(l) \qquad \text{III-11}$$
$$W_6(l, R) = f_4(l) \ln R + f_4^*(l)$$

Utilization of these results in III-5 gives

$$f_1(l)T + f_1^*(l) \ln R + f_2(l)T + f_2^*(l) = W_2(T, R)l + W_5(T, R) \qquad \text{III-12}$$

Differentiating III-12 with respect to $l$ yields

$$W_2(T, R) = \frac{df_1}{dl}T + \frac{df_1}{dl}\ln R + \frac{df_2^*}{dl} + \frac{df_2^*}{dl} \qquad \text{III-13}$$

For $W_2$ to be a function only of $T$ and $R$ requires that

$$\frac{df_1}{dl} = C_{11} \qquad \frac{df_2}{dl} = C_{21} \qquad \text{III-14}$$
$$\frac{df_1^*}{dl} = C_{11} \qquad \frac{df_2^*}{dl} = C_{21}$$

or

$$f_1 = C_{11}l + C_{12} \qquad f_2 = C_{21}l + C_{22} \qquad \text{III-15}$$
$$f_1^* = C_{11}^* + C_{12}^* \qquad f_2^* = C_{21}^* + C_{22}^*$$

Hence from III-8 and III-4 the "equation of state" for the low tension range is

$$t = (C_{11}l + C_{12})T + (C_{11}^*l + C_{12}^*)\ln R + (C_{21}l + C_{22})T + C_{21}^*l + C_{22}^* \qquad \text{III-16}$$

A similar equation can be derived for the higher tension range. Sufficient data are not available at this time to evaluate the constants in III-16.

## Literature Cited


1. Barkas, W. W., "Swelling Stresses in Gels," His Majesty's Stationery Office, London (1945).
2. Bryant, G. M., TEXTILE RESEARCH JOURNAL **23**, 788 (1953).
3. Roseveare, W. E. and Poore, E. L., *J. Polymer Sci.* **14**, 341 (1954).
4. Roseveare, W. E., unpublished data.
5. Smith, T. L., *J. Polymer Sci.* **20**, 89 (1956).
6. Treloar, L. R. G., *Trans. Faraday Soc.* **48**, 567 (1952).


*Manuscript received October 11, 1957.*

# Nonsilicate Stabilization of Hydrogen Peroxide Bleach Solutions

**David M. Cates and Winifred H. Cranor**

*The Textile Research Center, School of Textiles, North Carolina State College, Raleigh, North Carolina*

**Abstract**

Alkaline solutions of hydrogen peroxide are stabilized by addition of calcium chloride and disodium phosphate. Evidence is given that stabilization may be due to the formation of $CaHPO_4$ as precipitate.

THE stability of highly purified hydrogen peroxide solutions is well established [4]. There are a great many substances, however, that catalyze peroxide decomposition even when present in trace concentrations, particularly in alkaline solution. Since bleaching of cellulosic fabrics in mill practice is normally carried out in alkaline solution that may contain dissolved or suspended catalytic impurities, a stabilizing agent is added to prevent wasteful decomposition. Moreover, the uncontrolled release of oxygen from hydrogen peroxide is said to degrade cellulose chemically, so that an additional function of the stabilizer is to prevent this degradation by controlling the decomposition rate. A stabilizer may also serve to buffer the solution at the desired pH level and to provide detergent and penetrant action [4].

The most widely used stabilizer in textile plants is sodium silicate. Silicate has all of the aforementioned advantages, but associated with these are disadvantages that have often proved a source of trouble. The silicate apparently forms insoluble compounds with calcium and magnesium which deposit on the surface of equipment and fabric and are difficult to remove. The result is that cloth is frequently abraded by the silicate deposits; also, the presence of insoluble compounds on the cloth leads to difficulties in the dyehouse.

Recently, Easton and Feldman [2] reported the successful use of nonsilicate stabilized peroxide solutions. The system which they used consisted of an alkaline peroxide solution containing calcium chloride and disodium phosphate. The purpose of this paper is to present the results of experiments carried out in this laboratory that give some information about the stabilizing action of this system as well as the composition of the stabilizing agent.

In most of the present work, the concentrations in solution of hydrogen peroxide, sodium hydroxide, and calcium chloride were held constant and the stability of the peroxide determined as a function of concentration of disodium phosphate. A precipitate of calcium phosphate and/or calcium hydroxide was present in all of the solutions, the composition of the precipitate depending upon the amount of disodium phosphate present. In some of the experiments, the composition of the precipitate was determined by analyzing the filtrate and precipitate separately as a function of concentration of disodium phosphate.

## Experimental

Solutions containing reagent grade hydrogen peroxide, sodium hydroxide, calcium chloride, and disodium phosphate were made up to a specified volume and maintained for 90 min. at 90° C. in a constant temperature bath. In most of the work the composition of the reaction solution was held constant except for the amount of $Na_2HPO_4$ that was added. Stock solutions of reagent grade $Na_2HPO_4$, NaOH, and $CaCl_2$ were made up, and the required addition of each was always made from the same stock solution.

The reaction flasks in some experiments were 25-ml. volumetric flasks and, in others, 50-ml. Erlenmeyer flasks. Both types of flasks were ground-glass stoppered; the stopper was kept in place throughout reaction to prevent evaporation. After each experiment the reaction flask was washed out with 1 *N* $HNO_3$ before cleaning with distilled water. This procedure was followed to make certain that

unremoved traces of precipitate, soluble in nitric acid, did not influence subsequent reactions carried out in the same flask.

In the initial work, redistilled water was used for dilution. After reaction, the flask was removed from the constant temperature bath and immediately diluted by addition of cooled redistilled water. In all of the other experiments ordinary distilled water was used for dilution; after reaction, the reaction solution was first cooled to room temperature by placing the flask in a beaker of cooled water and then diluted to volume with distilled water. The decomposition of hydrogen peroxide in each solution was determined.

In some of the experiments both filtrate and precipitate were analyzed. The procedure was the following. The solution flask was removed after a reaction time of 90 min. at 90° C. and immediately cooled to room temperature. The solution was then filtered through a sintered glass funnel and the filtrate made up to 100 ml. volume with distilled water. The precipitate was dissolved by passing 25 ml. of standard 0.1 *N* HCl drop by drop through the sintered glass funnel, applying suction. The precipitate solution was then made up to 100 ml. with distilled water. The following analyses were performed on aliquots of the filtrate and precipitate solutions:

*Filtrate*

The amount of $H_2O_2$ decomposed was determined by titration with 0.1 *N* standard potassium permanganate [3]. The pH of the diluted filtrate was measured. Successive endpoints for NaOH and $Na_2HPO_4$ were obtained by potentiometric titration using standard 0.01 *N* HCl [5]. The amounts of NaOH and $Na_2HPO_4$ used during reaction were then calculated from the known original amounts added. The amount of calcium used during reaction was determined by titration with the disodium salt of ethylenediamine tetraacetic acid using Eriochrome Black T as indicator [1].

*Precipitate*

The "peroxide" content of the precipitate was determined by titration with standard 0.01 *N* potassium permanganate. The 25 ml. of 0.1 *N* HCl used to dissolve the precipitate was in excess of the alkali content of the precipitate. The excess acid was determined by potentiometric titration using standard 0.01 *N* NaOH. The difference between excess acid and the known amount of acid originally added was taken as the sum of the $OH^-$ and $HPO_4^=$ content of the precipitate. The amount of calcium present in the precipitate was determined by titration with the disodium salt of ethylenediamine tetraacetic acid.

## Results and Discussion

*Stability of $H_2O_2$ Solutions When Concentration of $Na_2HPO_4$ is Varied*

The stability of hydrogen peroxide was determined as a function of the concentration of disodium phosphate, the concentrations of hydrogen peroxide, sodium hydroxide, and calcium chloride being held constant. In part of the experiments, solutions were used in which the concentrations of all components were relatively dilute; the results are shown in Figure 1. The data in Figure 1 include two series of experiments; in one series (initial experiments), only the decomposition of hydrogen peroxide was determined, whereas in the other (repeat experiments), both peroxide decomposition and final pH of the solution were measured. In the rest of the work, solutions were used in which the concentrations were 14 times those used in the case of the dilute solutions; the results are given in Table I and in Figure 2.

In the case of the dilute solutions, a flat maximum in percent hydrogen peroxide decomposed was found in the range of 0.015–0.06 mmol. $Na_2HPO_4$ added (see Figure 1, initial experiments; the results of the repeat experiments will be discussed below). It was noticed that a precipitate was obtained in each solution and that the amount of precipitate appeared to increase with larger additions of $Na_2HPO_4$.

It was thought that this precipitate consisted of

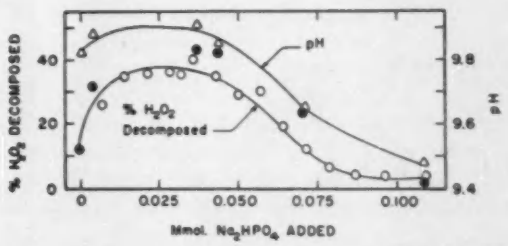


**Fig. 1.** % $H_2O_2$ decomposed in dilute solution as function of mmol. $Na_2HPO_4$ added. % $H_2O_2$ decomposed: ○ initial experiments; ● repeat experiments; △ pH, repeat experiments. Concentration in solution (mmol./ml.): $Na_2HPO_4$, varied; $CaCl_2$, 0.00368; NaOH, 0.0058; $H_2O_2$, 0.14. Reaction volume of 35 ml. Initial experiments: redistilled water used for dilution. Repeat experiments: distilled water used for dilution.

a mixture of calcium hydroxide and calcium phosphate and possibly that the stability of the hydrogen peroxide was related to the composition of the precipitate. Accordingly, a series of experiments was carried out in which the peroxide filtrate and precipitate were analyzed separately for the various components. Concentrations were increased ten-fold over those used in the dilute solutions, and the reaction volume was reduced from 35 ml. to 25 ml. In effect, concentrations were increased to 14 times the concentrations that were used in the dilute solutions. The results are shown in Table I and in Figure 2.

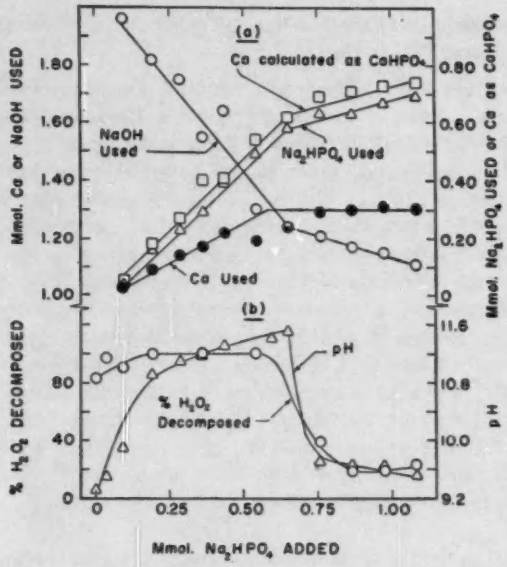


**Fig. 2.** Analysis of hydrogen peroxide solutions as function of mmol. $Na_2HPO_4$ added. Concentration in solution (mmol./ml.): $Na_2HPO_4$, varied; $CaCl_2$, 0.0515; NaOH, 0.0825; $H_2O_2$, 1.95. Reaction volume of 25 ml.

The "used" values of Table I correspond to differences between quantities originally added to the reaction solution and quantities found in the filtrate; each value was therefore taken to be the amount of the component appearing in the precipitate. The average calcium used represents the average between the amount found by actual titration of the precipitate and the amount that was calculated to be present in the precipitate based upon titration of the filtrate. The values for calcium calculated as $CaHPO_4$ were determined by assuming that the quantity of NaOH used, obtained by titration of filtrate solutions, was present in the precipitate as $Ca(OH)_2$. The amount of calcium represented by NaOH used was subtracted from the average calcium used, and the difference was taken to be calcium as $CaHPO_4$.

The role of the "peroxide" content of the precipitate (see Table I) is not clear. It is possible that the peroxide may exist as calcium peroxide, adsorbed hydrogen peroxide, or as a molecular complex. The values obtained for peroxide in the precipitate were somewhat erratic, and were ignored in the calcula-

**TABLE I. Analysis of Decomposed Hydrogen Peroxide Solutions**

Concentration in solution (mmol./ml.): $Na_2HPO_4$, varied; $CaCl_2$, 0.0515; NaOH, 0.0825; $H_2O_2$, 1.95. Reaction volume of 25 ml.

| *Mmol.* $Na_2HPO_4$ added | 0 | 0.037 | 0.094 | 0.191 | 0.284 | 0.361 | 0.434 | 0.542 | 0.650 | 0.758 | 0.867 | 0.975 | 1.084 |
|---|---|---|---|---|---|---|---|---|---|---|---|---|---|
| $H_2O_2$ in ppt. | * | * | 0.69 | 1.23 | 0.50 | 0.77 | 0.44 | 0.26 | 0.05 | 0.22 | 0.14 | 0.27 | 0.32 |
| Calcium used, filt. | * | * | 1.06 | 1.09 | 1.16 | 1.17 | 1.24 | 1.18 | 1.25 | 1.30 | 1.30 | 1.30 | 1.30 |
| Calcium used, ppt. | * | * | 1.00 | 1.09 | 1.12 | 1.17 | 1.20 | 1.19 | 1.23 | 1.28 | 1.29 | 1.31 | 1.29 |
| Average | * | * | 1.03 | 1.09 | 1.14 | 1.17 | 1.22 | 1.19 | 1.24 | 1.29 | 1.30 | 1.31 | 1.30 |
| NaOH used, filt. | * | * | 1.96 | 1.82 | 1.75 | 1.55 | 1.64 | 1.30 | 1.24 | 1.21 | 1.17 | 1.15 | 1.11 |
| $Na_2HPO_4$ used, filt. | * | * | 0.04 | 0.16 | 0.23 | 0.29 | 0.39 | 0.49 | 0.58 | 0.63 | 0.63 | 0.67 | 0.69 |
| Total | * | * | 2.00 | 1.98 | 1.98 | 1.84 | 2.03 | 1.79 | 1.82 | 1.84 | 1.80 | 1.82 | 1.80 |
| Total NaOH and $Na_2HPO_4$ used, ppt. | * | * | 1.85 | 2.08 | 1.98 | 2.01 | 2.00 | 1.84 | 1.82 | 1.87 | 1.83 | 1.89 | 1.87 |
| $Na_2HPO_4$ remaining in filtrate | * | * | 0.06 | 0.03 | 0.06 | 0.07 | 0.05 | 0.05 | 0.07 | 0.13 | 0.24 | 0.31 | 0.39 |
| Calcium calculated as $CaHPO_4$ | – | * | 0.05 | 0.18 | 0.27 | 0.40 | 0.40 | 0.54 | 0.62 | 0.69 | 0.71 | 0.73 | 0.74 |
| Final pH of filtrate diluted to 100 ml. vol. | 9.32 | 9.50 | 9.90 | 10.92 | 11.10 | 11.20 | 11.30 | 11.40 | 11.50 | 9.70 | 9.65 | 9.65 | 9.50 |
| % $H_2O_2$ decomposed | 83.3 | 97.5 | 91.0 | 100 | * | 100 | * | 100 | * | 38.3 | 18.3 | 18.5 | 22.9 |

* Not measured.

tions. A reasonable picture emerges when this is done, as will be seen below.

According to Figure 2(a), the amount of NaOH used decreases rapidly at first and then tends to level off at about 0.65 mmol. $Na_2HPO_4$ added, whereas the amounts of calcium and $Na_2HPO_4$ used increase rapidly and linearly, leveling off in the same range. In the case of calcium, the data reveal that all of the calcium originally added was used after addition of 0.65 mmol. $Na_2HPO_4$. This behavior indicates that a competition exists in the reaction solution between $OH^-$ and $HPO_4^=$ ions for $Ca^{++}$ ions, which is reasonable in view of the relative insolubility of hydroxide and phosphate salts of calcium.

The curve for calcium as $CaHPO_4$ in Figure 2(a) coincides within experimental error with the curve for $Na_2HPO_4$ used. Since the $CaHPO_4$ figures were calculated from experimental data that were independent of experimental values for $Na_2HPO_4$ used, this agreement is evidence that the precipitate consists of a mixture of $Ca(OH)_2$ and $CaHPO_4$.

The effect of increasing additions of $Na_2HPO_4$ on pH is shown in Figure 2(b). The pH passes through a maximum at about 0.65 mmol. $Na_2HPO_4$ added and then decreases rapidly to a pH of about 9.5. Prior to the addition of any $Na_2HPO_4$, the solution pH has the low value of 9.3 because much of the $OH^-$ originally added has been precipitated as $Ca(OH)_2$. Addition of $Na_2HPO_4$ to the solution results in competition between $HPO_4^=$ and $OH^-$ ions for $Ca^{++}$ ions; increasing quantities of hydroxide ion are freed from calcium hydroxide in the precipitate and pass into solution, as indicated by the NaOH used curve, raising the pH. In the vicinity of 0.65 mmol. $Na_2HPO_4$ added, virtually all of the calcium ions have been precipitated, either as the hydroxide or as the phosphate in proportions dependent upon the relative solubilities. Further addition of $Na_2HPO_4$ causes slight displacement of hydroxide ion from calcium hydroxide in the precipitate, in a manner predictable by the mass action law; most of the added $HPO_4^=$ ions, however, remain in solution, buffering the solution to pH 9.5–9.6 This can be seen from the results in Table I for $Na_2HPO_4$ remaining in the filtrate.

Figure 2(b) shows that the stability of the peroxide parallels closely the pH of the solution as increasing amounts of $Na_2HPO_4$ are added. The $H_2O_2$ decomposed increases from 83% for zero addition of $Na_2HPO_4$ to 100% and then decreases rapidly to 20% after addition of about 0.65 mmol. $Na_2HPO_4$.

There was some question as to whether or not conclusions based on the results of Figure 2, obtained with relatively concentrated solutions, were applicable to the more dilute solutions used in the initial experiments of Figure 1. For this reason, repeat experiments using dilute solutions were run in which pH and percent decomposition of $H_2O_2$ were checked at six different levels of phosphate addition. The results are shown in Figure 1. The peroxide decomposition again was observed to pass through a flat maximum. The slight difference between the results of the initial and repeat experiments of Figure 1 is believed to arise from small differences in procedure. The pH in the case of the repeat experiments increased slightly from an initially low value and then decreased and levelled off at about 9.5 for high additions of phosphate. Although the change in pH is much less pronounced than was the case in Figure 2(b), the trend in both dilute and concentrated solutions was the same. From this correspondence of results, it was felt that the description previously applied to the more concentrated solutions is essentially true for the dilute ones.

Because the stability of peroxide parallels closely the changes in pH brought about by phosphate addition, it may be considered possible that the formation of calcium phosphate in the precipitate does not itself bring about any stabilizing action. There can be little doubt that a decrease in pH ordinarily leads to smaller rates of peroxide decomposition, since the instability of $H_2O_2$ in alkaline solution is well known. The correlation between pH and peroxide decomposition is shown in Figure 3, where the data relating to pH from Figures 1 and 2(b) are plotted.

The pH effect alone is insufficient to explain the results, however. For example, in the case of the concentrated solutions of Table I, the pH of 9.3 was obtained when no phosphate was added, compared to the pH of 9.5 for 1.084 mmol. of phosphate added. Yet the respective decompositions of 83% and 23% were found. This suggests that the calcium phosphate precipitate does have a stabilizing effect and that calcium hydroxide is relatively ineffective. Similar results are obtained in dilute solution, as can be seen in Table II(a). Table II(a) shows that hydrogen peroxide is much more stable in the presence of calcium phosphate precipitate than in its absence,

even though the pH in the former case is somewhat higher.

*Stability of $H_2O_2$ in Dilute Solution in Presence of Constant Amounts of $Ca^{++}$ and $HPO_4^{=}$ Ions*

Some additional experiments were carried out in which the stability of $H_2O_2$ was examined when the concentrations of both NaOH and $H_2O_2$ were varied. The concentrations of $Ca^{++}$ and $HPO_4^{=}$ ions were kept constant at a level which would achieve the maximum stabilization shown in Figure 1. The results are given in Table II(b) and in Figures 4 and 5.

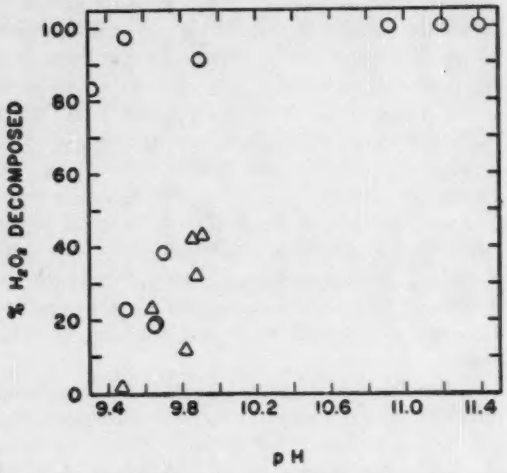


**Fig. 3.** % $H_2O_2$ decomposed as function of pH when only $Na_2HPO_4$ concentration is varied. $H_2O_2$ concentrations (mmol./ml.): △, 0.14; ○, 1.95.

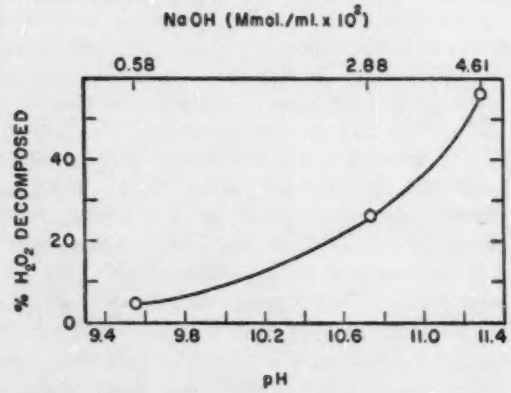


**Fig. 4.** % $H_2O_2$ decomposed as function of pH when only NaOH concentration is varied. Concentration in solution (mmol./ml.): $Na_2HPO_4$, 0.00535; $CaCl_2$, 0.00368; NaOH, varied; $H_2O_2$, 0.14. Reaction volume of 35 ml.

Table II(b) shows that an eight-fold increase of $H_2O_2$ concentration causes a reduction of pH, as expected, and that peroxide stability is not much affected.

Figure 4 shows that an eight-fold increase in NaOH concentration, while maintaining all other concentrations constant, greatly increases pH and the instability of the peroxide. Higher decomposition is caused by increasing the amount of hydroxide ion; the effect of the hydroxide ion apparently is to raise the pH and to reduce the amount of calcium phosphate precipitate by competing with $HPO_4^{=}$ ions for $Ca^{++}$ ions. It is clear, however, that at the high pH of 11.3 which was attained, complete decomposition would be expected in the absence of stabilizer instead of the 56% that was actually realized.

Figure 5 illustrates the results obtained when the concentrations of both $H_2O_2$ and NaOH are increased eight-fold, while maintaining their relative concentrations constant at a ratio of 24:1, respectively. As expected, pH was raised slightly, and this was reflected in a higher rate of decomposition.

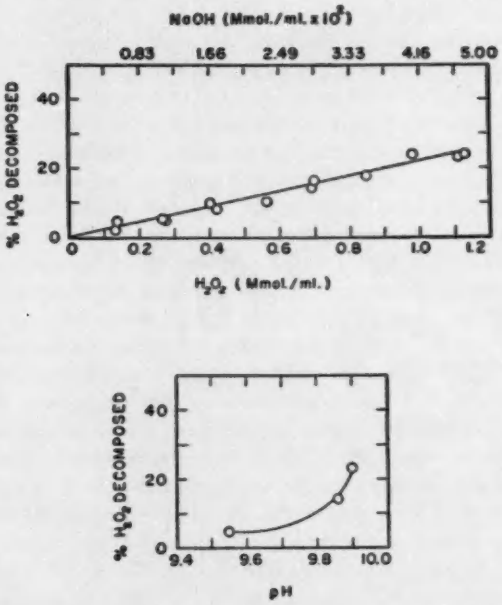


**Fig. 5.** % $H_2O_2$ decomposed when concentrations of both NaOH and $H_2O_2$ are varied. Concentrations in solution (mmol./ml.): $Na_2HPO_4$, 0.00535; $CaCl_2$, 0.00368; NaOH, varied; $H_2O_2$, varied. Reaction volume of 35 ml.

## Summary

Alkaline solutions of hydrogen peroxide are stabilized by addition of calcium chloride and disodium phosphate. Evidence is given that stabilization may be due to the formation of $CaHPO_4$ as precipitate.

In hydrogen peroxide solutions in which the concentrations of NaOH and $CaCl_2$ are held constant, the solution pH and amount of calcium phosphate formed in the precipitate depend on the amount of $Na_2HPO_4$ that is added. The data indicate that a competition exists in the reaction solution between $OH^-$ and $HPO_4^=$ ions for $Ca^{++}$ ions. Initially, the addition of phosphate ion to the solution results in freeing hydroxide ion from calcium hydroxide precipitate, raising the pH of the solution. When all of the calcium ions have been precipitated, either as hydroxide or as phosphate, further addition of phosphate causes some displacement of hydroxide ion from calcium hydroxide in the precipitate, but most of the phosphate ions remain in solution as buffering agent. The final solution pH reached in the present work was about 9.5, where the hydrogen peroxide was much more stable than it was in solutions maintained at the same or lower pH's in the absence of calcium phosphate.


## Literature Cited


1. Bersworth Chemical Company, "The Versenes," Technical Bulletin No. 2, Section III, Page 6.
2. Easton, B. K. and Feldman, P., *Textile Bulletin* **82**, 77 (1956).


**TABLE II. % $H_2O_2$ Decomposed in Dilute Solution**

(a) $Na_2HPO_4$, $CaCl_2$, NaOH concentrations varied. $H_2O_2$ concentration constant at 0.14 mmol./ml.; reaction volume of 35 ml.

| $Na_2HPO_4$ mmol./ml. | $CaCl_2$ mmol./ml. | NaOH mmol./ml. | % $H_2O_2$ decomposed | Final pH of reaction solution (diluted) |
|---|---|---|---|---|
| 0 | 0 | 0.00058 | 100 | 9.55 |
| 0.0031 | 0 | 0.00058 | 74.4 | 9.05 |
| 0.0031 | 0.0037 | 0.0058 | 1.43 | 9.48 |

(b) $H_2O_2$ concentration varied.

Concentration in solution (mmol./ml.): $Na_2HPO_4$, 0.00535; $CaCl_2$, 0.00368; NaOH, 0.0058; reaction volume of 35 ml.

| $H_2O_2$ mmol./ml. | % $H_2O_2$ decomposed | Final pH of reaction solution (diluted) |
|---|---|---|
| 0.14 | 4.41 | 9.55 |
| 1.12 | 3.42 | 8.60 |


3. Kolthoff, I. M. and Sandell, E. B., "Textbook of Quantitative Analysis," New York, Macmillan, 574 (1952).
4. Schumb, W. C., Satterfield, C. N., and Wentworth, R. L., "Hydrogen Peroxide," New York, Reinhold, 515, 578 (1955).
5. Zall, D. M., Wagman, E., and Ingler, N., *Anal. Chem.* **27**, 277 (1955).


*Manuscript received January 15, 1958.*

# Letters to the Editor

## Maximum Alkali-Combining Capacity of Wool

Wool Textile Research Laboratories
Commonwealth Scientific and Industrial Research Organization
Geelong, Australia
February 11, 1958

To the Editor
TEXTILE RESEARCH JOURNAL

*Dear Sir:*

The maximum amount of alkali which combines with proteins, especially those rich in cystine, is difficult to measure due to the extensive degradation which takes place at high pH. However, much less degradation takes place in alkaline solutions containing high concentrations of certain salts, and it has now been found that the alkali-combining capacity of wool can be determined in sodium hydroxide solutions saturated with these salts. The mean value obtained from these experiments is 11.8 g.-equiv. $OH^-/10^4$ g. dry wool (Table I), which agrees reasonably well with the average value of 12.2 calculated from the sums of the arginine, lysine, $\alpha$-amino group, tyrosine, and histidine contents of wool given by various authors [3, 4, 8, 10, 12].

Merino 64's wool was used, either loose or as a plain weave worsted fabric. It was purified by Soxhlet extraction for 6 hr. with petroleum ether, followed by cold ethanol extraction for 24 hr. (for the fabric only), and then rinsing in several changes of distilled water. After standing in 0.001 *N* HCl for 2 days, it was washed with several changes of distilled water daily until the pH of the water did not change overnight. The ash content of the fabric was 0.07% and of the loose wool, 0.05%.

Each sample (about 5 g.; dried for 2 hr. at 105° C.) was wet out *in vacuo* in 100.0 ml. of sodium hydroxide solution saturated with either sodium chloride or sodium thiosulfate. The conditions of treatment are given in Table I. Samples of solution, withdrawn at various times, were diluted and titrated with 0.1 *N* HCl to the phenolphthalein endpoint. (Sample volumes and dilutions were such that titrations were approximately 20 ml., an error of ±0.02 ml. in a titration giving an error of ±0.3 g.-equiv. $OH^-/10^4$ g. wool.) When successive titres had become approximately constant, the wool was removed, allowed to stand in 0.5 *N* HCl for 15 min., and then rinsed in distilled water for several days until the washings were chloride-free. The change in weight, cystine [14], and primary amino groups (using the ninhydrin method as applied to wool [9]) was estimated in each sample. Bromine-oxidizable sulfur [6] was determined in some of the residual solutions.

The striking protection from degradation given by the salt solutions is shown by the weight losses in Table I. Treatment for 2 hr. at 25° C. in 1.286 *N* NaOH in saturated sodium chloride, or in 1.266 *N* NaOH in the absence of salt, gave weight losses of 2% or 56% respectively.

Three degradative reactions have been considered in arriving at corrections to be applied to the results.

1. Hydrolysis of primary amide groups would be expected to take place under the conditions used; some $NH_3$ was detected in solution with Nessler's reagent. One $OH^-$ would be lost per amide group hydrolyzed and an equivalent amount of $NH_3$ formed. Some $NH_3$ would be titrated to the phenolphthalein endpoint, compensating for an equivalent amount of $OH^-$ reacted, and the amounts not titrated must have been insignificant since, in the presence of salts, the calculated amounts of alkali combined did not vary when different indicators were used. This was not the case with the pure sodium hydroxide solutions (Table I).

2. Hydrolysis of peptide bonds would use one $OH^-$ per peptide bond hydrolyzed if no protein material went into solution; allowance has been made for this by assuming that one $OH^-$ has been used for every new amino group found in the wool.

3. Table I shows that some cystine reacts when wool is treated in alkaline salt solutions. If the reaction could be represented simply as R.S.S.R. → R.S.R. + S [1], no $OH^-$ would be used in the overall reaction and no correction would need to be applied to the alkali binding figures. However, a positive nitroprusside test was given by the residual

**TABLE I. Combination of Wool with Alkali**

| NaOH conc., *N* | Salt used | Temp., °C. | Time, min. | Weight loss, % | Cystine, mole/$10^6$ g. dry wool | $NH_2$ groups, equiv./$10^6$ g. dry wool | $OH^-$ combined,* equiv./$10^6$ g. dry wool | Corrected $OH^-$ combined,† equiv./$10^6$ g. dry wool |
|---|---|---|---|---|---|---|---|---|
| 0.492 | NaCl | 25 | 60 | | | | 10.6 | |
| | | | 120 | | | | 11.8 | |
| | | | 240 | | | | 12.4 | |
| | | | 360 | 0.4 | 3.4 | 2.12 | 12.8 | 11.6 |
| | | | 420 | 0.6 | 3.2 | 2.14 | 12.9 | 11.5 |
| 1.256 | NaCl | 25 | 15 | | | | 10.8 | |
| | | | 30 | | | | 13.4 | |
| | | | 60 | 1.2 | 3.1 | 2.22 | 13.7 | 12.1 |
| 1.286 | NaCl | 25 | 120 | 2.0 | 2.5 | 2.25 | 14.0 | 11.8 |
| 1.237‡ | NaCl | 25 | 30 | | | | 13.8 | |
| | | | 60 | 1.3 | 3.0 | 2.20 | 14.0 | 12.3 |
| 1.262 | $Na_2S_2O_3$ | 25 | 30 | | | | 10.9 | |
| | | | 60 | | | | 13.6 | |
| | | | 120 | 1.4 | 2.8 | 2.23 | 13.8 | 11.9 |
| 2.444 | NaCl | 25 | 5 | | | | 11.6 | |
| | | | 15 | | | | 14.0 | |
| | | | 30 | 1.7 | 2.5 | 2.24 | 14.4 | 12.2 |
| 1.231 | NaCl | 2 | 180 | 0.1 | 3.6 | 2.18 | 12.0 | |
| | | | 360 | 1.0 | 3.2 | 2.20 | 12.8 | 11.3 |
| | | | 960 | 2.1 | 2.8 | 2.30 | 13.1 | 11.1 |
| 1.266 | — | 25 | 15 | 9.1 | 3.1 | 2.40 | 12.8§ | (11.0) |
| | | | 120 | 56 | 1.0 | 2.98 | 16.1§ | (11.6) |
| | (Untreated wool) | | | | (4.6) | (2.10) | | |

* Calculated by assuming that the concentration of NaOH inside the wool is the same as in solution.

† Allowing for one $OH^-$ used per peptide bond hydrolyzed and one $OH^-$ lost per cystine residue decomposed.

‡ Purified Merino loose wool used.

§ These figures were obtained using phenolphthalein in the titrations; with bromthymol blue or methyl orange, the values found were 11.3 or 6.3 respectively, instead of 16.1.

solutions, showing that not all the sulfur lost from wool was in the form of free sulfur. Bromine-oxidizable sulfur, estimated in some of the solutions, was found to be equivalent to the decrease in cystine content of the wool. Thus, in the absence of any more definite information, it appears likely that the correction of one $OH^-$ lost per bromine-oxidizable sulfur atom in solution, as used previously [7, 13], is the best that can be made. The correction appears to be justified by the constancy of the corrected alkali uptakes in Table I, but it may be too high.

This new method should prove useful, in conjunction with acid-binding determinations, for measuring the total number of protein side chains which have reacted during chemical treatments. If the reaction is specific for a particular side chain, the method provides a means of analysis for the groups in question. Also, the treatment of wool with NaOH in saturated salt solutions offers a convenient means of studying the reaction of combined cystine with alkali, since very little protein goes into solution and cystine degradation is apparently the only reaction taking place to any great extent. Certain salts also protect soluble proteins from denaturation [2, 5, 11] and would, presumably, also prevent extensive breakdown by alkaline solutions so that the alkali binding of a wide variety of proteins could be studied by making use of concentrated salt solutions. Further, protein reactions which take place only in strongly alkaline solution could be carried out in the presence of high concentrations of salts to prevent the excessive degradation normally associated with these reactions.

### Acknowledgments

I am grateful to Dr. M. Lipson for many valuable discussions and to Miss L. Boardman for assistance with the experimental work.

### Literature Cited

1. Blackburn, S. and Lee, G. R., *Biochim. et Biophys. Acta* **19**, 505 (1956).
2. Burk, N. F., *J. Phys. Chem.* **47**, 104 (1943).
3. Corfield, M. C. and Robson, A., *Biochem. J.* **59**, 62 (1955).
4. Graham, C. E., Waitkoff, H. K., and Hier, S. W., *J. Biol. Chem.* **177**, 529 (1949).
5. Greenstein, J. P., *J. Biol. Chem.* **130**, 519 (1939).

6. Harris, M., *J. Research Nat. Bur. Standards* **15**, 63 (1935).
7. Horner, J. L., *Trans. Faraday Soc.* **50**, 1000 (1954).
8. La Fleur, K. S., *Am. Dyestuff Reptr.* **34**, 395 (1945).
9. McPhee, J. R., TEXTILE RESEARCH JOURNAL **28**, 303 (1958).
10. Simmonds, D. H., *Australian J. Biol. Sci.* **7**, 98 (1954).
11. Simpson, R. B. and Kauzmann, W., *J. Am. Chem. Soc.* **75**, 5139 (1953).
12. Speakman, J. B., *J. Soc. Leather Trades' Chem.* **37**, 37 (1953).
13. Steinhardt, J. and Harris, M., *J. Research Nat. Bur. Standards* **24**, 335 (1940).
14. Stricks, W., Kolthoff, I. M., and Tanaka, N., *Anal. Chem.* **26**, 299 (1954).

J. R. MCPHEE

# A Tex-Cotton Count Conversion Scale

Southern Utilization Research
and Development Division
1100 Robert E. Lee Boulevard
New Orleans, Louisiana
February 17, 1958

To the Editor
TEXTILE RESEARCH JOURNAL

*Dear Sir:*

A universal numbering system, called tex, defined as the number of grams per 1000 meters of material, was approved at the 1956 Plenary Conference of the International Organization for Standardization (1956). The tex system was endorsed by Committee D-13, American Society for Testing Materials, October 1956; the system has been described in several articles [1, 2, 3, 4].

A useful conversion scale is proposed (Figure 1) which might be of interest in production line or research fields as a convenient method of converting from cotton count to tex, or vice versa, based on the relationship that tex = 590.54/cotton count. The scale is applicable to both yarns and rovings with sizes which are common and popular in U. S. textile mills. Either the upper or lower portion of the scale may be used as a starting point for any desired conversion; however, it may be found more convenient to follow the procedure outlined below. The scale is designed as a substitution for massive conversion tables when only the approximate value is needed.

Directions for using the scale are as follows:

1. For yarn—read directly from the scale
   Example: 11's cotton count = 54 tex
   28's cotton count = 21 tex
   30 tex = 20's cotton count
   42 tex = 14's cotton count
2. for roving—
   A. To find tex value with number of hank roving known:
      a. For 0.75 and lighter hank roving: Move the decimal point of the hank roving (example: 1.1 hank roving) one digit to the right. Locate this number (11) on the upper portion of the scale, read its corresponding value (54.0), and multiply by 10 to obtain the equivalent tex value (540).
      b. For roving heavier than 0.75 hank: Move the decimal point of the hank roving in question (example: 0.70 hank roving) two digits to the right. Locate this number (70) on the lower portion of the scale, read its corresponding value (8.4), and multiply by 100 to obtain the equivalent tex value (840).
   B. To find the number of hank roving with tex known:
      a. For roving of 800 tex or lighter: Move the decimal point of the tex (example 300.0-tex roving) one digit to the left.

**Fig. 1.** Conversion scale.

Locate this number (30) on the lower portion of the scale, read its corresponding value (20), and multiply by 0.10 to obtain the equivalent hank roving (2.0).

b. For roving heavier than 800 tex: Move the decimal point of the tex (example: 840.0-tex) two digits to the left. Locate this number (8.4) on the upper portion of the scale, read its corresponding value (70) and multiply by 0.01 to obtain the equivalent hank roving (0.70).

### Literature Cited

1. Anon., *Man-Made Textiles* **33**, No. 391, 45 (1956).
2. Bates, A. W., *J. Textile Inst.* **48**, P255–267 (1957).
3. Röder, H. L., *Rayon Rev.* **10**, No. 4, 130–139 (1956).
4. Whittier, B. L., *Textile World* **107**, No. 8, 88–89, 170 (1957).

Gain L. Louis

# Cause of Wool Felting

Institute of Organic Chemical Technology
Technical University
Budapest, Hungary
April 23, 1958

To the Editor
Textile Research Journal

*Dear Sir:*

The purpose of this investigation was to observe the role played by the entanglement of wool fibers placed on the surface of or immersed in water. The heterogeneous swelling of the cortical components; i.e., the para- and orthocortex [1], may be considered as the cause of the entanglement of the wool fibers.

If in the process of swelling of the differently oriented (thus, to a differing degree, anisotropic) cortex components, the difference of length arising as a consequence of genetic shrinkage disappears, the crimpiness of the fiber disappears too [3]. As a result of further swelling, the more highly oriented layer, as a consequence of the difference in anisotropy, will change its dimension along the axis of the fiber, to a small extent. In the less oriented cortical

**Fig. 1.** The entanglement of a wool fiber (Grade C) in distilled water at 20°. The points around which the fiber curves in taking up the next formation are marked with circles.

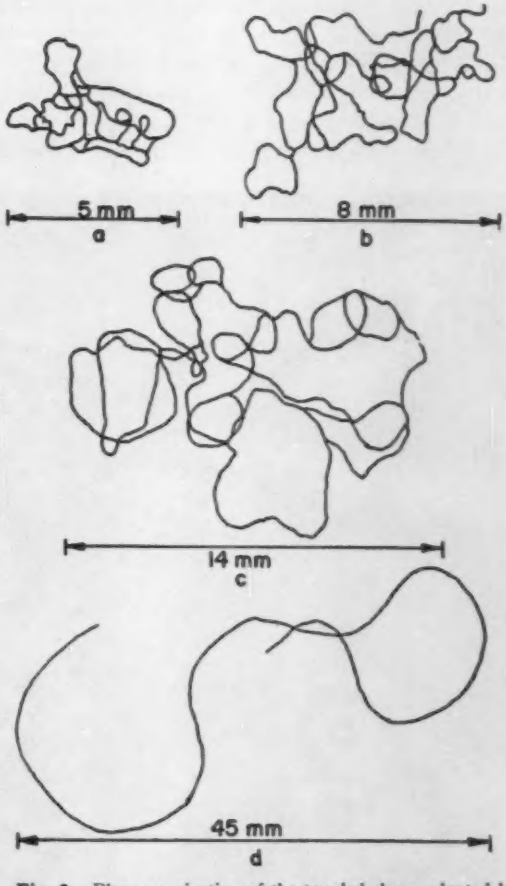


**Fig. 2.** Planar projection of the tangled shape adopted by various wool fibers placed on distilled water. a = AAA grade, b = A, c = B, and d = C grade.

component, the difference of dimensional change caused by swelling, acting in the direction of the longitudinal axis, will continue to be greater. After a certain stage in swelling, any further swelling will necessarily cause the elongation of the less oriented component as compared to the more highly oriented segment. Since there is no possibility of sliding between the two layers, even in case of a greater swelling, new stresses must arise acting in the opposite direction to those causing the crimpiness of the fiber. If the swelling and accordingly the stress is large enough, this will lead to the bending of the fiber and to the formation of new curvatures. In this case the curvature is of opposite direction to the crimp. During the formation of these new curvatures the fiber makes large movements and becomes entangled with others (Figure 1).

Our experiments suggest that there are no new curvatures to be found on the place of each crimp, and no spiral form appears. At this stage of swelling an irregular shape will be formed even if, by the use of swelling agents, a greater swelling is brought about than that caused by water (Figure 2).

It may be suggested that in the process of felting the movement of wool fibers will cause displacement in various directions as a result of internal influences and thus cause entanglement with other fibers. The loops and knots formed in the course of the entanglement impede the complete displacement of the fiber from the felt. Thus it is the entanglement that produces the felting effect from the sliding movement of the fibers.

To prove this, 20 wool fibers parallel to each other were placed on the surface of water and their entanglement observed (Figure 3). They all appeared to become entangled. The movements leading to the entanglement did not occur at the same time; accordingly, we observed several places where the fibers were twisted together and wound around each other.

From this the conclusion may be drawn that the entanglement and movement of wool fibers in water is accompanied by intertwining, and this phenomenon may be a basic principle of felting.

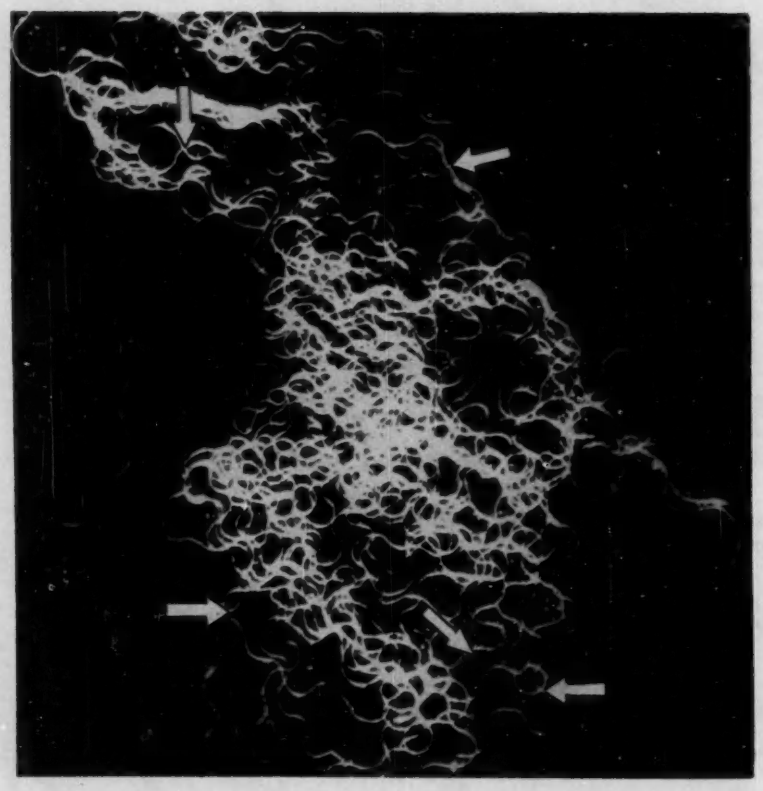

**Fig. 3.** Twenty parallel fibers of AAA grade wool placed on distilled water at 20°, after 2 min. exposure. At the places marked by arrows, the fibers entwined.

The other factors referred to by Speakman [2] naturally also influence the felting of fibers, but are important only for those fibers which are inclined to felt formation due to their spontaneous entanglement, and only after the spontaneous entanglement has been accomplished.

From this standpoint it is clear that in order to characterize the felting power of a wool it is not sufficient to consider merely the hysteresis of the extension and contraction curve, or the directional friction of the fiber. A third parameter is also necessary—the tendency to entanglement. This may be expressed by the ratio L:D, where L is the length of the nonentangled fiber and D is the radius of the sphere that may be plotted around the entangled fibers.

We have found that the ability of a fiber to become entangled varies with such conditions as temperature and the concentration of electrolyte. Moreover, acid and alkaline damage is shown up more sensitively by the tendency to entanglement of a fiber than by the usual tests [4].

### Literature Cited

1. Dobozy, O. K., *L'Ind. Text.* No. 843, 109 (1957).
2. Speakman, J. B., *J. Textile Inst.* **22**, T339 (1931).
3. Zilahi, M. and Dobozy, O. K., *Acta Techn. Acad. Sci. Hung.* **9**, No. 1–2, 65 (1954).
4. Zilahi, M. and Dobozy, O. K., *Magy. Text. Techn.* No. 2, 42 (1955).

O. K. DOBOZY

# Dynamometric Measurements on Wool Fibers in Tops: Mean Value of Specific Strength, Work of Stretching, and Rate of Loading

Peltzer & Fils S. A.
102 Rue David
Verviers, Belgium
March 17, 1958

To the Editor
TEXTILE RESEARCH JOURNAL

*Dear Sir:*

The electronic integrator-differentiator, described in a previous paper [1], has been applied to the determination of the work of stretching and rate of loading on 350 wool fibers taken out of five tops. Fineness measurements on the individual fibers were also made; they were used to evaluate the specific strength and to set up various correlations between the dynamometric parameters of the tops and the cross-sectional area of the fiber.

A paper collecting all these results, comparing them with results obtained by other authors, and adding some comment, was presented by F. Monfort, M. Franck, and J. Grignet to the Technical Committee of the International Wool Textile Organization at its meeting in Paris, December 1957. This paper appeared in *Bulletin de l'Institut Textile de France*, No. 72, February 1958.

We here summarize the most important original results from that paper, which is a continuation of the one previously published [1].

The experiments were considered from an industrial point of view. Starting from dynamometric measurements on fibers extracted from five tops, covering the whole normal fineness range, from 19.5 to 33$\mu$, it was hoped to set up some relations between the dynamometric parameters and the geometrical parameters of the fibers, mainly the fineness. A more distant purpose was to verify if the assemblies of fibers used in the industry (batch of wool top) could be characterized by sufficiently uniform dynamometric parameters, and if these parameters could be deduced from the mean geometrical parameters of the top. In this case, it would be possible to avoid the dynamometric measurements on individual fibers, not practicable for routine control.

We also call attention to the limitations of the experiments. The results are obtained for tops of different origins, but these tops have been washed, carded, and combed in the same mill, under the same conditions.

The dynamometric measurements were made on 1 cm. of fiber, in air, using a Fafegraph Stein dy-

namometer, working with constant rate of extension. The mean time to break was 20 sec. ± 3 sec. For each fiber, a determination of length and weight led to the evaluation of the mean cross-sectional area $a$, assuming a cylindrical form and a constant specific weight. On the load–extension diagram were read the breaking load $F_R$, and the loads $F_{20}$, $F_{25}$, and $F_{30}$ at 20, 25, and 30% extension respectively.

On the rate of load vs. time recordings were picked up the maximum rate of load (corresponding to the Hookean zone), which led to the evaluation of the Young's modulus, and the rate of load at break.

Finally, the work of stretching vs. time recordings provide the work at break $W_R$, and the works $W_{20}$, $W_{25}$, and $W_{30}$, corresponding respectively to 20, 25, and 30% stretching.

The conclusions are as follows:

1. The mean breaking load[1] $(1, F_R)$ is very nearly proportional to the cross-sectional area $(1, a)$.

2. The mean loads $(1, F_{20})$, $(1, F_{25})$, and $(1, F_{30})$ are very nearly proportional to the cross-sectional area $(1, a)$.

These results were obtained by averaging the loads and the cross-sectional areas of the fibers within each top. The five points provided by this method showed a good adjustment on a mean straight line. The adjustment was very good for $F_{20}$, $F_{25}$, and $F_{30}$, and good for $F_R$, the deviation from the mean line being 0, −7.8, −8.2, +6.4, and +4%.

3. The mean specific strength $\rho = F_R/a$ seems to be independent of the cross-sectional area $(1, a)$.

4. The mean stresses $F_{20}/a$, $F_{25}/a$, and $F_{30}/a$ at 20, 25, and 30% stretching seem to be independent of the cross-sectional area.

These results were obtained by averaging the ratios $F_R/a$ (or $F_{25}/a$, etc.) for the fibers within each top. The five values obtained presented fairly small deviations from a horizontal mean line that could be led through the common zone of the confidence intervals.

The specific strength $\rho_R = F_R/a$ was found equal to about 16.3 kg./mm.²

In every respect, one can say that if some difference exists between the specific strengths of the tops considered, it is very little and can be neglected for industrial calculations (spinning, etc.).

5. The mean work of stretching at break $W_R$ is nearly proportional to the cross-sectional area.

6. The mean works of stretching $W_{20}$, $W_{25}$, and $W_{30}$ are very nearly proportional to the cross-sectional area.

The results are obtained by averaging the work $W$ and area $a$ for all the fibers within each top and setting up a correlation between the five values of work and the five corresponding values of area.

The coefficient of variation of the $W_R$ in a top is about 60%; for $W_{20}$, $W_{25}$, $W_{30}$, about 42%.

7. The mean value of the maximum rate of load $dF/dt$ increases with the cross-sectional area. Values range from 2.58 g./sec. to 8.94 g./sec.

The diagram $(1, dF/dt)$ vs. $(1, a)$ has the form of a curved line with the concavity upwards. The C.V. of the values in a top is about 40%. The rate of load goes through a maximum for an extension of about 1.4%.

8. The mean values of the Young's modulus are included between two closely lying limits.

Although it is difficult to say that the Young's modulus is independent of cross section, it is remarkable that the mean values range from 236 to 293 kg./mm.², in a relatively narrow range.

The C.V. of the Young's modulus of the fibers in each top is about 20%.

9. The mean value of the rate of load at break increases with the cross-sectional area.

The values obtained range from 0.225 g./sec. to 0.902 g./sec. The curve "$dF/dt$ at break" versus area has its concavity turned upwards. The C.V. of the values in each top is about 70%.

10. The mean value of the rate of load at break is about one-tenth of the mean value of the maximum rate of load for each top.

The values found for the work of stretching at break and the Young's modulus agree with these cited by other authors [2].

[1] The expressions $(1, F_R)$, $(1, a)$, etc. are notations for the mean, due to R. C. Palmer. In this paper $(1, F_R)$ and $(1, a)$ are the arithmetical means, obtained by numerical sampling.

For further details, see F. MONFORT, *Annales Scientifiques Textile Belger*, June 1958.

## Literature Cited

1. Grignet, J. and Monfort, F., TEXTILE RESEARCH JOURNAL **28**, 47 (1958).
2. Meredith, R., *J. Textile Inst.* **36**, T127 (1945).

J. GRIGNET
F. MONFORT